A STUDY OF SEMICONDUCTOR STRAIN GAUGES

Thesis

A STUDY OF SEMICONDUCTOR STRAIN GAUGES

Submitted for the Degree of Bachelor of Philosophy

BRIAN PICKTHORNE

OPEN UNIVERSITY

ELECTRONICS DISCIPLINE

Date of Submission: OCTOBER 1986
Date of Award: 1.5.87

OCTOBER 1986

ABSTRACT - Semiconductor Strain Gauges

Piezoresistance is the change in the electrical resistance of a material due to the application of a strain and is employed for measuring strain. The effect in semiconductors was reported in 1954 by Smith and it was mainly in America, during the following decade, that the investigation and development of semiconductor strain gauges took place. Recent literature in this sphere is somewhat scant.

This investigation examines the theoretical basis of piezoresistance in semiconductors, explores the manufacture and properties of semiconductor strain gauges and reviews factors which influence their properties, such as dopant level and type. In comparison to metal foil or wire gauzes it is shown that the gauge factor of semiconductor strain gauges is high. However, at elevated temperatures they display the following undesirable features to a greater extent than metal foil or wire strain gauges:

(a) T.C.R. : temperature coefficient of resistance

(b) T.C.G.F. : temperature coefficient of gauge factor

(c) Apparent strain induced by differential thermal expansion between the gauge and substrate

(d) A non-linear strain/resistance characteristic which varies with temperature.

Investigations were undertaken regarding the behaviour, use and testing of typical semiconductor strain gauges and recommendations are made based upon the findings. This includes the bonding of semiconductor strain gauges, gauge non-linearity and gauge energization circuits. Studies of bridge circuits were also carried out and a special bridge/amplifier system, which was devised for use with semiconductor strain gauges, is described and assessed. Investigations of the thermal characteristics are then reported and suggestions made concerning the compensation of these effects. Following this, details of the photosensitivity of semiconductor strain gauges are presented. A photoconductive effect was detected, and the photo-transient response of typical semiconductor strain gauges was found to be much more marked than their static response.

In a final section two significant potential applications of semiconductor strain gauges are outlined:

First, the use of semiconductor strain gauges in nuclear radiation fields was explored. The results indicate that such an application is feasible. The second application is the use of semiconductor strain gauges, and the special bridge/amplifier unit, for condition monitoring of automotive engine sub-units. It was again found that this application proved feasible, within the particular contexts explored.

Conclusions are finally drawn concerning the relative properties of semiconductor and other electrical strain gauges. Consideration is given to possible improvements to semiconductor strain gauges, and suggestions are made concerning future developments and further investigations arising as a result of this study.

OCTOBER, 1986

ACKNOWLEDGEMENTS

I am indebted to many people for their help, support, encouragement and advice.

In particular, I would like to thank Dr D A Gorham for his guidance, advice, interest and friendship. My thanks must also be given to Oliver Cox for his help and interest.

Grateful thanks are due to Mr G Bancroft, Vice President European Marketing, Kulite Semiconductors Limited, for information and help concerning semiconductor strain gauges and to Mr B L Welsh of the Royal Aircraft Establishment, Bedford.

Thanks are also due to Dr L G Earwaker of Birmingham Radiation Centre for the provision of facilities for irradiating semiconductor strain gauges.

Furthermore I must thank Mr J A Mackinnon of the National Engineering Laboratory and Mr J George of the Thermodynamics Laboratory at North Worcs. College for the provision of facilities for engine monitoring.

Finally I wish to thank Miss J Thomas for typing this thesis.

LIST OF CONTENTS

LIST OF FIGURES

LIST OF TABLES

CHAPTER 1

INTRODUCTION, THEORY AND BACKGROUND

Introduction, theory, properties and background

1.1 GENERAL INTRODUCTION

The piezoresistive effect was initially reported in 1856 by Lord Kelvin[1]. Piezoresistance is the change in the electrical resistance of a material due to the application of a stress. The effect was subsequently employed as a means of monitoring or measuring strain by devices generally known as electrical strain gauges. Strain may be simply expressed as $d\ell/\ell$, such that $d\ell$ is the change in the original length ℓ. It is a dimensionless quantity and is often conveniently expressed as microstrain or "μ" strain (where μ is 10^{-6}). This is measured in terms of the change in the electrical resistance of the electrical strain gauge when the material, on which the gauge is mounted, is stressed. The applied stress may be a simple tension, a shear stress, a hydrostatic pressure or a combination of these.

In the late 1920's and 1930's attempts were made to produce electrical strain gauges of higher gauge factors than metal foil or wire gauges. Basically, the gauge factor k is the ratio of the fractional change in

resistance with applied stress (with respect to the initial resistance) divided by the strain ε (see section 1.3). Amongst these early attempts were the use of carbon piles[2] and strips cut from carbon resistors[3]. These were found to display unsatisfactory zero shift and hysteresis characteristics, as well as a large variation of resistance with temperature change.

In 1954 the piezoresistive effect in the semiconductor materials silicon and germanium was reported by Smith[4]. Explanations of the effect were initially given by Herring[5], Eisner[6], Herring and Vogt[7] Morin et al.[8], Mason and Thurston[9] amongst others. Studies leading to these developments began in the preceding decade[10,11]. However, it was chiefly in America, during the late 1950's and early 1960's, that strain gauges manufactured from semiconductor materials were investigated and their applications explored (see, for example, Mason[12,13], Geyling and Forst[14], Vogt[15,16] and others[17]). These gauges were found to have significantly larger gauge factors than metal foil or wire gauges. Nevertheless, as will later be discussed, a number of shortcomings were observed[18,19] concerning the behaviour of semiconductor strain gauges.

During the 1970's there were still some papers published regarding the properties and applications of semiconductor strain gauges (for example, [20,21,22,23, 24,25]). In the current decade there has been little published work in this context (see Mallon et al.[26,27,28], Sze[29], Kanda[30], Yamada et al.[31], Baker [32], and Welsh et al.[33]), as observed by Hearn[34(a)], and also by Mackinnon[34(b)]. Some developments have been reported, with regard to the related area of piezoresistance in polycrystalline silicon, by Seto[35], Nishidon et al.[36], Germer and Tödt[37] and French and Evans[38]. However, this specialized area is outside the concern of this study. It is against the background outlined here that this investigation was undertaken.

1.2. AIMS AND OVERVIEW OF THE INVESTIGATION

It is intended that while the principles, behaviour and applications of semiconductor strain gauges will be considered in depth, a broad picture of these key aspects should also emerge. Consequently, following a discussion of appropriate background theory, an outline of the relevant properties of silicon and germanium is presented. Then semiconductor strain gauge manufacture and general properties are detailed and discussed. Next the theory of piezoresistance in semiconductors is considered in detail,

in order to provide a basis for the experimental investigations which follow.

The investigations reported involved both a qualitative and quantitive examination of the performance, properties and uses of typical semiconductor strain gauges. They include a study of the bonding of gauges, an exploration of the linearity of their response and factors influencing this, the thermal properties of gauges and also their photoelectric sensitivity. Means of compensating for various effects were analysed and explored so that practical recommendations could be made regarding particular measures. Strain gauge energizing circuits, bridge and compensating circuits were studied experimentally so that suggestions could be made concerning their improvement and employment. A special low drift, low noise integrated linear amplifier and bridge system, developed for use with semiconductor gauges, was constructed and its performance examined.

Potential applications which exploit the properties of semiconductor strain gauges, along with the integrated bridge/amplifier system used in conjunction with these gauges, were subsequently explored. One application involved a feasibility study of the use of semiconductor strain gauges for monitoring small static and dynamic strains in a nuclear radiation environment. The other

study explored the potential use of semiconductor strain gauges, for the "condition monitoring" of various internal combustion engine sub-units. Proposals concerning possible applications of semiconductor strain gauges are subsequently presented.

Conclusions, regarding the overall implications of the theoretical and empirical examination of semiconductor strain gauges, arising from this investigation are then drawn. Finally suggestions are made of aspects for development or further investigation, which have been identified as a consequence of this study.

1.3 BACKGROUND THEORY

The electrical resistance R, of a metallic conductor, is given by the relation:

$$R = \rho \ell / A \qquad 1.3.1$$

where ρ is a the resistivity, ℓ is the length and A is the cross-sectional area of the material. In the case of metallic conductors ρ is more or less constant for a given metal, so R changes mainly with changes in ℓ and A. However, in semiconductors changes in ρ have a dominant effect. In this case ρ is inversely proportional to the product of the number of charge carriers n_i and their average mobility μ_a. The resistivity is given by:

$$\rho = 1/(n_i \mu_a e) \qquad 1.3.2$$

e is the electronic charge.

Hence, the electrical resistance of a semiconductor is:

$$R = \rho \ell / A = \frac{1}{\sigma_c} \frac{\ell}{A} \qquad 1.3.3$$

$$= \ell/(n_i \mu_a e A) \qquad 1.3.4$$

σ_c is the conductivity.

As previously indicated, the piezoresistive effect is defined as the change in the electrical resistance of a material due to an applied stress.

Since, for a conductor, $R = \rho \ell / A$, then, when there is a strain induced dimensional change $d\ell$ in an original dimension ℓ, A changes by dA;

$$\text{where } dA/A = -2\nu \, (d\ell/\ell). \qquad 1.3.5$$

Here ν is Poisson's ratio which is the ratio of the magnitude of the transverse strain to longitudinal strain.

Therefore the new resistance R' is given by:

$$R' = \rho\ (\ell + d\ell)(A + dA)^{-1} \qquad 1.3.6$$

$$= (\rho/A)[\ell + d\ell][1 + dA/A]^{-1} \qquad 1.3.7$$

$$= (\rho/A)[\ell + d\ell][1 - (dA/A) + \ldots]$$

$$= (\rho/A)[\ell + d\ell][1 + 2\nu(d\ell/\ell) + \ldots]$$

$$\text{Hence } R' = (\rho/A)\ell + (\rho/A)[d\ell + 2\nu d\ell + \ldots] \qquad 1.3.8$$

Thus, for a conductor, the change in resistance dR, due to a strain induced dimensional change $d\ell$, is to a first order:

$$dR/R = (d\ell/\ell)(1 + 2\nu) \qquad 1.3.9$$

In this equation the "one" is the effect of the increase in length of the gauge. The term "2ν" is the effect of the lateral contraction of the cross-sectional area due to a longitudinal stress.

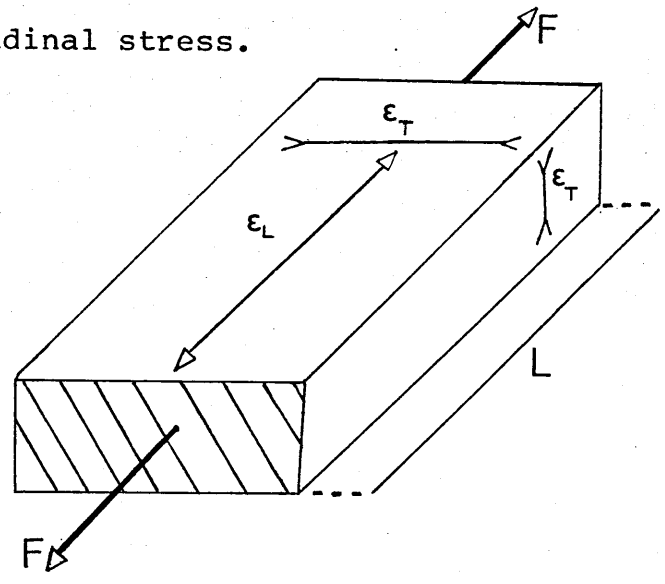

Bar subject to longitudinal strain

Figure 1. 3. 1.

As shown in figure 1.3.1, applying a tensile stress to a metal bar increases its length causing a longitudinal tensile strain ε_L and reduces the cross-sectional area giving rise to a transverse compressive strain ε_T .

For small strains the gauge factor k, of a piezoresistive strain gauge is given by:

$$k = (dR/R)/\varepsilon \qquad 1.3.10$$

Thus k is a measure of the sensitivity of the strain gauge to applied strain. For metallic conductors k generally has values in the range 2 to 4.5. From equation 1.3.9 the value associated with geometric changes is $1 + 2\nu$ (i.e. about 1.6). Thus, another effect is also involved, namely the effect of strain on resistivity.

The semiconductor materials germanium and silicon have the same crystal structure as diamond and each unit cell is symmetrical about its centre. Consequently, germanium and silicon are not piezoelectric substances and do not generate a voltage when strained. Nevertheless, they exhibit large piezoresistive coefficients in certain directions. The resistance change occurs under all conditions of static and dynamic strain. For silicon the fractional change of resistance for a given strain reaches values which are about one hundred times greater than are found for metals.

In intrinsic semiconductors the effect of an applied stress is such that both the number of charge carriers and their average mobility changes. (The sign and magnitude of the change depends on the type of semiconductor material, the carrier concentration and its crystallographic orientation with respect to the applied stress - as will later be outlined). When subjected to a simple tension or compression, with the current through the material along the stress axis, the relative change in resistivity is given by:

$$d\rho/\rho_o = \pi_L \sigma \qquad 1.3.11$$

(π_L is the longitudinal piezoresistive coefficient and σ is the stress). For different stress systems similar equations apply but with different values of π_L.

Thus, for semiconductors (and metals) the gauge factor k does not simply depend upon the change in electrical resistance due to an induced dimensional change $(1 + 2\nu)$ as given by equation 1.3.9 but also, and far more predominantly, on the change in resistivity with strain ($\pi_L E$). Hence, for semiconductors the gauge factor is given by:

$$k = (1 + 2\nu) + (\pi_L E) \qquad 1.3.12$$

E represents Young's modulus for the semiconductor material.

For a doped* or extrinsic semiconductor the number of charge carriers n_i is held at a fixed level by the density of the doping atoms, but the mobility μ_a can change when the semiconductor is strained. A simple view of what happens is as follows. (See, for example Herring[5] and Keyes[39].)

In k space, the constant energy surfaces corresponding to the conduction band minimum in silicon can be represented by 6 ellipsoids of revolution around the co-ordinate axes, as shown in figure 1.3.2.

(see figure overleaf)

* see section 1.4.

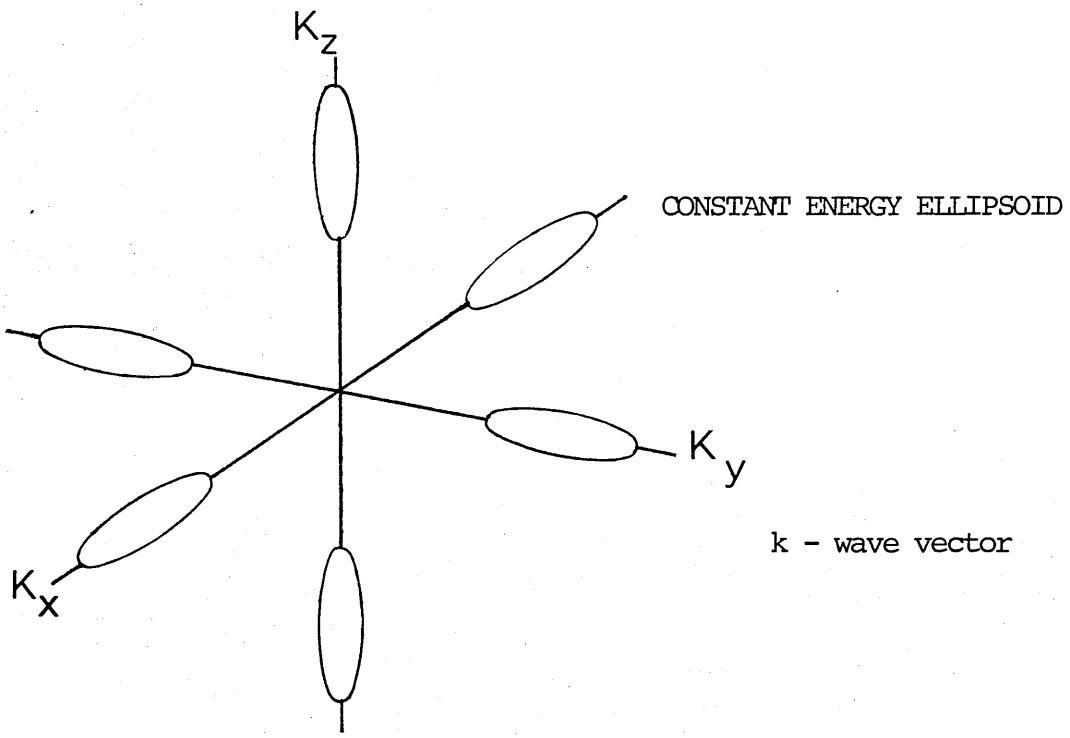

Constant energy ellipsoids for electrons in silicon

Figure 1.3.2

The motion of electrons on each of these surfaces is described by an anisotropic mass tensor. Since effective mass is related to energy band curvature, it can be seen from the figure that the effective mass of a carrier in one particular minimum is low along the co-ordinate axis and high perpendicular to it. Hence mobility is high along the axis and low perpendicular to it. When a field is applied along, say, the k_x axis, then electrons in the x minima will respond with high mobility, and electrons in the y and z minima will respond with a low mobility. Thus the average, measured mobility μ_{obs} will be an average of these:

$$\mu_{obs} = {}^{1}/_{3} (\mu_H + 2\,\mu_L) \qquad 1.3.13$$

where μ_L and μ_H are the low and high values respectively. When strain is applied, the energy levels shift, anisotropically, and so the relative populations of the x, y and z minima change. Hence, the relative number of carriers with high or low mobility changes and so the average mobility is different.

Figure 1.3.3 shows the effect for strain and resistance measured along 3 different directions in the crystal.

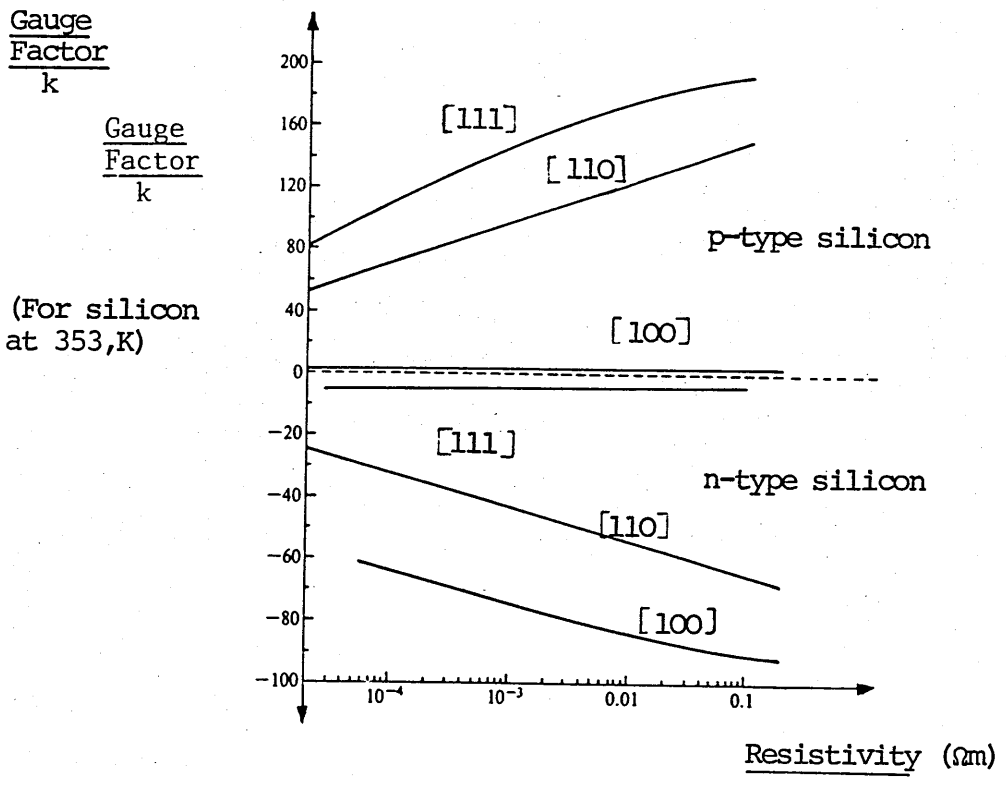

Resistivity and gauge factor measured along different crystal directions [40]

Figure 1.3.3

As illustrated by figure 1.3.3, for n-type silicon the strongest effect occurs in the [100] direction, when one pair of minima are fully affected and the other four (see figure 1.3.2) are not affected. If a strain is applied along the [111] direction there is very little change in resistance, as symmetry necessitates, while along the [110] direction strain has an intermediate effect. For p-type material the directions which exhibit low or high sensitivity are different from those for n-type material. This is because of the different symmetry of the valence band structure. For p-type silicon the gauge factor has positive values, while for n-type silicon the gauge factor has negative values.

Figures 1.3.4 and 1.3.5 show typical strain sensitivity curves for p-type silicon and n-type silicon, respectively. As can be seen from these graphs the slope is not constant, in other words the gauge factor k, for semiconductor materials, varies with the applied strain level. This is in marked contrast with the behaviour of metal foil or wire strain gauges (see typical response of metal foil gauge shown in figure 1.3.4).

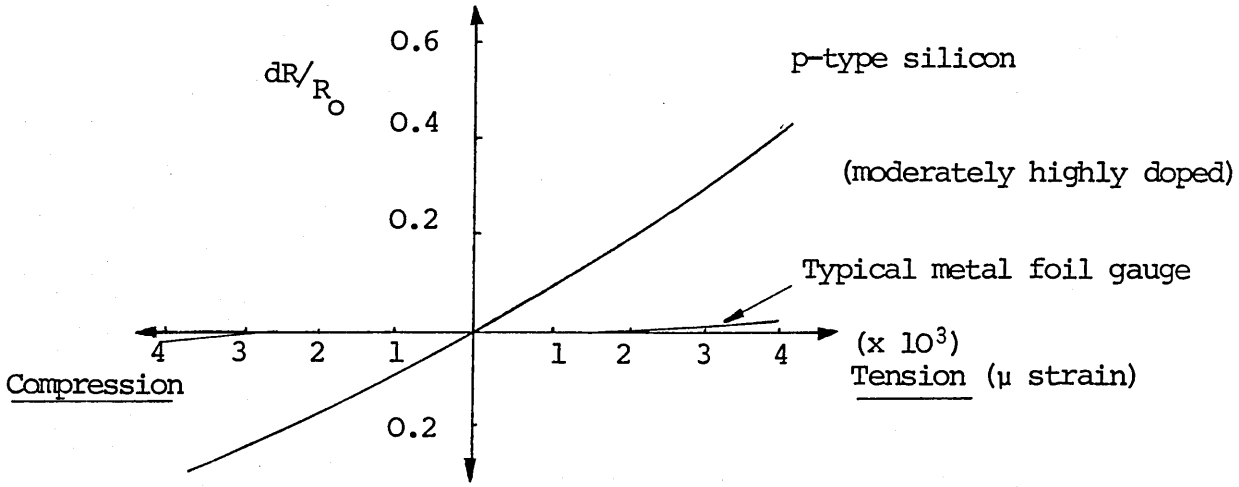

Strain sensitivity for p-type silicon semiconductor strain gauge

Figure 1. 3. 4.

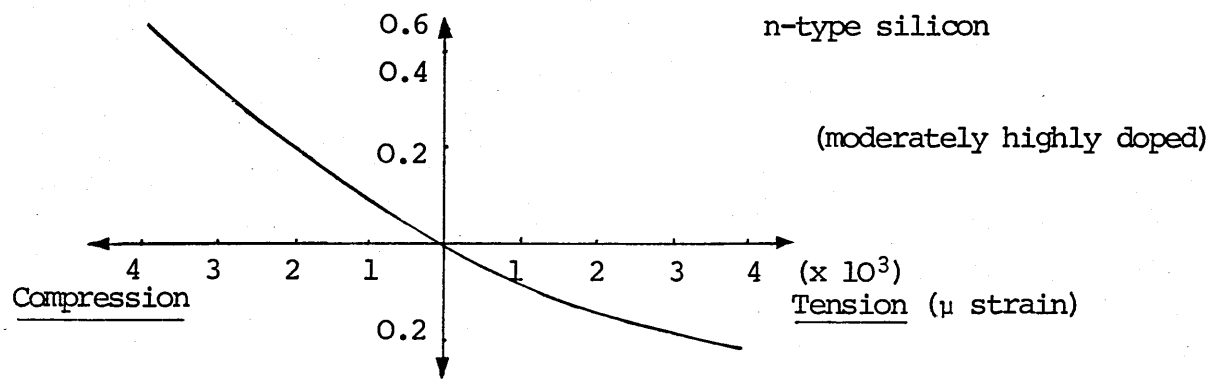

Strain sensitivity for n-type silicon semiconductor strain gauge.

Figure 1.3.5

Gauge factors for semiconductor strain gauges are large. For example, they may be in the range + 100 to + 175 for gauges manufactured from p-type silicon and from - 100 to - 140 for gauges made from n-type silicon. Strain gauges manufactured from germanium have a gauge factor around 50 and are less common than silicon strain gauges. The relevant properties of these materials are given in Table 1.

Material	Young's Modulus E (N/m^2)	Longit.piezo.coeff π_L (m^2/N)	Resistivity ρ (ohm m)
SILICON			
p-type	18.7×10^{10}	9.36×10^{-10}	11.7×10^{-2}
n-type	13.0×10^{10}	10.20×10^{-10}	7.8×10^{-2}
GERMANIUM			
p-type	15.5×10^{10}	6.58×10^{-10}	15.0×10^{-2}
n-type	15.5×10^{10}	10.10×10^{-10}	16.6×10^{-2}

Values are for lightly doped material (i.e. about 10^{-21} atoms m^{-3}) at low levels of strain.

Table 1

Properties of silicon and germanium at room temperature

N.B. The crystal orientations (Miller indices) for all the above values are [111] except for n-type silicon which is [100]. The values given for π_L are maximum values, for the conditions stated. In other words, the maximum strain sensitivity for p-type silicon and p-type and n-type germanium is in the [111] direction, but for n-type silicon maximum strain sensitivity is in the [100] direction (see figures 1.5.2 and 1.5.3).

Silicon not only has a high piezoresistive coefficient π_L but also an anisotropic modulus of elasticity with a maximum (see Table 1) which is almost equal to that of steel. In addition, it has a low density (2,300 kg m^{-3}) and, under favourable conditions, can be bent to a small radius of curvature (e.g. about 2mm radius for a gauge 0.01mm thick). Thus flexible strain gauges can be made using silicon.

The thermal conductivity of silicon is quite high (about 330 $Wm^{-1}K^{-1}$). It is relatively strong, with the breaking stress of thin filaments reaching about 2×10^9 N/m^2. Moreover, it exhibits negligible mechanical creep or hysteresis (up to almost 800K) and shows no plastic deformation prior to yield.

The fact that silicon may be formed into small flexural elements, and the aforementioned properties, makes it quite suitable for strain gauge use. However, it needs to be handled with a measure of care when used for certain strain measurements, if it has no backing layer to help reinforce and protect it.

1.4 SEMICONDUCTOR STRAIN GAUGE MANUFACTURE, ELECTRONIC AND GENERAL PROPERTIES.

To provide the necessary foundations and background, so that explanations may be presented concerning the subsequent investigations of the applied properties of semiconductor strain gauges, reference will be made to their manufacture, electronic and basic general properties. As pointed out earlier, it is silicon, rather than germanium (or other materials) which is currently chiefly employed for semiconductor strain gauges. Hence, reference will mainly be made to strain gauge manufacture using silicon. (Nevertheless, in general, the same basic manufacturing processes apply to gauges made from other semiconductors).

Single crystals of silicon of high purity are required for semiconductor strain gauges. The first operation in the fabrication process is the cutting of slices from the silicon boule perpendicular to the longitudinal axis of the crystal. This is the [111] axis for p-type silicon and generally the [100] axis for n-type silicon. To assist in locating the appropriate crystallographic axis a flat is usually cut on one side of the ingot. This may be cut quite easily using a diamond saw.

The process of the diffusion of dopants into the silicon is carried out because the number of charge carriers in pure or intrinsic silicon is relatively low and so the resistivity is high. To produce p-type semiconductor material impurity atoms of velency 3 (such as boron) are required. This leads to conduction by positive holes. However, to produce n-type semiconductor material impurity atoms of valency 5 (such as phosphorus) are required and conduction is by free electrons.

One technique employed for this purpose involves heating slices of silicon in a radio-frequency tube furnace to more than 1300K and passing on inert carrier gas, which contains a minute amount of the appropriate dopant, through the tube and allowing it to circulate around the silicon. Depending upon the length of time for which diffusion occurs, the rate of gas flow and the concentration of the impurity atoms in the gas, it is impossible to attain a specific impurity concentration in the silicon wafer. Gaseous diffusion is the most common technique, although there are a number of alternatives.

This wafer is subsequently lapped and polished to the required finished thickness (e.g. 0.01 mm thick). Following this, measurements are made of the resistivity so that the electrical characteristics of the semiconductor material are known and can be categorized appropriately. Photolithography is employed to produce, from the wafer,

the pattern of gauges and required geometric detail (this is done by conventional means using positive or negative photoresists. A process of wet and dry etching (including anisotropic etching and electrochemical etching) enables the manufacture of thinned flexural membranes and complex peripheral geometry gauges. Controlled thin structures are also obtained by the employment of conductivity selective etching.

Typical semiconductor strain gauge sizes and geometries are shown in figure 1.4.1. For special high quality gauges a layer of silicon dioxide is built up on the surface of the silicon wafer. There are gaps or "windows" left in the layer to enable the required electrical connections to be made. To ensure that these regions of the wafer are very heavily doped, so that they have low resistivity, a further diffusion process is carried out. This is done to minimise possible "diode effects" at the silicon and lead wire connection junction.

Connection pads are formed at the required positions on the gauges using masking and either electron beam evaporation, vacuum metalizing, d.c. or r.f. sputtering to deposit a thin film of metal on the gauge surface. Materials used for this include aluminium, platinum, gold, chrome-gold and copper.

ENLARGED GAUGE PROFILES

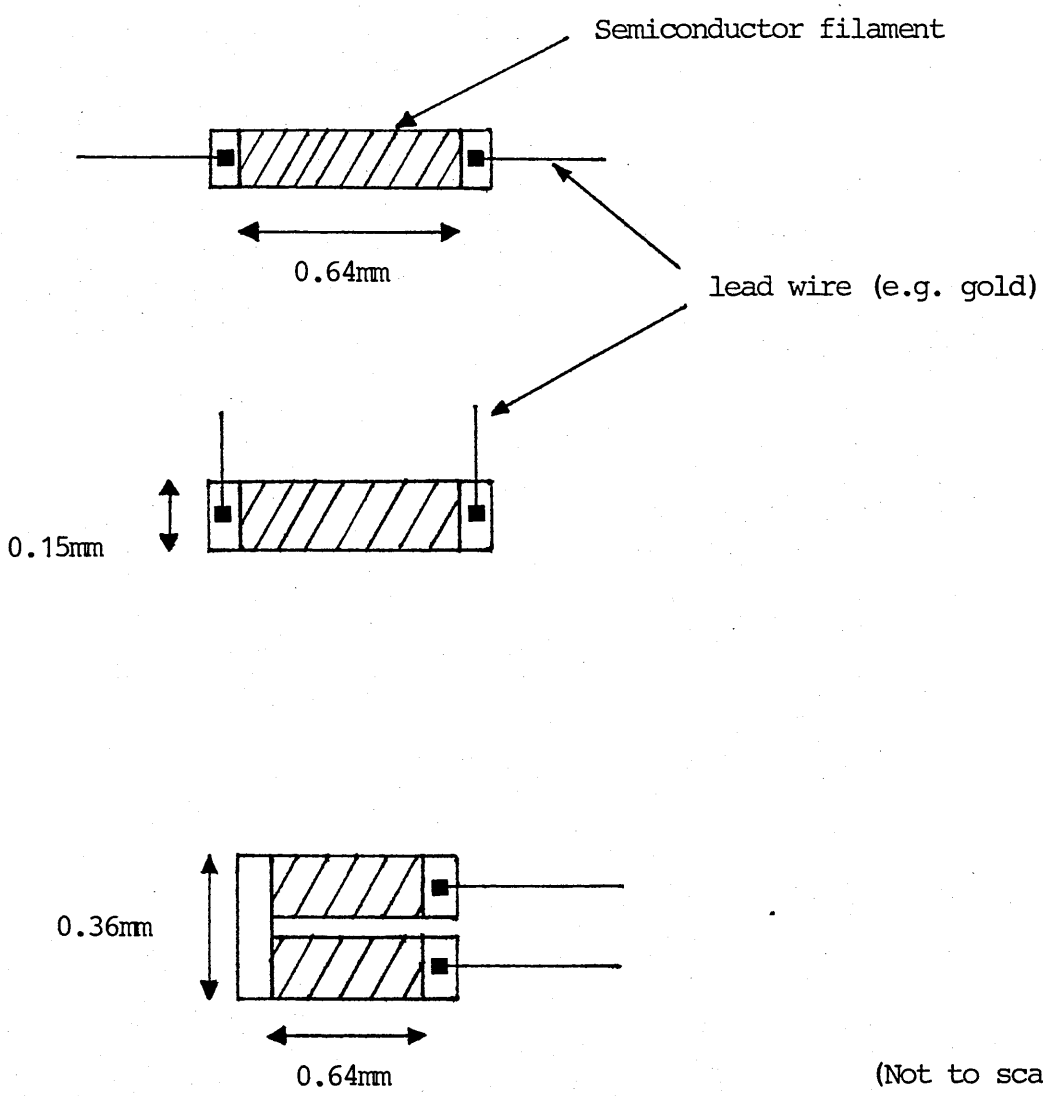

Examples of Semiconductor Strain Gauges

(backing not shown)

Figure 1.4.1

Separation of individual strain gauges from the wafer of semiconductor material involves a careful process of lapping and etching. Scribing, laser machining and ultrasonic machining may be employed. It is important that the presence of surface dislocations* is minimised because these act as stress weakness promoters and thus lower both the ultimate stress and fatigue life of the finished strain gauge. They can also affect the electrical properties of the gauge. Moreover, the thickness of the gauge is an important parameter and this needs to be typically of the order of 1×10^{-5} m, and uniform, if correct transmission of strain from the object specimen is to be achieved. More will be said in this context later, but is should be noted that Pearson et al.[41] confirmed that the ultimate strain of silicon crystals increases as the diameter is reduced, so a reduction in gauge cross section increases the ultimate strain.

The electrical connections to strain gauges are commonly made by thermo-compression bonding, ultrasonic bonding, resistance welding, soldering or brazing. Materials used for the connecting leads include 99.9 per cent pure gold, platinum or aluminium.

* Single crystals are readily available with dislocation densities of less than 1×10^{6} m^{-2}.

Semiconductor strain gauges which have no plastic or other backing material have the highest sensitivity to strain but are more prone to damage during mounting and use. For this reason semiconductor gauges which are sealed or encapsulated are also manufactured. The materials chiefly used for this are epoxy resins (e.g. cycloaliphatic type). Sealing techniques employed include glass fusion sealing, and centrifuging or vapour deposition is used to apply the sealing layer.

Gauges are often supplied in sets of 4 gauges which have been made from the same wafer of semiconductor. These are matched for resistance to a tolerance of about $\pm$ 2% at a particular ambient temperature. Due to variations in uniformity of diffused impurities, and other variations due to manufacturing methods, the resistance matching of gauges over a wide temperature range is difficult, and so computer-assisted matching using large batches, from the same wafer, is employed by some manufacturers. This enables sets of gauges to be provided which are resistance matched to $\pm$ 0.2% over a temperature range of 110K. Some sets of gauges are resistance matched to $\pm$ 1% of the nominal resistance at room temperature. To achieve this a large number of gauges, (perhaps 1000 or more) from the same wafer of semi conductor, are mounted into test rigs and put into a special oven capable of giving a range of constant temperatures. Then the resistance variations of each gauge, at three different temperatures, over a range

of 110K are recorded. Best fit groups of four gauges are then selected.

1.5 THEORY OF PIEZORESISTANCE IN SEMICONDUCTORS

Silicon and germanium have cubic crystal structures and belong to the group having the highest symmetry of the 5 classes comprising the cubic system. As will be shown, the piezoresistive effect (section 1.3) can be described mathematically by 3 basic equations, each relating the electric field components, E, current density j, and stress components σ .

For a completely anisotropic semiconductor, E is a function of the 3-dimensional distributions of j and σ as follows:

$$\underset{\sim}{E} = E\,(j_1,\ j_2,\ j_3,\ \sigma_{11},\ \sigma_{22},\ \sigma_{33},\ \sigma_{12},\ \sigma_{23},\sigma_{33}) \qquad 1.5.1$$

Where 1, 2 and 3 are the crystallographic axes of the semiconductor (see figure 1.5.1). The subscripts of stress (σ) which are equal indicate normal stress, and those which are different indicate shear stress.

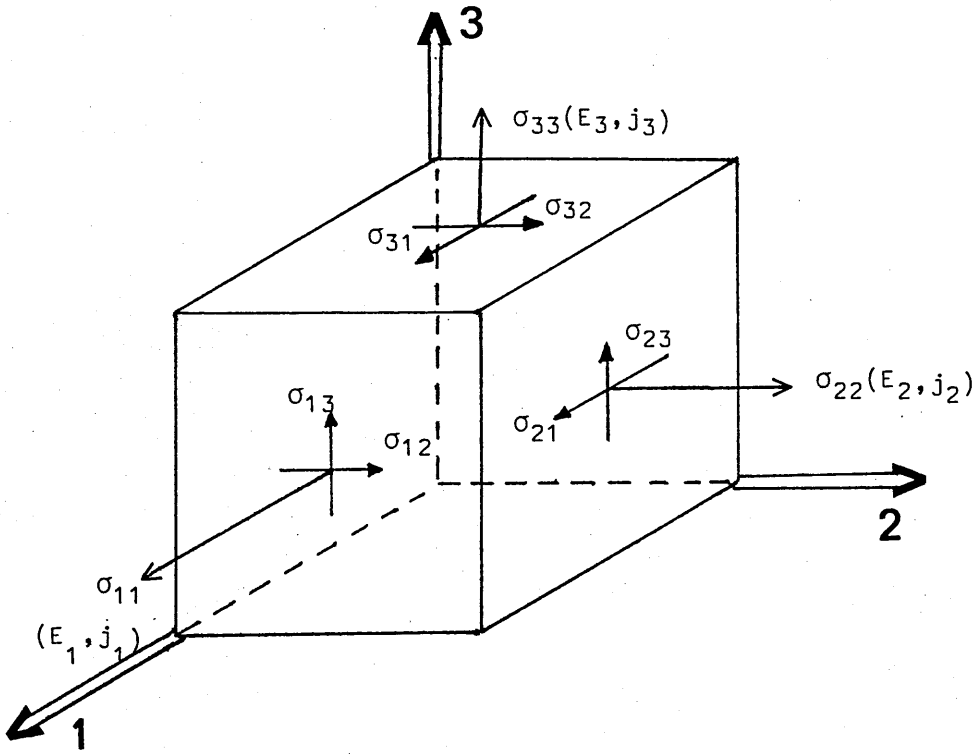

Element of Semiconductor Crystal

Figure 1.5.1.

Although the general expression for electric field strength E represents a complex tensor relationship, it has been shown by Mason and Thurston[9] that, for a material having the symmetry of silicon and germanium, the electric field strength components are represented by:

$$E_1/\rho = j_1[1 + \pi_{11}\sigma_{11} + \pi_{12}(\sigma_{22} + \sigma_{33})] + j_2\pi_{44}\sigma_{12} + j_3\pi_{44}\sigma_{13}$$

1.5.2

$$E_2/\rho = j_2[1 + \pi_{11}\sigma_{22} + \pi_{12}(\sigma_{11} + \sigma_{33})] + j_1\pi_{44}\sigma_{12} + j_3\pi_{44}\sigma_{23}$$

1.5.3

$$E_3/\rho = j_3[1 + \pi_{11}\sigma_{33} + \pi_{12}(\sigma_{11} + \sigma_{22})] + j_1\pi_{44}\sigma_{13} + j_2\pi_{44}\sigma_{23}$$

1.5.4

Here ρ is the (isotropic) resistivity at zero stress and π_{11}, π_{12} and π_{44} are the piezoresistive coefficients on the principal axes. (The latter can be displayed as a 6 x 6 matrix, as Mason and Thurston[9] have described). These coefficients vary both with the type of material and with temperature. The subscripts of these coefficients can be more readily comprehended when considered in terms of the following five practical cases of stress patterns and current density:

(i) current and uniaxial stress along the same crystal axis:

$$E/\rho = j\ (1 + \pi_{11}\sigma) \qquad 1.5.5$$

(ii) Current and uniaxial stress along <u>two</u> orthogonal crystal axes:

$$E/\rho = j(1 + \pi_{12}\sigma) \qquad 1.5.6$$

(iii) Current along one crystal axis and pure uniaxial stress operating in a plane <u>normal</u> to this axis:

$$E/\rho = j \qquad 1.5.7$$

(Thus there is no effect on resistance)

(iv) at a (hydrostatic) pressure p then:

$$E/\rho = j[1 + p\ (\pi_{11} + 2\pi_{12})] \qquad 1.5.8$$

(v) With shear stress τ, operating in a plane defined by two of the crystal axes, and current flowing along one of these, the effect along the other axis is:

$$E/\rho = j\ (\pi_{44}\tau) \qquad 1.5.9$$

In practice both the stress and the current are along the length of the semiconductor strain gauge (even though this direction may not actually be a crystal axis). Then the "effective" longitudinal piezoresistive coefficient π_L may be found in terms of the direction cosines ℓ_1, m_1, n_1 of π_L with respect to the crystal axes since:

$$\pi_L = \pi_{11} + 2\,[\pi_{12} - \pi_{11} + \pi_{44}][\ell_1^2 m_1^2 + m_1^2 n_1^2 + n_1^2 \ell_1^2] \qquad 1.5.10$$

Now, $\ell_1^2 m_1^2 + m_1^2 n_1^2 + n_1^2 \ell_1^2$ is a maximum when $\ell_1 = m_1 = n_1 = 1/\sqrt{3}$, consequently, when $\pi_{12} - \pi_{11} + \pi_{44}$ 0 the maximum piezoresistive effect will occur along a crystal direction designated [111]. However, when $\pi_{12} - \pi_{11} + \pi_{44} < 0$ the maximum piezoresistive effect will be along a crystal axis such as [100]. Figures 1.5.2 and 1.5.3 show the two cubic crystal directions [111] and [100] respectively.

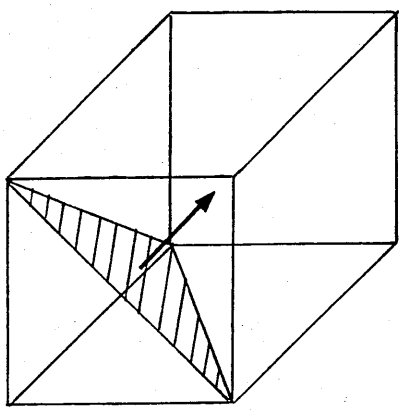

Cubic Crystal [1,1,1] direction.

Figure 1.5.2

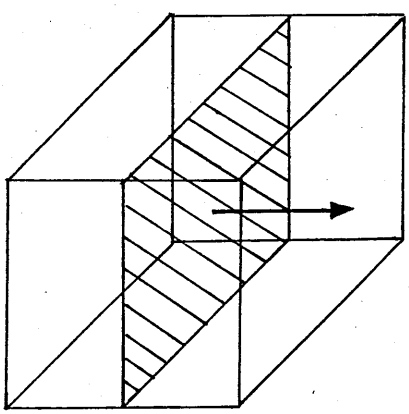

Cubic Crystal [1,0,0] direction.

Figure 1.5.3

Both the magnitude and temperature dependance of the piezoresistive coefficients of semiconductors are a function of the impurity concentration. A number of investigators, such as Kerr and Milnes[42], have explored these factors. It has been found that relatively low impurity concentrations produce a high gauge factor k. However, this also results in a high temperature coefficient of sensitivity T_s, as can be seen from figure 1.5.4. [r is the temperature coefficient of resistance. T_s is the sensitivity (i.e. change in output voltage with applied strain) expressed in percent per kelvin].

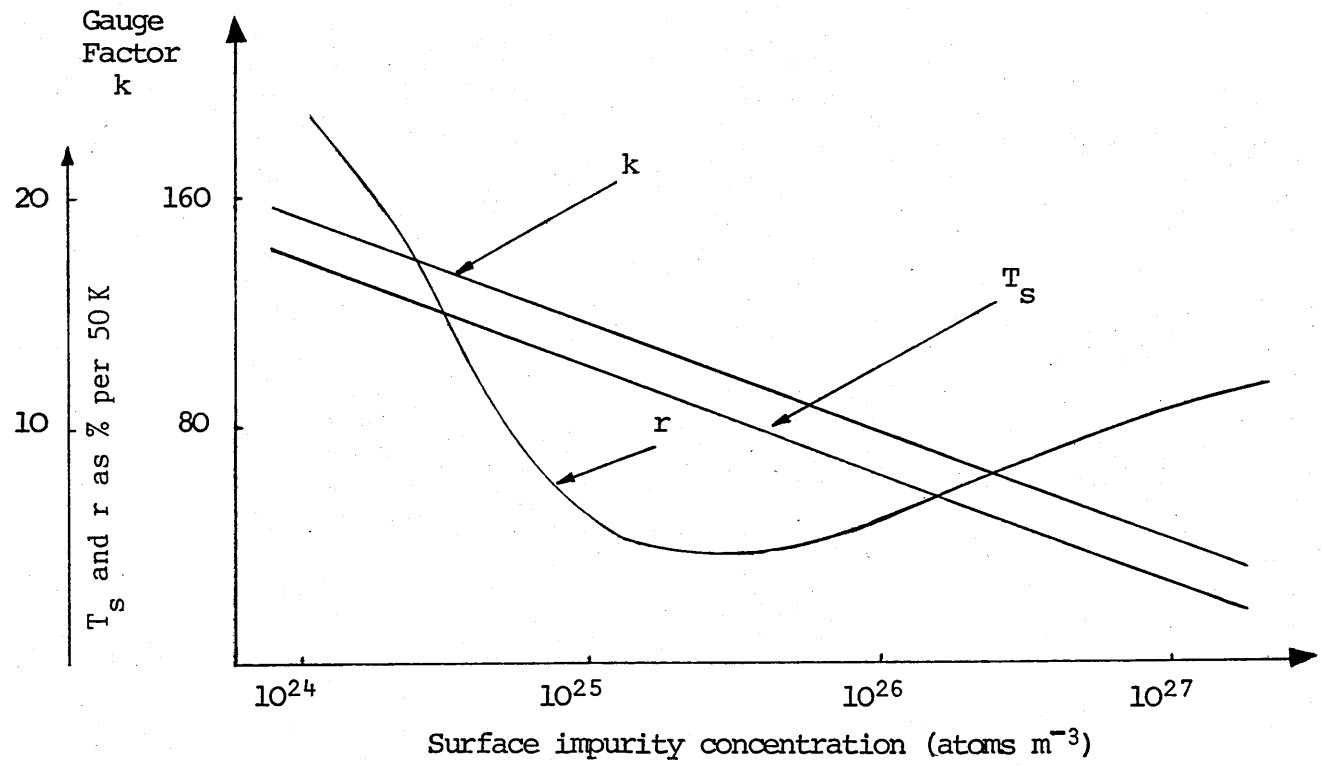

The piezoresistive properties of diffused layers on silicon

Figure 1.5.4.

A temperature coefficient of resistance r, which is large enough to enable the passive compensation of the temperature coefficient of sensitivity T_s (e.g. by constant current energization), is desirable. As shown in figure 1.5.4. this may be achieved by the use of either high or low dopant levels.

It must be noted, however, that if low dopant levels are used a higher gauge factor is attained, but at the expense of a high temperature coefficient of sensitivity (particularly the linearity of the compensated temperature coefficient of sensitivity is adversely affected) over an extended temperature range.

Mallon et al[43] report that, if relatively degenerate dopant levels are employed, it is then possible to use what they term "integrated sensors", which are integrated circuits containing piezoresistive sensing elements, at low (cryogenic) temperatures. (e.g. semiconductor strain gauges with dopant levels greater than 2×10^{25} atoms m^{-3} have been found to be suitable for use in cryrogenic applications).

For a given surface impurity concentration it has been found that strain gauges made from n-type silicon have a higher temperature coefficient of sensitivity than gauges made from p-type silicon. Consequently, piezoresistive elements of n-type silicon are generally not used, apart

from monolithic gauges (single strip gauges such as are used for compensation with p-type gauges). Nevertheless, because π_{11} is the dominant piezoresistive coefficient the employment of n-type silicon gauges provides added flexibility in strain gauge response in various stress fields. Tufte and Stelzer[44,45] found that, for n-type silicon at high surface impurity concentrations (10^{26} atoms m^{-3}) π_{44} was quite high. This could provide increased flexibility in the exploitation of the longitudinal , the transverse and the shear coefficients for the control of strain gauge response, in a range of stress fields.

It has been found from experimental observations of silicon and germanium[9] that, for different directions, the piezoresistive coefficients may be positive or negative or zero. As indicated in section 1.3, this means that, by judicious control of crystallography a gauge may be made to respond in a desired and controlled manner to positive, negative and shear stresses (either transverse or longitudinal). In p-type silicon the piezoresistive coefficient on the "44" principal axis[1] dominates and the longitudinal piezoresistive coefficient π_L may be made to be either positive or zero for various directions. Similarly, in respect of the transverse piezoresistive coefficient π_{44} dominates for p-type silicon and, in this case, the coefficient may be made to be either negative or zero for various directions.

1. ie. π_{44}

Different orientations have been found to be suitable for particular strain gauge applications. For example, using p-type silicon, the configuration which follows has been reported by Kurtz and Gravel[46] as being particularly suitable for strain gauges when there is a high transverse stress condition, such as in the centre of a diaphragm. This is where $\langle 110 \rangle$ is parallel to the gauge axis, $\langle 100 \rangle$ is perpendicular to the gauge axis and $\langle 110 \rangle$ is perpendicular to the plane of the gauge. (Under these conditions there is a maximum longitudinal piezoresistive coefficient under the constraint of an almost zero transverse piezoresistive coefficient).

1.6 COMPARISON OF SEMICONDUCTOR AND METAL FOIL OR WIRE GAUGES

The gauge factor k is much greater for semiconductor strain gauges than for metal foil or wire gauges. This means that very small magnitude strains may be measured or relatively large outputs from strain gauge circuits may be obtained (to drive relays, for instance) if semiconductor strain gauges are employed. However, as shown in figure 1.6.1, the change in the resistance of a semiconductor strain gauge with temperature is much greater than that of a wire or metal foil gauge, and small variations in temperature can thus produce marked changes in recorded strain values.

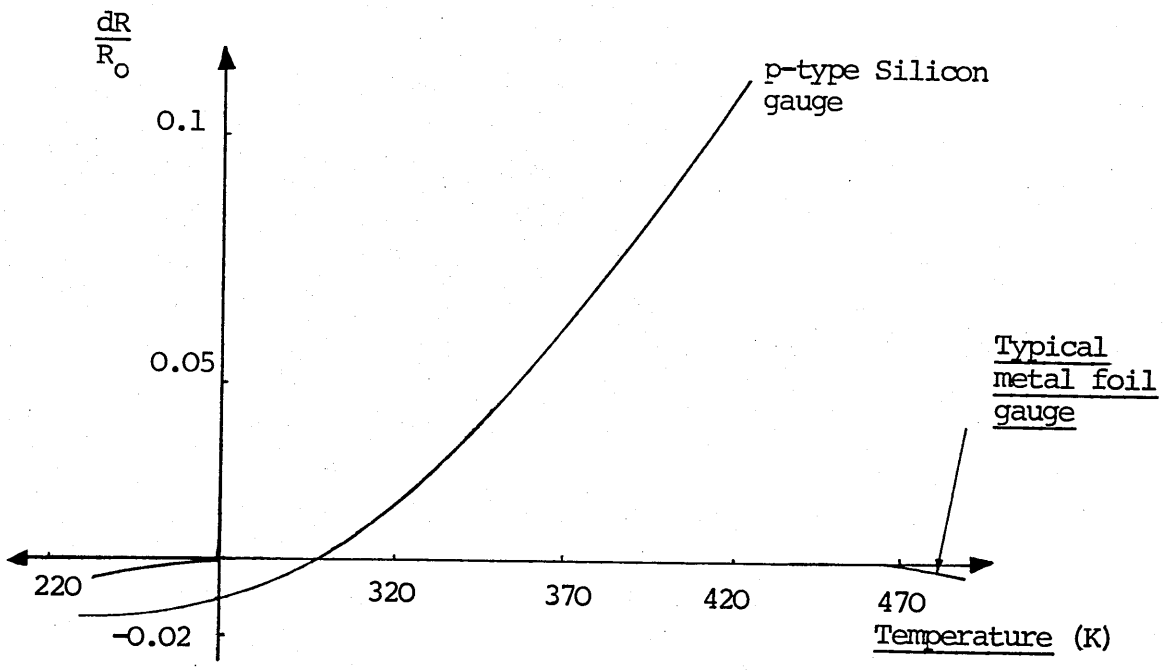

Temperature Sensitivity for Typical Semiconductor and metal foil strain gauges

Figure 1.6.1

Semiconductor strain gauges have very low hysteresis, which is only limited by the technique used for bonding. They also have a high fatigue life. For strain gauges currently manufactured this generally exceeds 10^8 fully reversed cycles at $\pm$ 1000 μ strain. The range of resistance values for semiconductor strain gauges is quite wide. Some gauges have unstrained resistances of 10 ohms at room temperature while others are available which have unstrained resistances of 10 kilohms or more at room

temperature. Furthermore, the elastic strain range for semiconductor strain gauges is usually up to more than 5000μ strain.

Not only does the gauge factor of semiconductor strain gauges markedly vary with temperature but also with the level of applied strain. This non-linearity of semiconductor strain gauges, compared to metal foil or wire gauges, is a performance imperfection which can, however, be compensated for, as will be shown (section 2.6). It will also be shown that compensation for temperature effects on semiconductor strain gauge performance can be provided. In addition, the photosensitivity of semiconductor strain gauges will be described. Finally, a comparison of semi-conductor and other types of electrical strain gauges will be provided (section 7.2).

1.7 SUMMARY

Piezoresistance is the change in the electrical resistance of a material due to an applied stress and the effect can be used to measure strain. The effect in semiconductors, which was reported by Smith[4] in 1954, is much greater than in metal foil or wire strain gauges. Much of the research and development concerning semiconductors strain gauges took place in America during the 1960's and recent literature in this context is sparse.

The principal aim of this investigation is a broad study of the theory and principles of piezoresistance in semiconductors and of the manufacture and properties of semiconductor strain gauges. Subjects to be covered include:-

(a) bonding of semiconductor strain gauges

(b) non-linearity of gauge resistance/strain response and compensation of this effect.

(c) semiconductor strain gauge energization, bridge circuits, compensating circuits and bridge output amplification

(d) semiconductor strain gauge thermal characteristics and their compensation

(e) static and dynamic photoelectric sensitivity of semiconductor strain gauges

(f) exploration of potential applications to exploit the properties of semiconductor strain gauges, including the development of an integrated bridge/amplifier system and a study of the behaviour of semiconductor strain gauges when subjected to a neutron flux.

Not only is the gauge factor k much larger than that of metal foil gauges (e.g. 100 times greater) but also either positive or negative - depending on the type of dopant employed. Considerable improvements in the manufacture of semiconductor strain gauges have resulted from the adoption of techniques employed in the manufacture of integrated circuits. Semiconductor strain gauges manufactured today are more closely matched, in terms of their resistance versus temperature charateristics, than those used in the 1960's.

The piezoresistive effect in semiconductors can be described mathematically by three basic equations relating the electric field components, current density and stress components. The maximum piezoresistive effect occurs along a crystal direction designated [100] for n-type silicon and [111] in the case of p-type silicon and both n and p-type germanium. An increase in dopant level gives rise to:-

(i) reduction in gauge factor

(ii) increase in the linearity of response to strain

(iii) reduction in temperature coefficient of resistance

(iv) increase in operating temperature range (increased doping lowers the minimum operating temperature)

A brief comparison of semiconductor and metal foil or wire strain gauges reveals that the former have very low hysteresis and a high fatigue life. Although they have a much larger gauge factor this varies significantly not only with temperature but also with the level of applied strain. In addition, they are reported as being photosensitive.

CHAPTER 2

SEMICONDUCTOR STRAIN GAUGE BONDING. GAUGE LINEARITY.

2.1 INTRODUCTION

The bonding of strain gauges can influence both their performance and reliability. Consequently, initial studies were undertaken concerning adhesives, bonding techniques, testing of bonds and the influence of the type of surface and environment on the behaviour of bonded semiconductor strain gauges. Suggestions, based upon the findings of these various studies, regarding measures to improve or test bonds are then presented.

Semiconductor strain gauges are somewhat non-linear with respect to their change of resistance with change in applied strain. A basic examination was thus also undertaken, after exploring the theoretical basis and problems associated with gauge non-linearity, of means of reducing non-linearity. This included an appraisal of the influence of dopant levels on gauge linearity and other factors concerning the compensation for non-linearity by electronic means.

2.2 SEMICONDUCTOR STRAIN GAUGE BONDING

In certain respects, as Stein[47] observes, the bonding techniques employed with semiconductor strain gauges are similar to those employed with metal foil or wire gauges and there is a range of adhesives manufactured for use at different temperatures.

Like metal foil or wire strain gauges semiconductor strain gauges are available either with or without a backing material. The backing material:

(a) provides for better handling of the gauge

(b) gives electrical insulation between the gauge and the test surface.

(c) presents a convenient surface for bonding to the object under test.

It must faithfully transmit the strain from the test surface via the adhesive to the strain gauge element.

Various properties are required of the backing material in view of these functions. These include good stability with minimum creep, high shear modulus to ensure complete transmission of strain, strength and flexibility, high insluation resistance and good bonding characteristics so that the adhesive adheres well with it. There are three basic types of backing material, each of these has its own properties and, thus, particular applications.

(i) Epoxy backing:

Gives good freedom from problems due to creep, provides high rigidity but is somewhat brittle.

(ii) Glass fibre reinforced epoxy-phenolic backing:

Similar properties to epoxy backing but it can be used over a wider range of temperatures.

(iii) Polyimide backing:

It is very flexible and tough yet suitable for a wide range of temperatures. This backing is widely used and can be employed for high levels of strain.

As indicated in section 1.4 semiconductor strain gauges are also manufactured in an encapsulated form. (It was noted that manufacturers do not recommend the use of solvent thinned cements with these gauges as the impervious substrate does not allow the escape of solvent gases during

cure). Thus, a brief study was also made of bonding using these, in addition to backed and unbacked gauges. Since unbacked gauges are not insulated it is necessary to apply a pre-coat of adhesive to substrates which are electrically conducting. More care is also needed in handling and in bonding unbacked gauges due to their brittleness.

Gauge manufacturers frequently quote values for properties such as thermal coefficients for unbonded gauges, and the bonding and base material can significantly modify such values. The behaviour and performance of semiconductor strain gauges is also influenced by the properties of the adhesive. In addition, as Mordan[48] emphasizes, gauge performance is critically dependent on the quality of the installation.

2.3 INVESTIGATION OF THE BONDING OF SEMICONDUCTOR GAUGES

An investigation of the bonding of typical, unbacked and encapsulated strain gauges was undertaken using various adhesives and three different types of substrates. Simple, oblong shaped gauges, of typical size 1 mm by 0.2 mm, were used as well as small pieces of foil which were used in place of gauges (thus saving the cost of employing many gauges for the investigations). Liquid synthetic adhesives were used and these were chiefly thermoplastic (e.g. polyacrylates) or thermosetting (e.g. epoxides and polyesters). A total of 10 adhesives were examined

comprising 3 polyesters, 2 polyacrylates, 4 expoxides and an inorganic adhesive. The three substrates employed were melamine strip, aluminium strip and stainless steel strip. The latter two were normal bright finish and all substrates were initially degreased using acetone.

The adhesives were applied using a small spatula and thin coates of adhesive (<0.1 mm) were employed. A number of the polyester and epoxy-resin adhesives used were two-component cements. These were mixed with careful control of both the composition and the homogeneity of the mixture. It was generally found that, in addition to the constancy of ambient temperature, these factors influenced both the required curing time and the quality of the bond. Where recommended, the amount of the catalyst was decreased by a few percent for ambient temperatures above 293K.

For gauges with no backing it was found that a total of 3 thin coats of adhesive gave the most reliable bond (i.e. a strong bond, free from air bubbles). This involved using a pre-coat, to provide electrical insulation on the steel and aluminium substrates, and applying a second coat after allowing the first coat to cure and checking that it was clean. Before the second coat was dry the gauges were placed in position and gentle but firm pressure applied using a thin rubber strip to provide uniform distribution. When the second coat of adhesive was dry a further coat was applied to provide protection. This covered the gauge up to the connecting leads, which were kept clear of the

substrate surface. Of the three coats applied the third coat was very slightly thicker.

In the case of the backed and encapsulated gauges and the foil test strips only two coats of adhesive were employed. (For some other tests of bond strength only 1 coat was used). These coats were all somewhat less than 0.1 mm thick and, as for the unbacked gauges, tweezers were used to position the gauges and the foil strips. Where appropriate, and in order to minimise possible prestrains (see section 2.4) bonds were cured at room temperature for the specified time. If no specified time was given by the manufacturer a period of 24 hours was allowed for curing, prior to tests being undertaken. Electrical connections to the strain gauge leads were made using low temperature solder and a variable temperature, thermostatic soldering iron. Observation of this process was facilitated by the use of an illuminated magnifier (x5).

After allowing an ageing period of 100 hours, examinations and tests were undertaken concerning the quality of the bonding for the different adhesives, surfaces and strain gauges (including the foil strips used as dummy gauges). Visual inspections of glue lines were carried out with the aid of a microscope and spot checks of adhesive thickness were undertaken using a dial gauge (reading to 0.01 mm). This provided information about the presence of air bubbles or flaws in the bond and the uniformity of the bond thickness.

A further test involved cutting through one end of the bond and then gradually peeling the strain gauge off the substrate. The ease of peeling and the surface appearance of the peeled area (i.e. the amount of residue on the substrate and the uniformity of adhesion) provided qualitative information concerning the condition of the bond. There were no facilities available to carry out a maximum elongation test, which would also reveal regions of weak or incomplete adhesion. However, in an attempt to estimate the distortion or dimensional change under sustained loading (creep), unbacked gauges were bonded to the same steel strip, with each of the different adhesives and a load applied which gave a tensile strain to the strip. Resistance readings were taken with a digital meter ($\pm$ 0.01 ohms) half hourly for 6 hours then hourly for 4 hours. The temperature was maintained at 293 ($\pm$1)K throughout. As will be outlined, none of the thermosetting adhesives displayed any detectable creep.

To obtain further information about the quality of bonding for the 3 different substrates and 10 adhesives, backed gauges each had their resistance measured with and without a rubber rod being gently pressed on their active surface. This short and slightly pointed rod was chosen because of its high elasticity and low thermal conductivity. In the cases where there was a differance between the two readings the gauge was cut and carefully peeled from the substrate then the bond was examined with

the aid of a microscope. It was generally found that there were either small air bubbles present or discontinuities in the bond between gauge and substrate. Thus, this simple test could help to identify possible flaws in bonds without the need to disturb the bond.

Finally, using both foil dummy gauges and unbacked gauges, a test was carried out on the resistance of the insulation (adhesive) for both steel and aluminium substrates. This was undertaken by connecting one side of a digital ohmmeter to one of the gauge connections (or the top of one side of the foil dummy gauge) and the other to the metal substrate. It was found that, for a properly bonded gauge, the resistance was generally in excess of 100MΩ at room temperature.

2.4 RESULTS, COMMENTS AND SUGGESTIONS CONCERNING BONDING

As Shields[49] points out, the peel strength of adhesives increases with adherend thickness and adhesive thickness, but decreases with increase in the modulus of elasticity of the adhesive. Brittle adhesives with high tensile strengths have low peel strengths. For gauges of the same surface area, bonded with the same glue line thickness, it was generally found, for the adhesives examined, that steel adherend gave a higher peel strength

than either aluminium or melamine (the latter generally being the lowest).

Of the adhesives tested it was found that the epoxy-resin and polyester adhesives (thermosetting) all gave acceptable bonding performance, as did the polyacrylate adhesives (thermoplastic). However the latter, which were cyanoacrylates, were hygroscopic and displayed a very small degree of creep at room temperature. The inorganic adhesive was generally found to give acceptable bonding performance but was far less convenient in use and somewhat viscous. Nevertheless, it was used for a particular application in a subsequent investigation because its thermal expansivity closely matched that of a particular (metal) substrate.

The epoxy-resin adhesives generally had recommended curing temperatures above room temperature and, as Parkins[50] has shown, this can result in induced prestrains on the bonded gauges when they return to room temperature. Moreover, Wake[51] reports that strong sunlight has a deteriorating effect on many polymers, including epoxides. Thus, polyester adhesives are suggested as being generally more suitable for bonding semiconductor strain gauges. One of these, with the trade designation "P2", gave one of the thinnest glue lines and the fewest air bubbles. It was thus adopted for use in the subsequent investigations of the performance, properties and uses of semiconductor strain gauges. It was

interesting that this adhesive is claimed by the manufacturer to have high moisture resistance and a relatively high operating temperature. However, as Pople[52] has pointed out, with regard to polyester adhesives used for strain gauges, there may be a need for thermal ageing (i.e. a post-cure period at a temperature elevated above the operating temperature) to avoid zero shift problems when the gauge is subsequently employed.

The advantages of backed or encapsulated semiconductor strain gauges, in terms of easier handling and bonding, must be set against the higher strain sensitivity of unbacked gauges. In respect of the actual bonding itself no significant difference was found between any of the gauges employed, although the unbacked gauges had a somewhat smaller area of contact than corresponding backed or encapsulated gauges.

2.5 FURTHER OBSERVATIONS CONCERNING BONDING

The effects of strain due to differences in the coefficients of thermal expansivity of the semiconductor strain gauge and material under investigation, must be carefully considered as must the type of adhesive used. Figure 2.5.1 illustrates, the situation when a strain gauge is bonded at an initial pre-compression ε which, after bonding is complete, changes to ε_c (due to the differences in the coefficients of thermal expansivity).

Bonded semiconductor
strain gauge

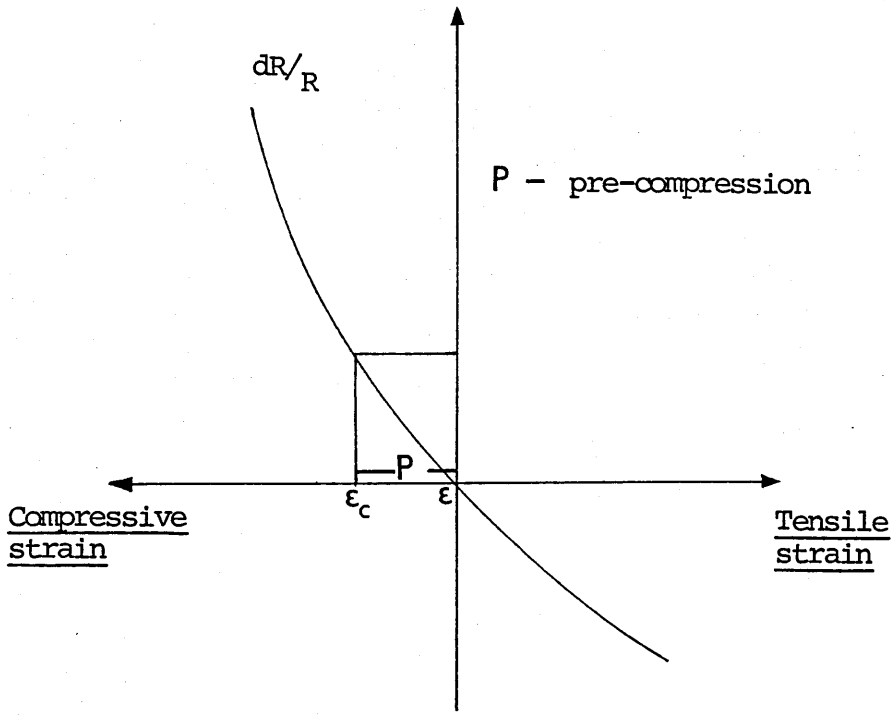

Pre-compression Effect on Strain Gauge.

Figure 2.5.1

Solder glass bonding, using comparatively low melting point powdered glass mixed with a solvent suspension medium, can be employed to bond semicondutor strain gauges to metals. The glass frit is heated progressively above the softening temperature of the glass which then flows and finally, at a higher temperature, the glass devitrifies. As a result, the strain gauge, which is

placed on top of the glass frit, is bonded to the metal surface under investigation. Initial heating evaporates the solvent suspension medium and, during curing, the glass crystallises. However, since the bonding occurs at an elevated temperature (over 670 K, in general) then the gauge is subjected to a compressive prestrain when cooled, because most metals have a coefficient of thermal expansivity somewhat greater than silicon. In the case of some metals the resulting compressive prestrain on the gauge may approach 4000 μ strain. In addition, the elevated temperature required means that some methods of attaching connecting leads to the gauge cannot be employed. Nevertheless, the technique provides bonding with good repeatability, and the gauge hysteresis is almost zero. When used for metals with low coefficients of thermal expansivity, particularly certain alloys, the compressive prestrain is also of a lower magnitude.

Bonding of semiconductor strain gauges using an electrostatic technique has been successfully employed in recent years. This uses a very thin wafer of inorganic glass, which is highly polished, sandwiched between the gauge and the metal surface under test. A high electric field which produces immense forces of attraction is applied across the assembly at the same time heating is also applied. The result is a very thin, high quality bond which is achieved at a somewhat lower temperature than would otherwise be possible. Moreover, the units have almost perfect mechanical and thermal repeatability, very

high long-term stability and zero hysteresis. However, the process requires very precise control, special components, strain gauges with optically flat backs, and very high surface cleanliness of gauge, wafer and test surface. Thus it is expensive and is currently only used for special applications, such as those in the aerospace testing industry.

2.6 SEMICONDUCTOR STRAIN GAUGE LINEARITY

Unlike metal foil or wire strain gauges, the strain sensitivity of semiconductor strain gauges varies significantly with the magnitude of the applied strain, that is, the resistance change versus applied strain characteristic can be noticeably non-linear, as indicated earlier (figure 1.3.4).

In the case of a semiconductor strain gauge subjected to a strain ε, at a constant temperature, the change is resistance dR compared to the unstrained resistance R, may be expressed generally as a polynomial of the form:

$$dR/R = C_1\varepsilon + C_2\varepsilon^2 + C_3\varepsilon^3 + \ldots\ldots \qquad 2.6.1$$

However, at practical levels of strain the ε^3 term, and higher orders of strain, make negligible contributions and can be ignored.

Thus equation 2.6.1 may be approximated to:

$$dR/R = C_1\varepsilon + C_2\varepsilon^2 \qquad 2.6.2$$

The terms C_1 , C_2 and C_3 are constants for a particular semiconductor. For n-type silicon, which has a maximum sensitivity along the [100] direction, at room temperature typical values (for lightly doped material) are $C_1 = -125$ and $C_2 = 26{,}000$. For n-type germanium, which has maximum sensitivity along the [111] direction, typical values (for lightly doped material) are $C_1 = -149$ and $C_2 = 52{,}600$ at room temperature.

The value of C_1 for p-type silicon is positve for lightly doped material and typical values are $C_1 = 175$ and $C_2 = 72{,}625$. At high levels of doping (e.g. such that the resistivity is about 2×10^{-4} Ωm) typical values are $C_1 = 119$ and $C_2 = 4{,}000$. Research[18] has shown that, over a wide range of doping levels and applied strains, p-type silicon strain gauges display a smaller deviation from linearity than n-type. The parabola shown dotted in figure 2.6.1 represents equation 2.6.2 and the bold line shows a typical gauge characteristic.

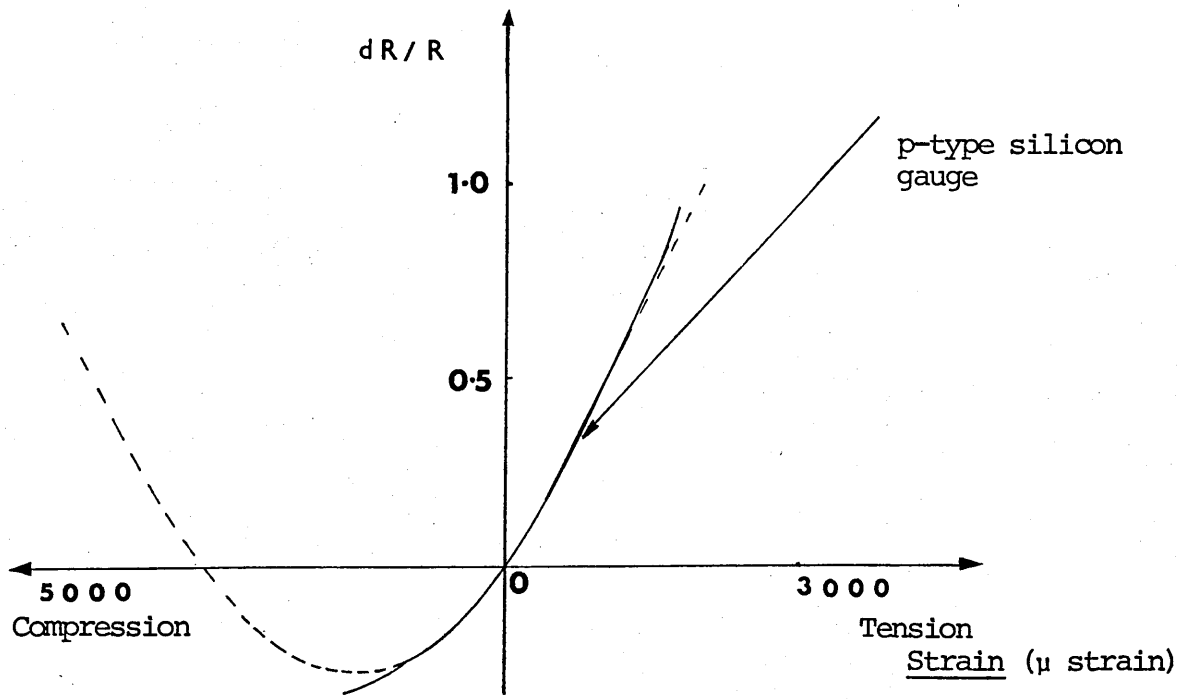

Relative Resistance change as a function of strain

Figure 2.6.1

The ε^2 term in equation 2.6.2 becomes significant at finite levels of strain and thus, if commencing with a resistance not equal to R, for an unstrained gauge condition, the slope (i.e. gauge factor k) at that point on the above curve would not be the same. Similarly, care should be taken when interpreting strain sensitivity curves (such as figures 1.3.4 and 1.3.5 in Chapter 1) because the gauge could already be subjected to a prestrain as a result

of the bonding technique used. As indicated in section 2.5, this is due to the difference in the coefficients of thermal expansivity between the gauge and the surface under test. The magnitude of this effect can be determined by comparing the static resistance of the bonded strain gauge to its static resistance prior to bonding (at the same temperature) and using this difference to estimate the prestrain.

The degree of non-linearity can be significantly reduced by employing higher levels of doping (e.g. for p-type silicon $> 10^{24}$ impurity atoms m^{-3}) with corresponding reductions in gauge resistivity. As a result of this the values of the constants in equation 2.6.2 are reduced, as given earlier, and a more linear relationship is thus achieved (i.e. the lower the resistivity the better the linearity).

Non-linearities of much less than $\pm$ 0.01% (over 1000 μ strain) are now attainable. In general, gauges manufactured from p-type material are more linear than those made from n-type material. However, gauges made from n-type material are slightly more linear in compression.

In many stress analysis contexts quarter bridge circuits are used, which means that non-linearity could well be particularly noticeable. Nevertheless, because strain levels in this context tend to be low and non-linearity is usually noticeable only at strain levels above

1000 μ strain, this is generally not a significant problem with modern semiconductor gauges using higher doping levels (see figure 2.6.2).

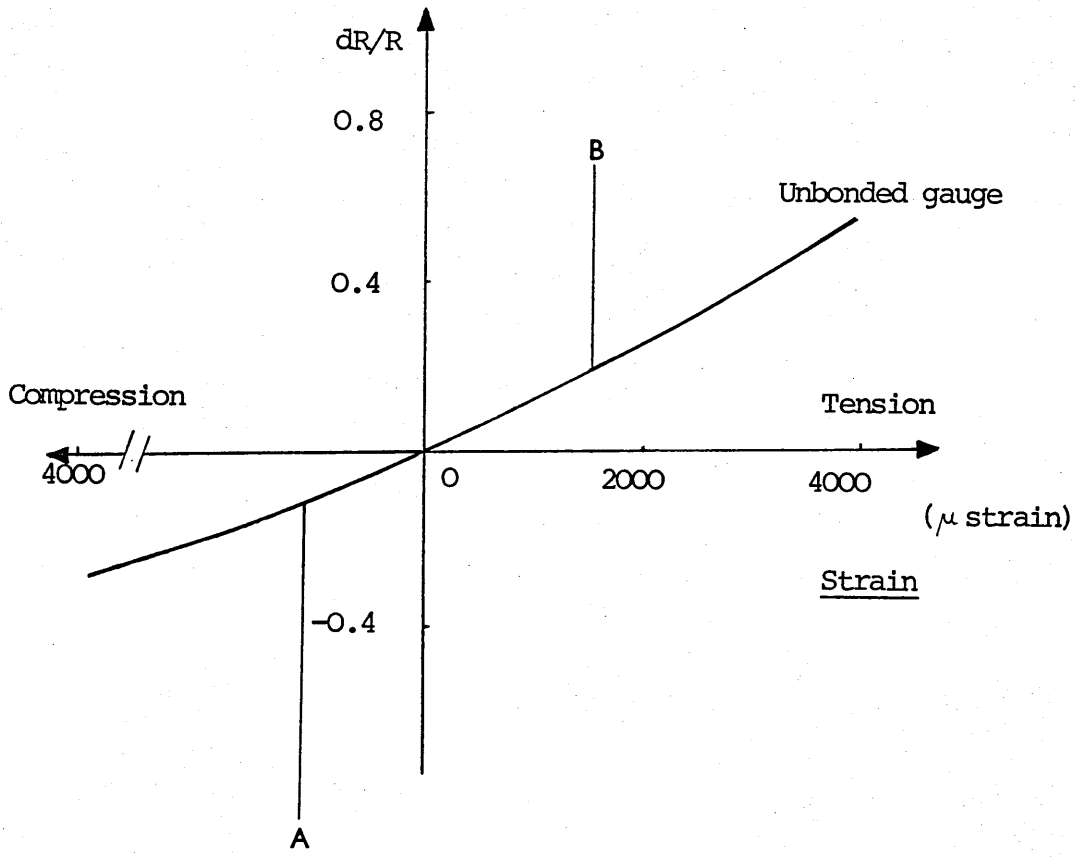

A-B Common overall range of use for single gauge

Resistance Change Versus Strain for heavily doped p-type Silicon (at 293K)

Figure 2.6.2

If fully active or half active Wheatstone bridge circuits are employed then, by cancellation of the non-linear terms in the transfer function, some degree of compensation for non-linearity can be achieved. Manufacturers of transducers using semiconductor strain gauges currently claim that, depending on mechanical design, non-linearities of 0.05% full scale, or less, can quite readily be attained in this way.

Account must also be taken of the inherent non-linearity of the electrical output of Wheatstone bridge circuits - particularly where 4 strain gauges are used and 2 are subjected to much lower applied strains (e.g. "diaphragm" type pressure transducers). Although this non-linearity is generally negligible it is not so when large asymmetries between gauges exist, and it is more significant in the case of semiconductor gauges also because of their greater strain sensitivity. The magnitude of the electrical non-linearity can be calculated (see section 3.4) and then allowance made for this. It is interesting that the basic non-linearity of the Wheatstone bridge circuit can be exploited to advantage, as pointed out by Sanchez and Wright[53]. More will be said about this, and other means of non-linearity compensation by circuitry which were investigated, in the next chapter.

2.7 SUMMARY

Semiconductor strain gauges are available with or without a backing material or encapsulated. The backing material provides for better handling of the gauge and gives electrical insulation between the gauge and test material. Good bonding characteristics, high shear modulus and very low creep are important properties required of the backing material. Typical materials used include polymide backing, epoxy backing and glass fibre reinforced epoxy-phenolic backing.

An experimental investigation was undertaken of the bonding of backed, unbacked and encapsulated semiconductor strain gauges using mainly thermosetting and thermoplastic adhesives. In all 10 common adhesives were employed using metal and plastic substrates. Most of the adhesives were found to provide adequate bonds but the thermosetting (i.e. epoxide and polyester) adhesives did not display any detectable creep and a polyester was chosen for later work, as bonds using this were found to be particularly free from air bubbles.

Tests of bonds were carried out, including peel strength, microscope examination of cut sections of bonds, pressure tests to reveal air bubbles or bond discontinuities and electrical resistance tests. No

significant difference, in terms of actual bonding was found between unbacked, backed or encapsulated gauges of similar surface area. Account may require to be taken of the effects of strain arising from differences in the coefficients of thermal expansivity of the gauge, adhesive and substrate when undertaking strain measurements over a range of temperatures.

Semiconductor strain gauges, unlike metal foil or wire gauges, have a non-linear resistance change versus applied strain characteristic. The characteristics of n-type and p-type silicon are somewhat different and it was noted that strain gauges made from the latter material display a smaller deviation over a wide range of applied strains.

It is possible to reduce the non-linearity of semiconductor strain gauges by increasing the dopant level. Gauge non-linearities of less than $\pm$ 0.01%, over a range of 1000 μ strain, can now be achieved. Gauges made from n-type material are slightly more linear in compression while gauges made from p-type material are more linear in tension.

In some cases, the magnitude of the non-linearity may be calculated and then allowance made for this. It is also possible to exploit the basic non-linearity of the Wheatstone bridge curcuit in order to provide a measure of compensation for gauge non-linearity.

CHAPTER 3

Semiconductor Strain Gauge Circuits

3.1 INTRODUCTION

The theory and practical aspects of semiconductor strain gauge circuitry require careful consideration. Factors which must be taken into account include the non-linearity of semiconductor strain gauges, the influence of both circuits and energization and the means of providing compensation for various effects.

In this chapter, various bridge circuits are described and analysed, and some suggestions are made concerning their applications.

3.2 BASIC SEMICONDUCTOR STRAIN GAUGE CIRCUITS

The greater sensitivity of semiconductor strain gauges, compared to wire or foil gauges, itself poses various problems with gauge circuitry. In addition, account must be taken of both the non-linearity and large temperature coefficient of gauge factor of

semiconductor strain gauges. Due to these factors, and the relatively higher resistance of semiconductor strain gauges, circuits with special compensation elements in their design may be required in some applications.

In order to measure accurately the change in resistance with applied strain a form of Wheatstone bridge circuit is particularly suitable, because it removes offsets and enables thermal compensation to be readily provided. Such bridge circuits (see figure 3.2.1) may be made using from 1 to 4 strain gauges of which one or more is 'active' (ie changes in resistance with applied strain). Many applications use either a fully active (4 active gauges) or half active (2 active gauges) bridge. If quarter active (ie 1 active gauge) and partially active (ie when 2 of the 4 gauges are subject to a fraction of the strain applied to the other gauges - as in some types of load cell) bridges are employed more account must be taken of the factors indicated earlier, such as the high temperature coefficient of semiconductor gauges. Account may also have to be taken of the non-linearities of Wheatstone bridge circuits with large resistance variations.

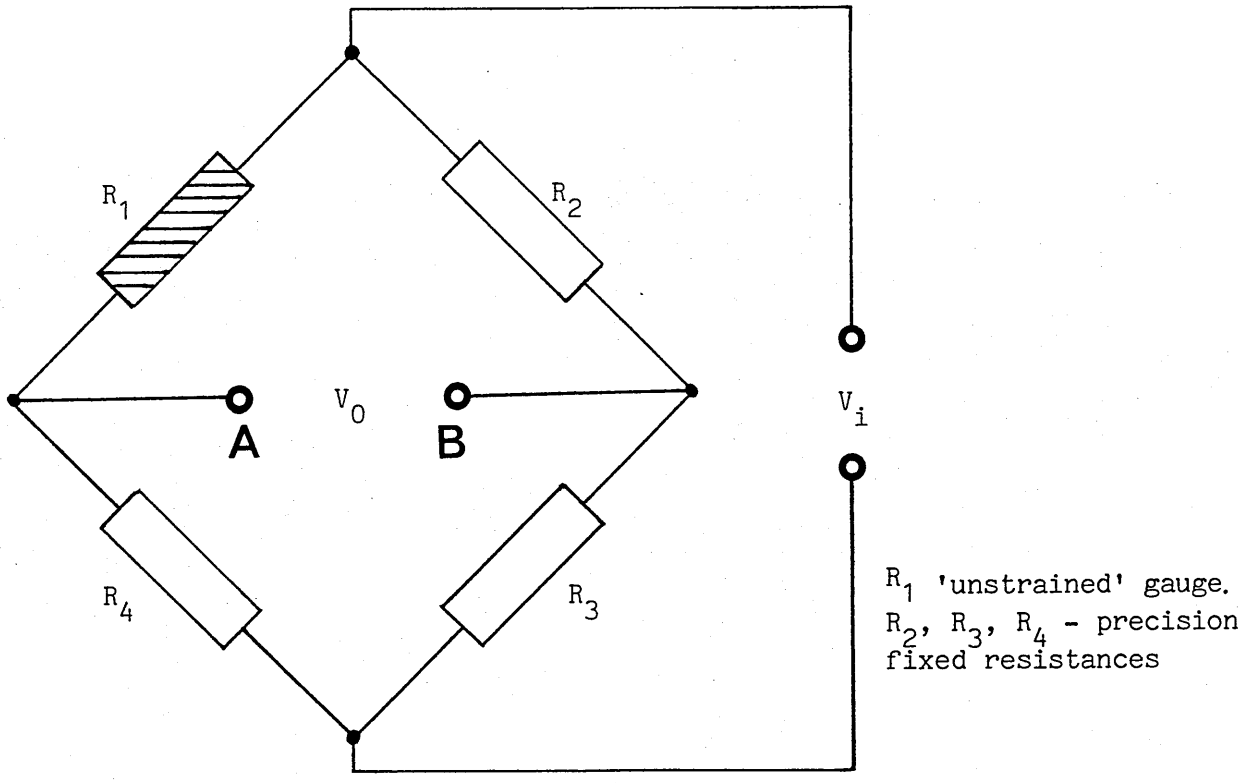

Basic Bridge Circuit

Figure 3.2.1

The Wheatstone bridge may be energized with either direct current or alternating current. Although alternating current was commonly used in the past for strain gauge applications (mainly because of drift and noise problems associated with discrete components used in direct current amplifiers) direct current bridge excitation is now frequently employed - using integrated circuits which have almost zero drift. The bridge is energized normally by applying a regulated voltage V_i across two opposite corners. Then a voltage output, which is

proportional to the excitation voltage V_i and the resistance change(s) of the strain gauge(s), appears across the signal terminals A, B. If the bridge is used at or close to the balance condition then the output voltage is either zero or almost zero. Hence, the small voltage changes due to the gauge(s) being strained may be measured with sensitive instruments to a high accuracy, which is a particular advantage of using such a bridge circuit.

To give zero output (ie V_0 = 0V) from the bridge (figure 3.2.1) the potential difference across R_4 equals the potential difference across R_3. Thus:

$$V_i[R_4/(R_4 + R_1)] = V_i[R_3/R_2 + R_3)] \qquad 3.2.1$$

Cross multiplying equation 3.2.1 gives:

$$R_4 (R_2 + R_3) = R_3 (R_4 + R_1)$$

This gives: $R_2 R_4 = R_3 R_1$ 3.2.2

The equation 3.2.2 is known as the balance equation and, in order to maintain balance if the resistance of the gauge changes by dR_1 (figure 3.2.2), then either R_4 or R_2 must be changed in the same direction, or R_3

must be changed in the opposite direction to the change of gauge resistance, by the necessary amount so that V_0 is zero again. Although a combination of changes in R_4, R_2 and R_3 could maintain the bridge in balance only one of these three is changed in practice. The null method, which is very precise, is considered to be only of use for static rather than dynamic strain measurement, because of the amount of time which is required to make the changes needed to restore balance. The surface strain ε is found from:

$$\varepsilon = \left(\frac{dR_1}{R_1}\right) / k \qquad 3.2.3$$

Where $\varepsilon = \frac{d\ell}{\ell}$ and k is the gauge factor.

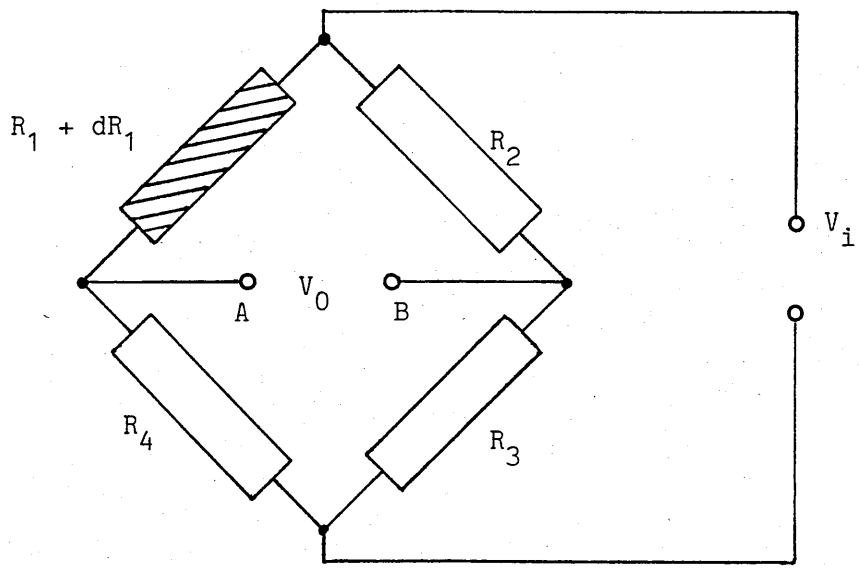

R_1 - 'strained' gauge.

R_2, R_3, R_4 - Precision fixed resistances.

Basic bridge circuit - 'strained' gauge

Figure 3.2.2

If the gauge in figure 3.2.2 is given an applied tensile strain then, in an originally balanced bridge, the resistance in the gauge arm of the bridge will increase by dR_1 to $R_1 + dR_1$. For a constant voltage input V_i and an open circuit output V_0 then:

$$V_0 = V_i\left[\frac{R_3 (R_4 + R_1 + dR_1) - R_4 (R_2 + R_3)}{(R_2 + R_3)(R_4 + R_1 + dR_1)}\right] \qquad 3.2.4$$

If $R_1 = R_2 = R_3 = R_4 = R$

then $V_0 = V_i \left[\frac{R(2R + dR) - 2R^2}{2R(2R + dR)}\right]$

which simplifies to: $V_i\left[\frac{dR}{4R + 2\,dR}\right]$ 3.2.5

If $dR \ll R$

then $V_0 \simeq V_i \left[\frac{dR}{4R}\right]$ 3.2.6

Since $k\varepsilon = dR/R$ then equation 3.2.6 may written as:

$$V_0 \simeq V_i \left[\frac{K\varepsilon}{4}\right] \qquad 3.2.7$$

This approximation applies to virtually all uses of conventional metal foil and wire strain gauges, but is often not satisfied by semiconductor gauges because of their high gauge factors, ie. $dR \not\ll R$.

As the out of balance mode gives an output voltage V_0 which is related to the strain experienced by the gauge it may be used for both static and dynamic strain measurements.

In some cases the Wheatstone bridge may be energized from a constant current rather than a constant voltage source. Such a case is when it is required to provide compensation for the temperature coefficient of gauge factor (see section 4.5) and another case is where improved linearity is required when high resistivity gauges are employed. More will be said regarding these and other aspects in subsequent sections.

3.3 NON-LINEARITY OF BRIDGE CIRCUITS

Wheatstone bridges display non-linear characteristics under certain conditions, such as when there are large changes in resistance, or when there are resistance changes which are non-symmetrical. As indicated in Chapter 1, the operational resistance changes of semiconductor strain gauges may be quite large; thus when used with Wheatstone bridge circuits the approximation used in equation 3.2.7 does

not hold. For example, in a bridge with a single active strain gauge R_1, such as shown earlier in figure 3.2.2, and with equal resistances in the other arms, the ratio of output to input voltage V_0/V_i is derived from equation 3.2.5:

$$\frac{V_0}{V_i} = \frac{1/2(dR_1/R_1)}{2 + (dR_1/R_1)} \qquad 3.3.1$$

In the case of semiconductor strain gauges the large resistance changes can mean that the deviation from linearity could reach 20%. However, the non-linearity can be markedly reduced in several ways.

One method is to increase the magnitude of the resistors R_3 and R_4 by a fixed factor f (eg 10) compared to R_1 and R_2 such that, assuming linear gauge response:

$$f = R_4/R_1 = R_3/R_2 \qquad 3.3.2$$

In this case the bridge output will be given by:

$$V_0 = V_i \{[R_4/(R_1 + R_4)] - [R_3/(R_2 + R_3)]\} \qquad 3.3.3$$

$$= V_i \left[\frac{R_1 f}{R_1 + dR_1 + R_1 f} - \frac{R_2 f}{R_2 + R_2 f} \right] \qquad 3.3.4$$

$$= V_i \left[\frac{R_1 f}{R_1 + (dR_1/R_1) + R_1 f} - \frac{1}{1 + f} \right] \qquad 3.3.5$$

$$= V_i \left[\frac{f}{1 + f + (dR_1/R_1)} - \frac{1}{1 + f} \right] \qquad 3.3.6$$

This may be written in the form:

$$V_o = V_i \left\{ \frac{1}{1+f} \left[f\left(1 - \left(\frac{dR}{R_1}1\right) \frac{1}{(1+f)} + \left(\frac{dR}{R_1}1\right)^2 \frac{1}{(1+f)^2} - \cdots - 1\right)\right]\right\} \qquad 3.3.7$$

Hence the degree of non-linearity between V_0 and dR_1/R_1 varies with f. However, the effect of increasing f to produce a greater reduction in bridge non-linearity is to reduce the output voltage; unless the bridge voltage is increased to compensate.

Another means of obtaining improved bridge linearity is to employ a shunt resistance in parallel with the gauge. In order to obtain this good linearity, however, there may be a very significant reduction in gauge sensitivity (which may be acceptable).

An alternative way of dealing with the problem of bridge non-linearity is to use the non-linear behaviour of semiconductor strain gauges to compensate for this. From equation 3.3.1, for a bridge with one active gauge of resistance R_1, the ratio of output voltage V_0 and input V_i is:

$$\frac{V_0}{V_i} = \frac{\frac{1}{2}(dR_1/R_1)}{2 + (dR_1/R_1)}$$

$$= \frac{(dR_1/R_1)/4}{1 + (dR_1/2R_1)} \qquad 3.3.8$$

(as $(dR_1/R_1)^2$ is $\ll 1$)

$$\simeq 1/4\ (dR_1/R_1)(1-[dR_1/2R_1] + ...) \qquad 3.3.9$$

$$\simeq \frac{dR_1}{4R_1}\left(1 - \frac{dR_1}{2R_1} + ...\right) \qquad 3.3.10$$

The non-linear calibration curve for p-type gauges can be written generally (see section 2.6) as:

$$dR_1/R_1 = \varepsilon(C_1 + C_2\varepsilon\ ) \qquad 3.3.11$$

The non-linear terms in equation 3.3.10 and equation 3.3.11 have opposite signs and, assuming C_2 is positive, good compensation may thus be

achieved by making the resistance of the two bridge ratio arms either larger or smaller than R_1, so that the bridge non-linearity matches that of the strain gauge. The only other adjustment required is to the input voltage V_i in order to maintain the optimum current through the bridge circuit.

3.4 SEMICONDUCTOR STRAIN GAUGE NON-LINEARITY COMPENSATION

Concerning the non-linear behaviour of semiconductor strain gauges (section 2.6) not only can improvements in linearity be achieved by the use of heavier doping levels but circuit compensation measures may also be employed. These compensation measures can be summarised as:

(a) Use of non-linearity of Wheatstone bridge

(b) Use of opposite pre-strained gauges in a push-pull arrangement

(c) Use of pairs of p-type and n-type silicon gauges with matched, opposite, characteristics.

(a) The use of the inherent non-linearity of Wheatstone bridge circuits, to provide compensation for semiconductor strain gauge

non-linearity, is as described in the previous section. However, as Parkins[50] has noted, the basic Wheatstone bridge circuit can only provide such compensation over a fairly specific range of applied strains. Nevertheless, by using semiconductors with a specific prestrain (perhaps 1000 μ strain) a linear output over a different range of applied strains may be achieved. The value of the factor f and the magnitude of the necessary prestrain will vary according to the type of semiconductor strain gauge.

(b) A significant reduction in the non-linearity of semiconductor strain gauges may be achieved by using either 2 or 4 strain gauges in a push-pull arrangement. One gauge (or pair of gauges) must be under pre-tension and the other gauge (or pair of gauges) under pre-compression of the same magnitude. Compensation is achieved because the non-linearities cancel out. A basic arrangement is shown in figure 3.4.1. As indicated, gauge A is under pre-tension and gauge B is under pre-compression by an equal amount.

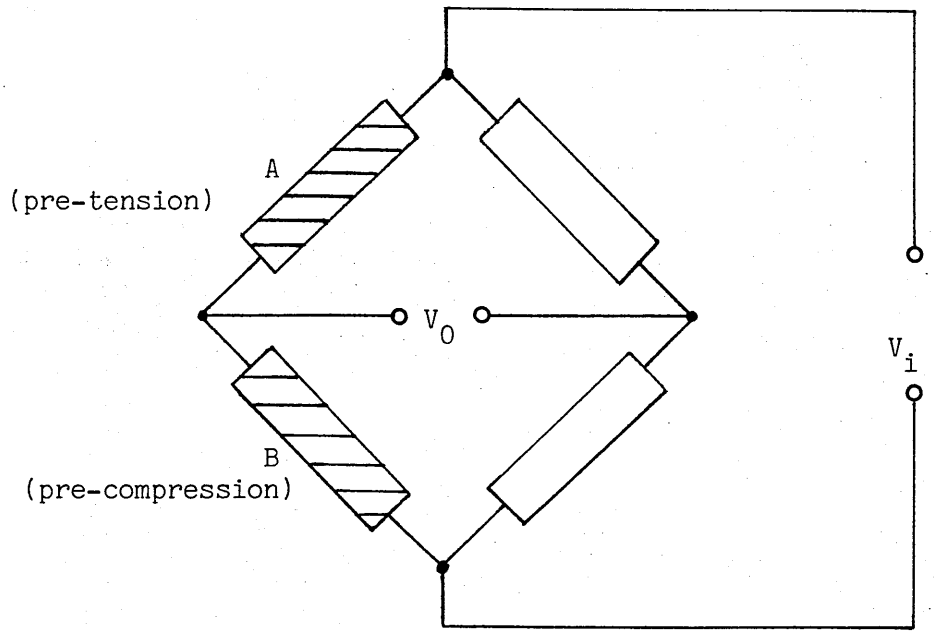

Non-linearity compensation using 2 gauges in a push-pull arrangement

Figure 3.4.1

Although not generally possible, if the strain gauge characteristics were both symmetrical about their origin then complete cancellation and a linear output over the whole working range of the gauges could be attained. The magnitude of compressional strain employed should not exceed a particular value (eg 500 μ strain) because at higher values there can be a significant increase in non-linearity.

It must not be overlooked that, since the resistance of gauge A will be different to that of gauge B, a full bridge analysis will be

required. In addition, since the magnitude of semiconductor strain gauge non-linearity is temperature dependent, as outlined in section 2.6, account of temperature changes may have to be made. (The arrangement shown if figure 3.4.1 does provide compensation for temperature.)

(c) If problems occur due to the magnitude of compressional strain then the same degree of compensation may be attained with the aid of matched pairs of p-type and n-type semiconductor strain gauges mounted side by side. Both gauges must be either in tension or in compression. Although it is posible to obtain gauges of similar gauge factor (and opposite sign) to provide compensation, the degree of compensation is limited because n-type gauges are not as linear as p-type gauges.

A further measure of compensation for non-linearity can be achieved by exploiting the property of p-type gauges that their linearity increases with an increase in tension and n-type which increase in linearity with increasing compression. Therefore, by using a matched pair of n-type and p-type gauges the degree of non-linearity can be reduced (within the constraints of strain magnitude and ambient temperature). Due to improvements in linearity associated with higher

levels of doping which is currently common, the overall degree of semiconductor strain gauge non-linearity compensation by circuitry is neither so great or so necessary as it formerly was.

3.5 SEMICONDUCTOR STRAIN GAUGE EXCITATION

There are several factors which must be taken into account when attempting to specify optimum excitation levels for semiconductor strain gauges. The highest voltage which can be applied is limited by the maximum temperature allowable, itself controlled by the amount of heat which is dissipated from the gauge to the test surface. This heat dissipation is a function of the adhesive thickness, the surface area of the gauge, the thermal mass of the adhesive and substrate, the thermal conductivity of the adhesive and substrate, the ambient temperature and the air flow around the strain gauge and the substrate. In addition, the resistance of the gauge must be taken into account.

Reference to manufacturer's data* shows that power dissipations of between 20 and 50 mW per gauge are generally acceptable (ie this gives acceptable performance stability without any risk of damage to the gauge). If high zero stability is not required, and the adhesive will function at higher temperatures, then 50-100mW power dissipation could be tolerated by larger gauges.

Manufacturer's data is often obtained with a constant voltage source and may be different if the gauge is energised by a constant current source.

To explore the effects of energization, a study of both constant current and constant voltage energization was undertaken. The investigation involved single active gauges operating at relatively low levels of applied strain (eg < 30 μ strain) and ambient temperatures of about 293K.

Figure 3.5.1 shows the basic constant current circuit which was used. This consisted of a voltage regulator (eg 7805), which provided a constant fixed voltage, connected so that the current through

* (For the gauges manufactured by Kulite used in this study.)

the resistance R_C, and hence through an external load, is constant. The power supply initially used was a smoothed d.c. power supply but this was found to have an unsatisfactory level of ripple, and so a 12V battery was subsequently employed.

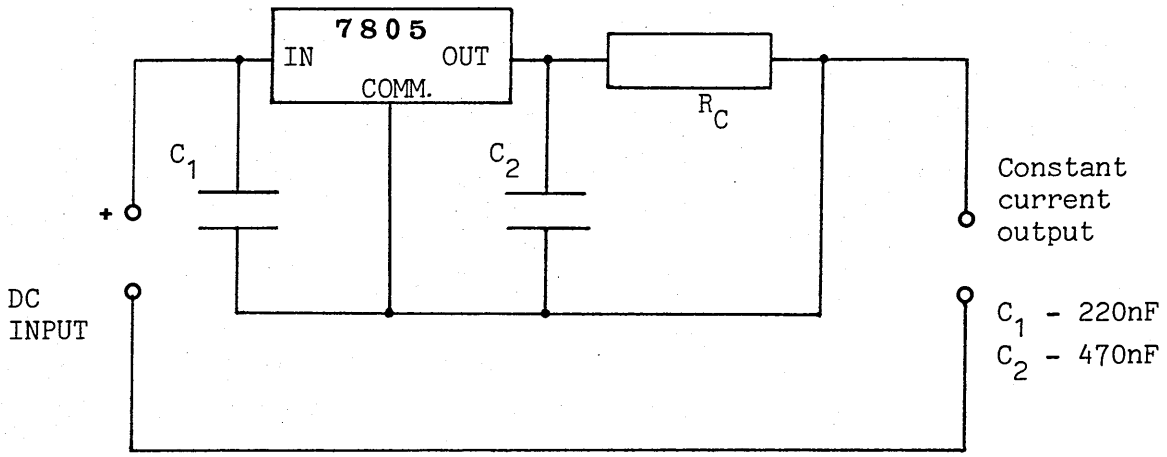

Basic Constant Current Circuit

Figure 3.5.1

A 7805 fixed 5V regulator and a resistor R_C of 470 Ω , was employed with strain gauges of about 350 Ω resistance at room temperature. These p-type silicon gauges were unbacked and were bonded, using P2 polyester adhesive detailed in the previous chapter, to stainless steel strip. Figure 3.5.2 shows the basic circuit used with the strain gauges.

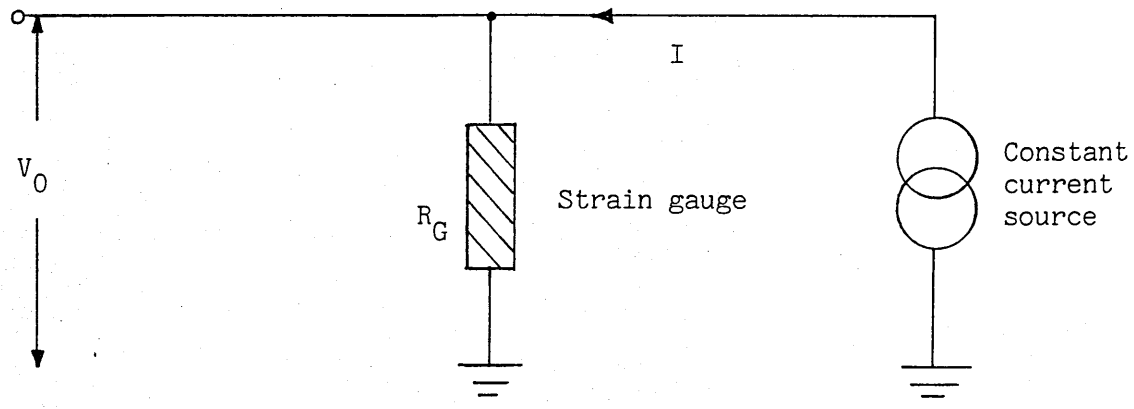

Basic Single strain Gauge Circuit: Constant Current Excitation

Figure 3.5.2

A sensitive digital voltmeter measured the change in potential difference across the gauge with applied strain. Tensile strains of a pre-determined magnitude were provided by a Hounsfield tensometer and, because of the high gauge factor of semiconductor strain gauges, typical strains applied were between 5 and 30 μ strain (although larger strains were examined). Readings of the strain gauge resistance were taken every 5 minutes for a total of 90 minutes. Gauge temperature was also measured every 5 minutes for 90 minutes using a thermocouple ($\pm$1K). A constant temperature bath was not available but, to reduce heat losses, the gauge was enclosed by a wooden draught shield (room temperature was 293 $\pm$1K).

The voltage change with this system is simply proportional to the change in the resistance of the strain gauge, and circuit non-linearity is eliminated because:

$$V_O = I\ (R_G + dR_G) \qquad 3.5.1$$

and changes in dR_G do not significantly affect I.

A corresponding study was undertaken using a constant voltage supply across the gauge and series resistance. The same semiconductor strain gauges were employed as for the constant current energization. Each strain gauge was put in series with a fixed resistor as shown in figure 3.5.3. This involved the use of voltage regulators (such as 7805) powered by a 12V battery, as with the constant current arrangement. In the later investigations of strain gauge circuits (section 3.6) a high quality stabilized d.c. power supply was employed in place of the battery, and found to be satisfactory.

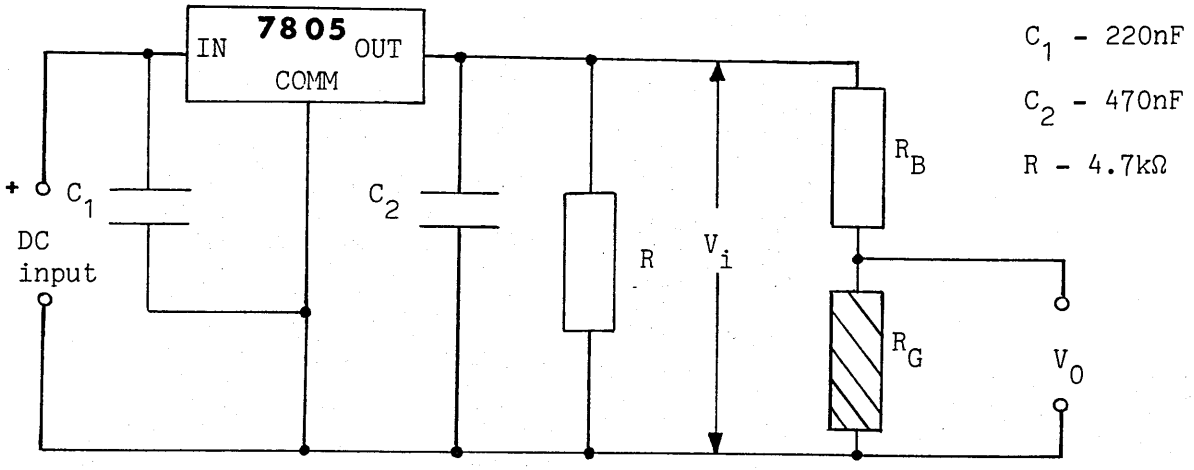

Basic Constant Voltage Circuit and Strain Gauge

Figure 3.5.3

A digital voltmeter was connected across the strain gauge as shown and the resistance R_B was chosen to have a similar resistance to the strain gauge with no applied strain (at room temperature). In this case currents in the gauge circuit were up to 10mA operating from a constant voltage of 5V. As in the case of constant current energization relatively low tensile strains were employed.

The results of these studies of gauge excitation are given in section 3.7, along with those obtained for constant current and constant voltage bridge energization investigations outlined in the following section.

3.6 EXPERIMENTAL BRIDGE CIRCUITS

Experimental investigations were undertaken, using various semiconductor strain gauges in the bridge circuits, under both static and dynamic strains. Bridge energization for these investigations was provided, initially, using the constant current and constant voltage circuits which were described in section 3.5 (see figures 3.5.1 and 3.5.3 for the basic respective circuits). The circuits used for constant voltage and constant current bridge energization are shown in figures 3.61. and 3.6.2 respectively.

Precision resistors (±0.1%) were used in the bridge and various types of resistors were tried in an attempt to match closely the temperature coefficient of resistance of the strain gauges (this is discussed in section 4.2). Mainly p-type silicon, relatively highly doped strain gauges of about 350Ω and 500Ω were used, but lower and higher resistance gauges were also studied. Mounting pads were used to connect the gauge leads, and it was found useful to mount the gauges on stainless steel strip so that the applied strain could be accurately controlled by various means. Relatively low levels of static and dynamic strains were employed, up to about 40μ strain.

Figure 3.6.1 shows the basic constant voltage bridge circuit which was employed using a 7805 integrated circuit. A 7815 integrated circuit was also later employed to provide a higher constant voltage. R_1 is the semiconductor strain gauge of gauge factor 120.

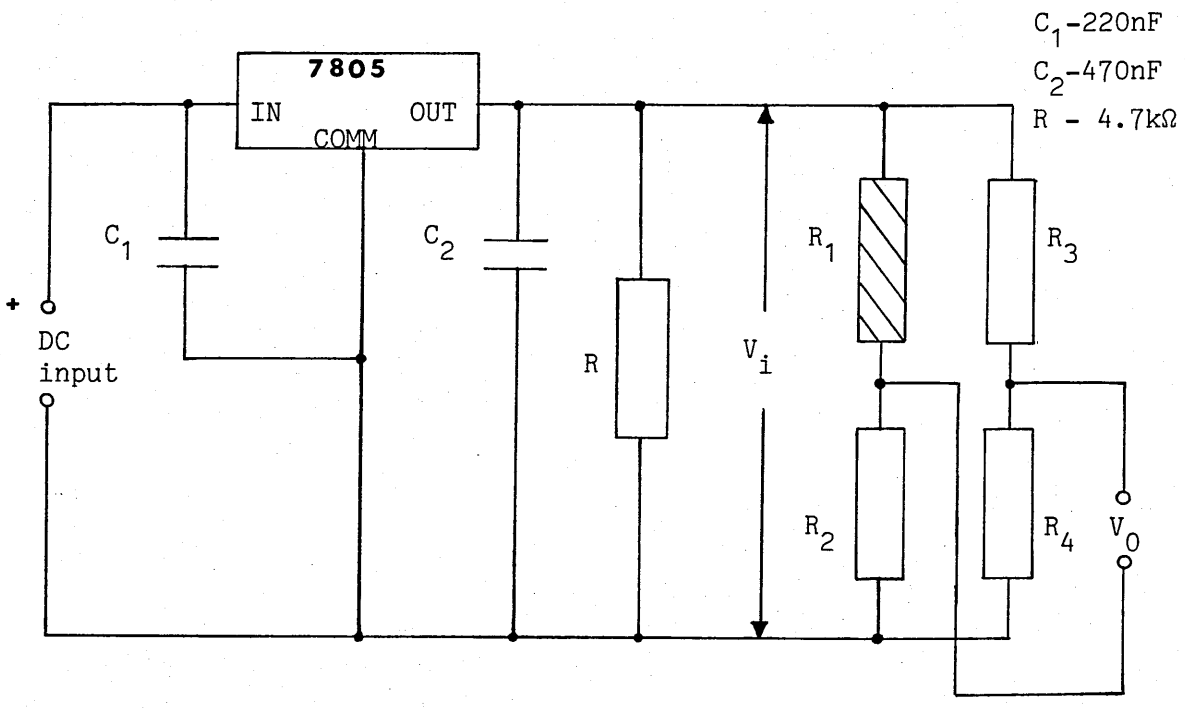

Basic Constant Voltage Bridge Circuit

Figure 3.6.1

For most purposes the bridge was used in the out of balance rather than null balance mode to allow dynamic as well as static strain measurement. The capacitors C_1 and C_2 (figure 3.6.1) are decoupling

capacitors which were found necessary to remove transient oscillations and R is a recommended load resistance. Resistors R_2, R_3, and R_4 are precision resistors.

Typical gauge currents with constant voltage energization were in the range from about 2 to 10mA and constant voltages of 5V and 15V were employed. Results were obtained (see section 3.7), for various silicon gauges and various applied strains, to be compared with corresponding results obtained using constant current bridge energization. In both cases monitoring of input and output voltages was carried out with digital voltmeters reading to an accuracy of 0.001mV. Currents were measured with digital meters reading to an accuracy of 0.01mA.

The basic constant current bridge circuit which was employed is shown in figure 3.6.2. Different constant currents from 2mA to about 10mA were used and various strain gauges and applied strains were employed for each constant current.

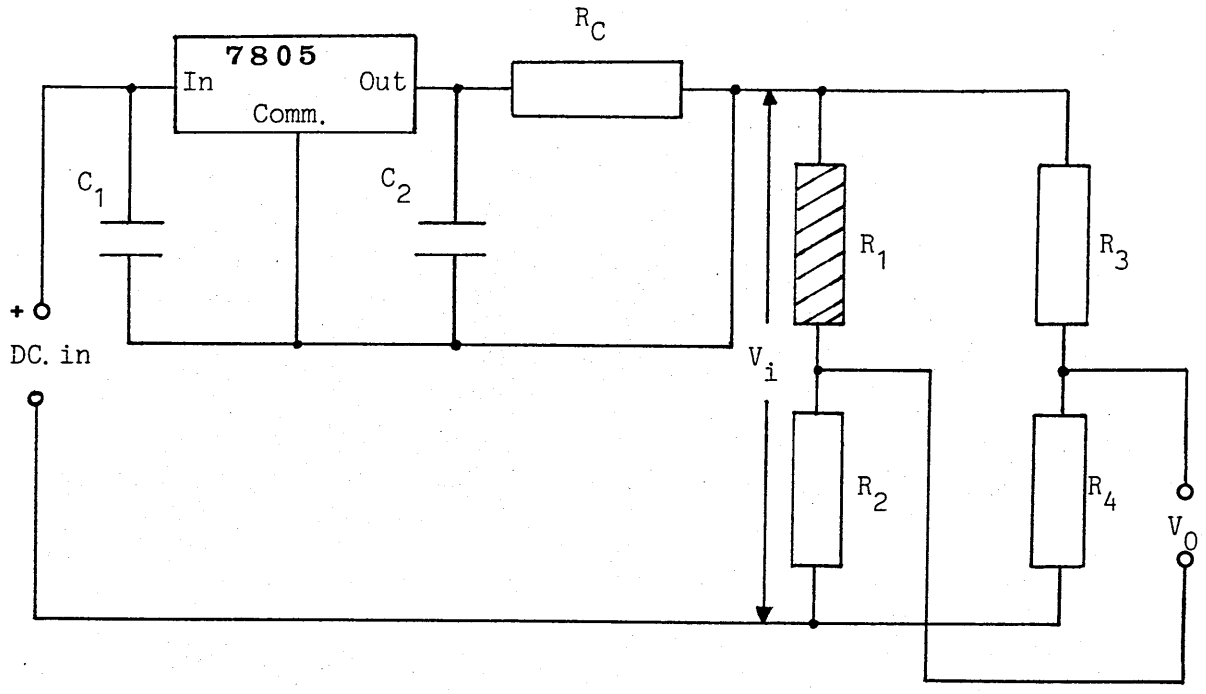

Basic Constant Current Bridge Circuit

Figure 3.6.2

The values of the capacitors and resistors used were the same as those employed in the constant voltage arrangement shown in figure 3.6.1.

In order to provide a particular current, an appropriate value resistor R_C, was selected. Typical results are given in section 3.7 (ii).

Following this investigation of constant voltage and constant current bridge energization, studies of half active and fully active bridge

arrangements were undertaken. The half active bridge systems explored

may be summarised as follows:

(a) Gauges mounted side by side and on the same face of the substrate. The 2 gauges were then connected to opposite arms of the bridge (figure 3.6.3)

(b) Gauges mounted back to back on opposite faces of the substrate. The 2 gauges were then connected to adjacent arms of the bridge (figure 3.6.4)

(c) Gauges mounted side by side on the same face of the substrate but with their active lengths at right angles to each other. The 2 gauges were then connected to adjacent arms of the bridge (figure 3.6.5).

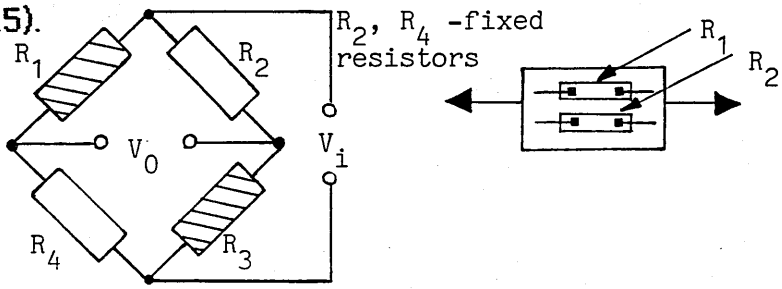

$V_0 \simeq 1/2\ k\ \varepsilon\ V_i$ (ε- strain)

(a) Half active bridge: gauges mounted side by side

Figure 3.6.3

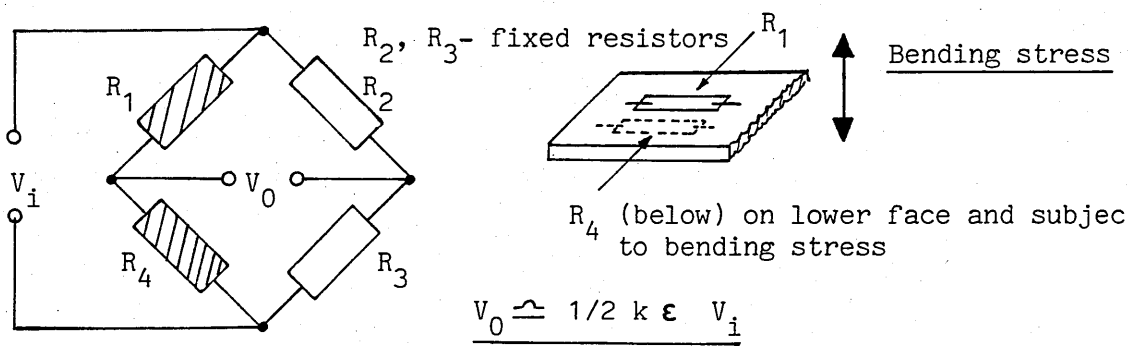

$V_0 \simeq 1/2\ k\ \varepsilon\ V_i$

(b) Half Active Bridge: Gauges Mounted Back to Back

Figure 3.6.4

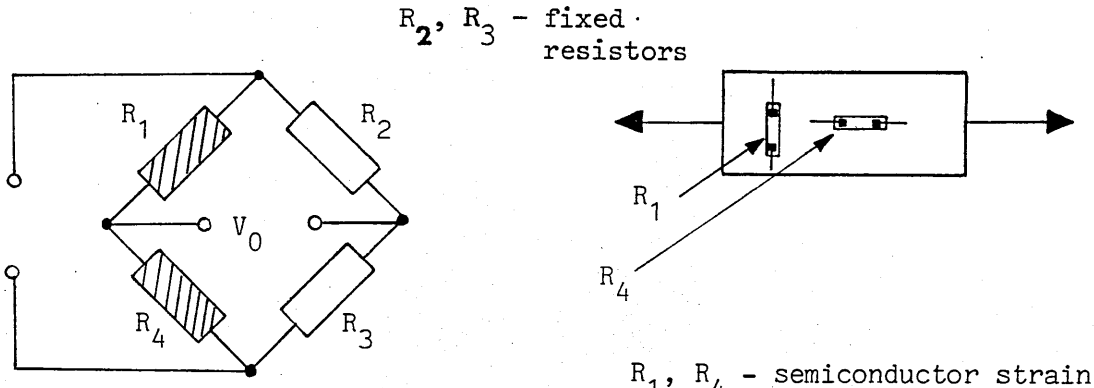

$V_0 \simeq \frac{(1 + \nu)}{4} K \varepsilon V_i$ (ν - Poisson's ratio)

(c) Half active bridge: gauges mounted with activelengths at right angles

Figure 3.6.5

The brief study of a fully active bridge involved the use of 4 strain gauges each connected to a separate arm of the bridge. These gauges were all mounted on the same steel strip, which was subjected to a bending stress.

Within each of these bridge circuits all the semiconductor strain gauges were matched for gauge factor and unstrained resistance at room temperature. Constant voltage bridge energization was employed. Initially a constant voltage of 5V was used and later 15V. Bridge input and output voltages were measured, as before, using digital voltmeters reading to an accuracy of 0.001mV.

The p-type silicon semiconductor strain gauges used were 'backed' type, for convenience, and were bonded to stainless steel strip

using P2 polyester adhesive cured at room temperature. Relatively small magnitude strains up to about 40 μ strain were employed since the gauge factors were 120 or more. Static strains were applied with a Hounsfield tensometer which provided uniform strains, and static bending stress was provided by clamping the steel strips in a horizontal clamp and attaching known loads to the unclamped end. Dynamic bending stress was provided by positioning coils of copper wire above and below the unclamped end of the strip and passing alternating current through the coils, so that the strips bent one way then the other. Different strain magnitudes and rates of change of strain were attained by changing the current through the coils and the frequency. The coils were positioned away from the gauges and no measurable current was induced in the gauges.

The investigations were carried out at room temperature (293K) with constant, artificial, ambient levels of illumination (300 lux). Later studies, which will be fully described in chapters 4 and 5 respectively, examined the effects of temperature and illumination on these gauges with different applied strains.

An attempt was made to amplify the bridge output using an operational amplifier. Brief details of the circuit employed with the bridge are given in Appendix 1.

3.7 RESULTS AND DISCUSSION

(i) Gauge excitation

In the studies of constant current and constant voltage gauge excitation (section 3.5) two main comparisons were made. These were of gauge thermal stability, in terms of the gauge resistance remaining constant, and change in output voltage with applied strain.

Figure 3.7.1 shows results obtained regarding gauge thermal stability for constant current energization, and figure 3.7.2 shows typical results obtained for constant voltage energization. These are for the same strain gauge, which was a p-type silicon gauge of gauge factor 120. The same characteristics shown in figure 3.7.1 were found when other silicon semiconductor strain gauges, having different gauge factors and resistances were employed.

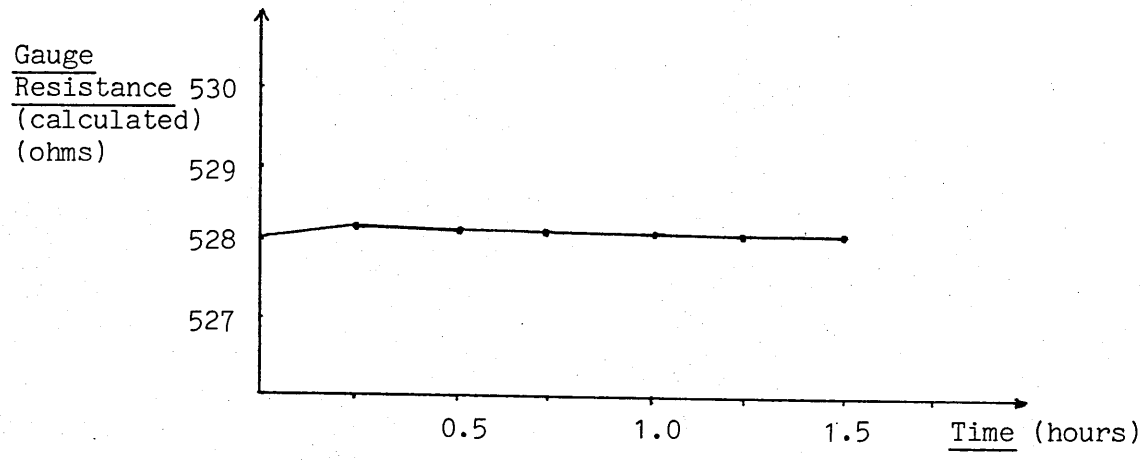

Thermal Stability: Constant Current Energization

Figure 3.7.1

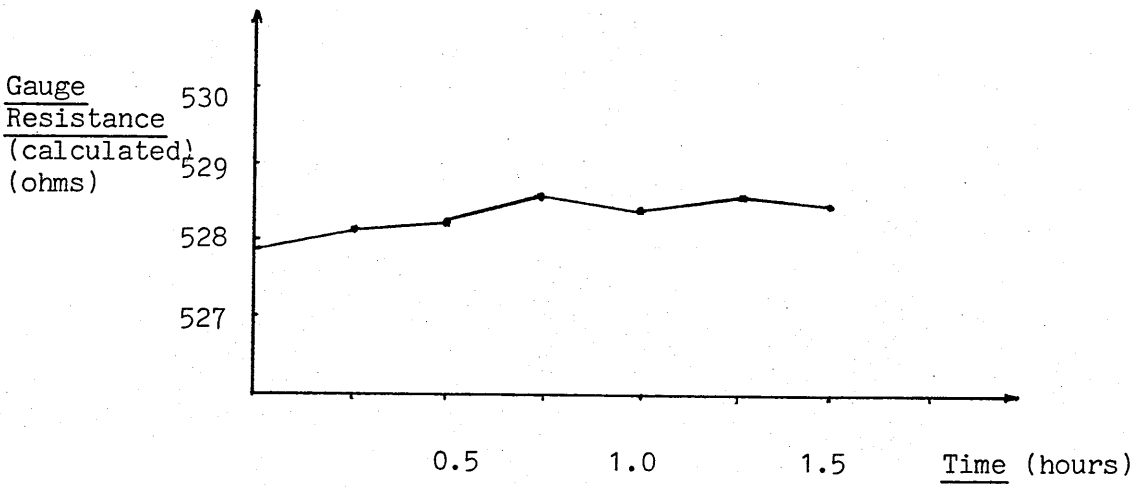

Thermal Stability: Constant Voltage Energization

Figure 3.7.2

The results were obtained under the same ambient temperature conditions (293±1K) in each case. For this gauge a temperature variation

of 1K corresponds to a resistance change of 1Ω. These results are for no applied strain on the gauge.

As can be seen from figures 3.7.1 and 3.7.2, there is a small but noticeable variation in the resistance of the strain gauge, over the same time period, for constant voltage energization compared to constant current energization. The probable reason for the variation seen in this instance is small variations in external temperature causing small variations in gauge resistance.

Although many authors (eg[54]) have recommended constant current energization as being more stable, with a positive temperature coefficient of resistance gauge constant voltage is probably better. The power dissipation causing self heating is: $VI = I^2R = V^2/R$. When the ambient temperature increases and the gauge resistance increases, then in the case of constant current energization the self-heating goes up, supporting the external change. However, for constant voltage the self heating (V^2/R) goes down, tending to compensate. In practice the circuit may well be a mixture of these two ideal conditions (such as the case of a simple potential divider), but constant current is still likely to be the

worst option. The present experiments have not indicated a significant difference between the two circuit conditions.

Typical results for change in output voltage dV, corresponding to change in applied strain are given in figure 3.7.3 for both constant current and constant voltage energization for the same p-type silicon semiconductor strain gauge. Applied strain levels used were relatively low so that gauge non-linearity, which increases with strain magnitude, was small. The results shown were obtained for a gauge of unstrained resistance 350 Ω at room temperature and gauge factor 120.

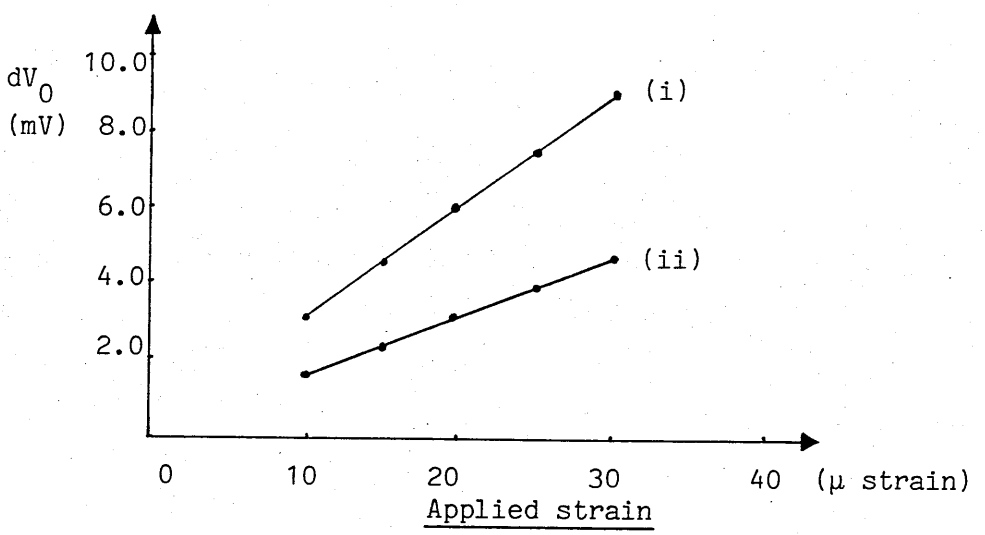

Output Voltage Change Versus Applied Strain

(i) Constant current gauge energization

(ii) Constant voltage gauge energization
Figure 3.7.3.

For constant current gauge energization (figure 3.5.2):

$$V_0 = IR_G$$

$$\text{so, } dV_0 = I dR_G \qquad 3.7.1$$

Now, for constant voltage gauge energization (figure 3.5.3):

$$V_0 = R_G/(R_B + R_G) \qquad 3.7.2$$

If $R_G \rightarrow R_G + dR_G$

$$\text{then: } V_0 = \frac{V_i (R_G + dR_G)}{R_G + dR_G + R_B} \qquad 3.7.3$$

$$= \frac{V_i (R_G + dR_G)}{(R_G + R_B)\left(1 + \frac{dR_G}{R_G + R_B}\right)} \qquad 3.7.4$$

$$\simeq V_i \frac{(R_G + dR_G)}{R_G + R_B}\left(1 - \frac{dR_G}{R_G + R_B}\right) \qquad 3.7.5$$

$$= \frac{V_i}{R_G + R_B}\left(R_G + dR_G - \frac{R_G\, dR_G}{R_G + R_B} + \ldots\right) \qquad 3.7.6$$

$$\simeq \frac{V_i}{R_G + R_B}\left[R_G + dR_G\left(1 - \frac{R_G}{R_G+R_B}\right)\right] \qquad 3.7.7$$

$$= \frac{V_i}{R_G+R_B}\left[R_G + dR_G\,\frac{R_B}{R_G+R_B}\right] \qquad 3.7.8$$

Since the unstrained output voltage, V_o

$$= V_i\left[R_G/(R_G + R_B)\right] \qquad 3.7.9$$

then, $dV_0 = \dfrac{V_i\, dR_G\, R_B}{(R_G + R_B)^2}$

corresponds to a resistance change of dR_G.

But original current $I_0 = V_i/(R_G + R_B)$

$$\therefore \quad dV_0 = I_0\, dR_G\left[\frac{R_B}{R_G+R_B}\right] \qquad 3.7.10$$

If $R_B >> R_G$, then $dV_0 \simeq I_0\, dR_G$ 3.7.11

as in the case of constant current.

If $R_B = R_G$, then $dV_0 = \frac{I_0\, dR_G}{2}$ 3.7.12

Experiments have supported this analysis. In a constant current circuit with I_0 = 7mA and dR_G = 1.26Ω for 30 μstrain, dV_0 was 8.8mV. A typical value for the same gauge and applied strain in a constant voltage circuit was dV_0 = 4.4mV.

Comparable results as in figure 3.7.3, were obtained when the strain gauge was subjected to compressive strains. Moreover, the same characteristics were observed when other silicon strain gauges, with different gauge factors and unstrained resistances, were subjected to similar tensile and compressive strains. Stein[54] recommended constant current energization for semiconductor strain gauges, but the results obtained using modern gauges, which are outlined here, do not suggest that it is better than constant voltage energization, except that dV_0 is higher.

(ii) Bridge excitation

The results shown of output voltage versus applied strain in figure 3.7.4 are for a symmetrical bridge using a p-type silicon gauge of unstrained resistance 350Ω and gauge factor 120. These results are for the gauge subjected to tensile strains at room temperature and are representative of other p-type silicon gauges of different unstrained resistances and gauge factors. The advantage of the bridge system compared to basic gauge systems is that offsets were removed when the bridge system was employed.

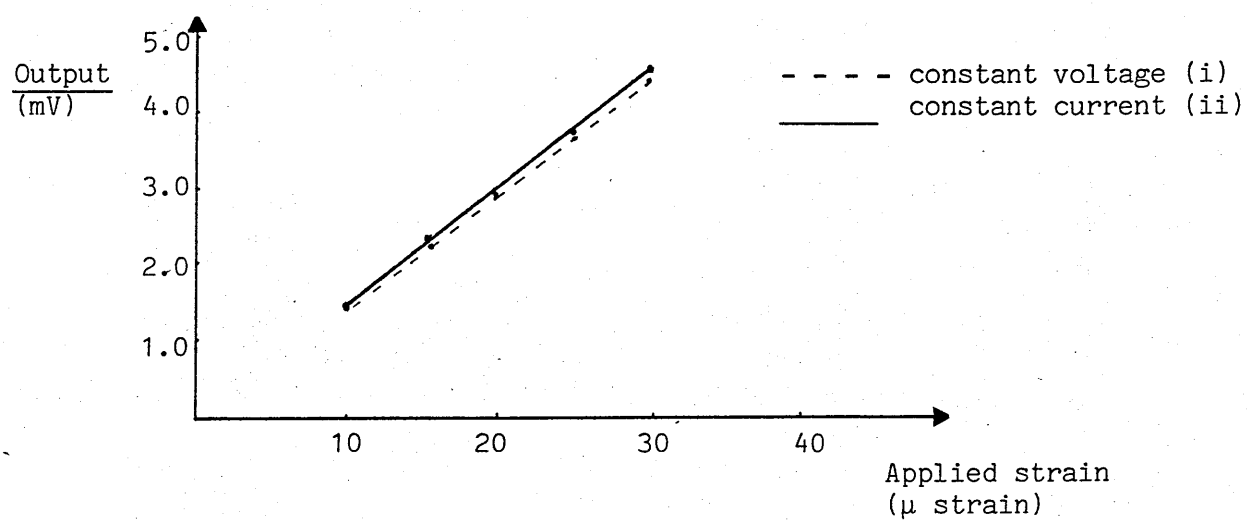

Bridge Output versus Strain for a 'quarter active' bridge
(i) Constant voltage energization
(ii) Constant current energization

Figure 3.7.4

For constant voltage Wheatstone bridge energization it was shown that output voltage (equation 3.2.5) is:

$$V_O = V_i \left[\frac{dR}{4R + 2dR} \right]$$

If the energization voltage for the constant current case is V_i in balance, then the constant current $I_0 = V_i/R$

Then, when a strain is applied,

$$V_0 = V_i' \left[\frac{dR}{4R + 2dR}\right] \qquad 3.7.13$$

where V_i' has changed to maintain the current constant. The new bridge resistance will be 2R and 2R + dR in parallel

$$\text{ie } R' = \frac{2R\,(2R + dR)}{(4R + dR)} \qquad 3.7.14$$

$$\text{Hence, } I_0 = \frac{V_i'\,(4R + dR)}{2R\,(2R + dR)} \qquad 3.7.15$$

$$= V_i/R, \text{ for constant current}$$

$$\therefore \quad V_i' = V_i \frac{2R\,(2R + dR)}{R\,(4R + dR)} \qquad 3.7.16$$

$$= V_i \frac{(4R + 2dR)}{(4R + dR)} \qquad 3.7.17$$

Thus, from equation 3.7.13,

$$V_O = Vi\left[\frac{4R + 2dR}{4R + dR}\right]\left[\frac{dR}{4R+2dR}\right] \qquad 3.7.18$$

$$= V_i\left[\frac{dR}{4R + dR}\right] \qquad 3.7.19$$

Compared with equation 3.2.5 for constant voltage energization, the only difference is the term dR instead of 2dR in the denominator. The figure 3.7.4 shows that there was no significant difference found in output voltage for constant current and constant voltage bridge energization using approximatley the same initial bridge voltage.

With regard to the brief study of half active bridges with different gauge configurations which was undertaken, Table 2 gives a

simple basis for comparison. All three pairs of gauges were of the same unstrained resistance at room temperature and the same gauge factor. The sample results in each case are of 30 μ strain, although the type of stress was not the same in each case.

CASE	LOCATION OF GAUGES	OUTPUT (dV)
(a)	In opposite arms of bridge (Gauges mounted side by side)	9.2 mV
(b)	In adjacent arms of bridge (Gauges mounted back to back)	9.1 mV
(c)	In adjacent arms of bridge (Gauge active lengths at right angles to each other)	5.8 mV
(A quarter active bridge gave 4.5mV)		

Sample Results for 'half active' Bridge with Gauges in Different Configurations using Constant Voltage Energization

Table 2

The sample outputs given in Table 2 were all obtained with a symmetrical bridge arrangement. For cases (a) and (b) the result is, allowing for temperature and small differences between gauges, double

that obtained for a quarter active bridge. This is in keeping with theory since, for a quarter active bridge (equation 3.2.7) the output voltage $V_0 \simeq V_i \left(\frac{K\varepsilon}{4}\right)$, and for half active bridge, as was indicated in section 3.6, for cases (a) and (b), $V_0 \simeq V_i \left(\frac{K\varepsilon}{2}\right)$. In case (c) the output voltage is higher by a factor of 1.3 (since $\nu = 0.3$ for steel) which is again in keeping with theory, because, as was shown, for this case $V_0 \simeq V_i \left[\frac{1+\nu}{4}\right] K\varepsilon$

When a full bridge system was used it was found, as expected, that when the 4 semiconductor strain gauges employed were subjected to the same applied strain (eg 30 μ strain) as applied to a single comparable gauge, the output was four times greater (ie 18.2 mV compared with 4.5mV) at the same ambient temperature. The only appreciable advantage observed in electronics terms, was that all the lead wires and connectors from the measuring point to the measuring system are outside the measuring circuit. This means that the errors arising from lead wires, connectors and plugs tend to cancel.

In all the subsequent work in this study constant voltage bridge energization has been used for simplicity, rather than constant current, since little difference was found between them.

It was found that satisfactory amplification of bridge outputs could be achieved using the operational amplifier arrangement outlined in Appendix 1.

3.8 SUMMARY

The advantages of using a Wheatstone bridge circuit with semiconductor strain gauges are that it avoids complications arising from large zero offsets and enables compensation to be provided for temperature effects.

Compensation for the non-linear resistance change versus applied strain characteristics of semiconductor strain gauges can be achieved by circuit compensation measures. One way of achieving this is to exploit the basic non-linearity of Wheatstone bridge circuits. Another way is to use either two or four semiconductor strain gauges in a push-pull arrangement such that non-linearities cancel out. A measure

of compensation may also be achieved by using a matched pair of p and n type gauges since the former increase in linearity with increase in tension and the latter increase in linearity with increasing compression.

Concerning excitation levels for semiconductor strain gauges account must be taken of heat dissipation and this is a function of adhesive thickness and the surface area of the gauge. Typical power dissipations may be up to 50 mW but larger gauges can tolerate 100 mW power dissipation, although zero stability may be reduced.

Although constant current energization has been recommended for use with semiconductor strain gauges by Stein[54] there was no evidence found which suggests that it is significantly superior to constant voltage gauge energization (which is also simpler to use). In fact, simple analysis suggests the opposite. However, constant current gauge energization produces a larger change in output voltage with applied strain than constant voltage energization under the same conditions, as the results obtained confirm.

There is no significant difference in bridge output with applied strain for constant current or constant voltage bridge energization.

However, depending on the gauge configuration, a half active bridge will give twice the output voltage of a quarter active bridge for the same applied strain, and a fully active bridge will give an output voltage which is four times greater. The advantage of this bridge is that, since all lead wires and connectors from the measuring point to the measuring system are outside the measuring circuit, then errors arising from lead wires and connectors tend to cancel. For all the bridge systems the out of balance mode is most practicable for dynamic strain measurement. If levels or changes of applied strain are small, and large output signals are required, an operational amplifier (Appendix 1) can be usefully employed with strain gauge bridge systems.

CHAPTER 4

Semiconductor Strain Gauge Thermal Characteristics and Temperature Effect Compensation

4.1 INTRODUCTION

Semiconductor strain gauges exhibit the following undesirable thermal characteristics, to a greater degree than wire or metal foil gauges:

(a) Temperature coefficient of resistivity

(b) Temperature coefficient of gauge factor

(c) Apparent strain induced by differential thermal expansion between the gauge and substrate

(d) Variation of gauge non-linearity with temperature change.

The latter only applies to semiconductor strain gauges and, like the first two, it is influenced by both the type and degree of doping of the semiconductor material.

An experimental investigation was undertaken of the temperature coefficient of resistance of silicon semiconductor strain gauges and then means of compensating for the shift in bridge zero with temperature change were explored. The basic theory of the temperature coefficient of gauge factor and the effect of dopant level on this was briefly examined prior to carrying out detailed investigations of measures devised to compensate for the temperature coefficient of gauge factor.

A brief investigation was then undertaken of means of compensating for temperature effects on gauge circuits. Following this, general observations and comments, concerning semiconductor strain gauge thermal characteristics and temperature effect compensation, are presented to reinforce and broaden the findings and conclusions.

4.2 TEMPERATURE COEFFICIENT OF RESISTANCE

The temperature, or thermal, coefficient of resistance (TCR) of a strain gauge relates to the change in resistance dR, of an unstrained gauge of initial resistance R at a given temperature, for a particular temperature change dT.

$$TCR = (dR/R)/dT \qquad 4.2.1$$

For an unstrained, bonded semiconductor strain gauge of resistance R_0 at temperature T_0, the resistance R_T, at an increased temperature T (where $T = T_0 + dT$) is:

$$R_T = R_0 (1 + r_B\, dT) \qquad 4.2.2$$

Where r_B is the bonded temperature coefficient of resistance of the semiconductor strain gauge.

The resistance, and variation of resistance with temperature, of extrinsic semiconductors decrease as the dopant level is increased. Moreover, since the number of dopant atoms in extrinsic semiconductor material is limited, at very high temperatures the resistance versus temperature charactersistic of an extrinsic semiconductor approaches that of intrinsic semiconductor material, which varies with temperature as:

$$\text{resistivity } \rho = \alpha\, e^{\beta/T} \qquad 4.2.3$$

α and β are constants and T is the absolute temperature.

The temperature variation of resistivity for heavily and lightly doped semiconductor material is shown in figure 4.2.1.

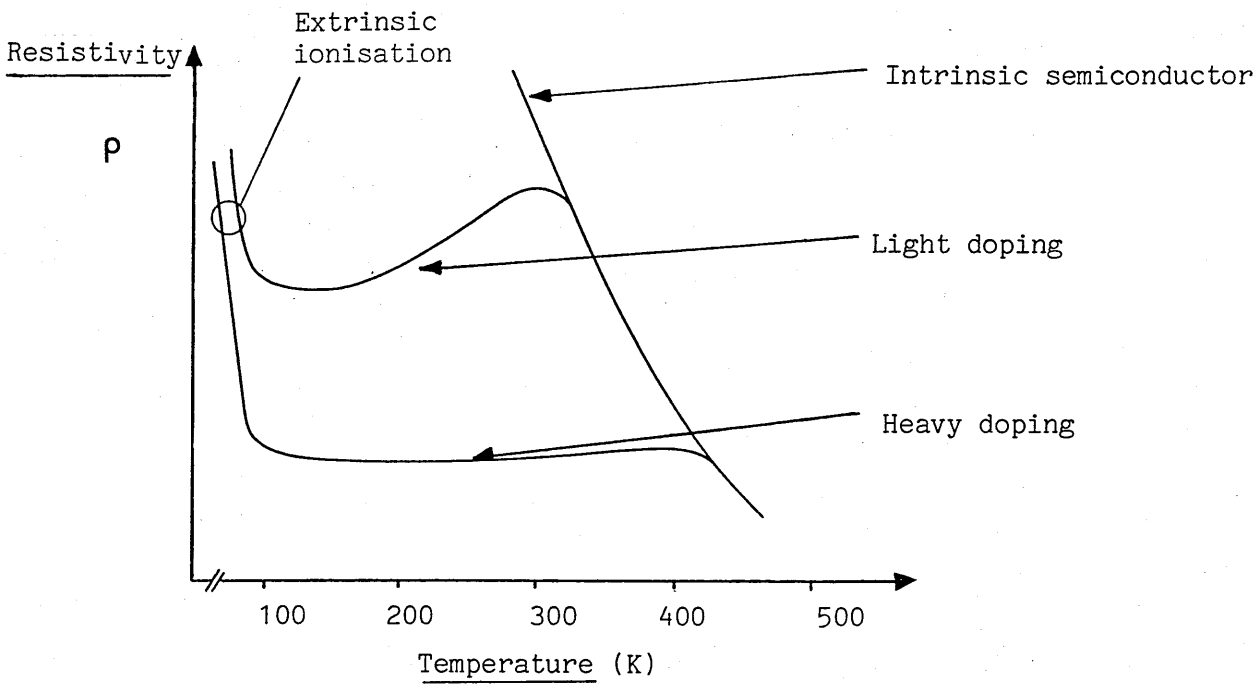

Temperature Variation of Resistivity for Heavily and Lightly Doped Semiconductor Material[55]

Figure 4.2.1

If the resistivity of a semiconductor strain gauge is relatively high (eg > $1 \times 10^{-2}\ \Omega$ m) due to a low dopant level, then the temperature

coefficient of resistance will be large. However, if the gauge resistivity is low (eg < 1×10^{-4} Ωm) then the temperature coefficient of resistance will be small (ie the resistance variation may be only a few percent for a temperature variation from room temperature to 350K). Typical relationships are illustrated by figure 4.2.2. Here R_0 is the resistance of the unstrained gauge at room temperature and R_T is the resistance of the gauge at increased temperatures up to 550K.

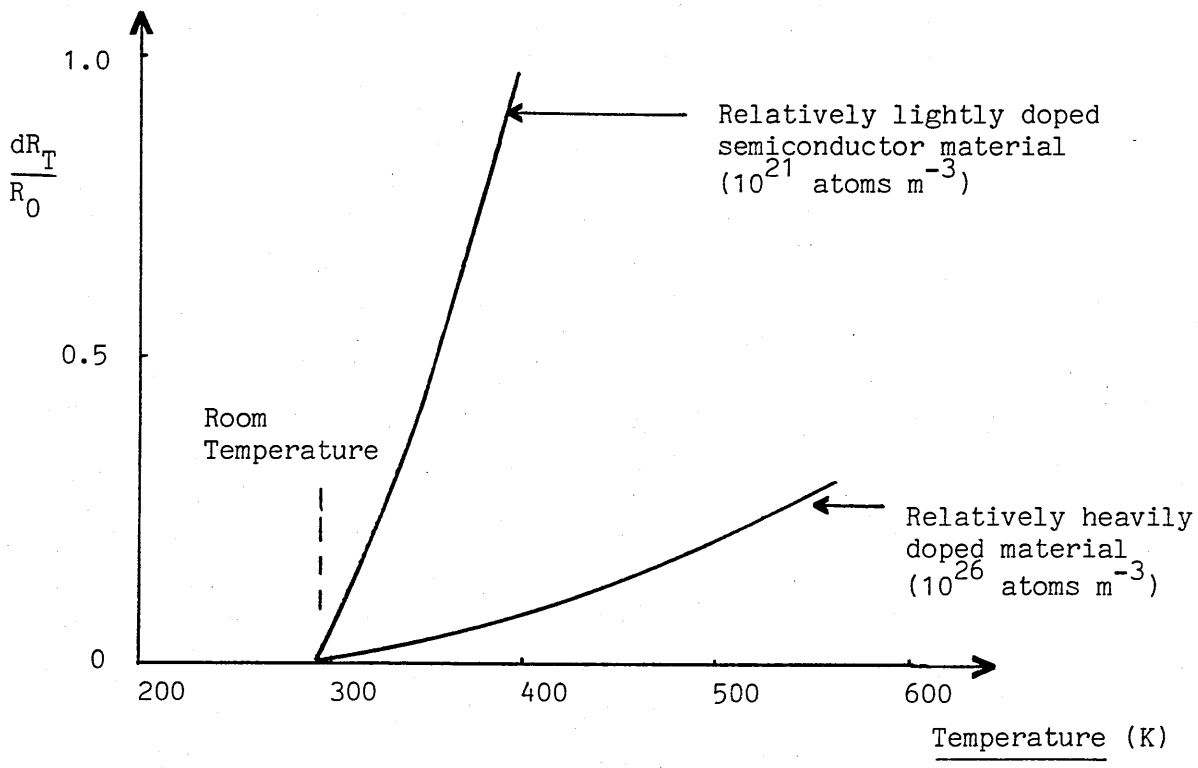

Relative Variation of Resistance of Silicon Semiconductor Strain Gauges with Temperature Variation

Figure 4.2.2

The characteristics illustrated by figure 4.2.2 are for p-type silicon [111] and n-type silicon [100]. Although the temperature coefficient of resistance is positive for the temperature range shown in figure 4.2.2, at very low temperatures it is negative.

For temperatures greater than approximately 600 to 700K semiconductor strain gauges behave according to the inverse (on a logarithmic scale) absolute temperature law of intrinsic semiconductors (equation 4.2.3) and exhibit a negative temperature coefficient of resistance. However, such temperatures are above those at which semiconductor gauges are generally employed.

Figure 4.2.3 shows experimental results obtained for the variation of resistance with temperature of an unstrained p-type silicon strain gauge of gauge factor 140. The gauge, which had a backing, was bonded, using P2 polyester adhesive as described in the previous chapter, to thin stainless steel strip 20 mm wide and 300 mm long. Initially this was placed in a thermostatically controlled refrigeration unit. It was later transferred to a thermostatically controlled oven. Resistance readings were taken over a range of temperatures (each accurate to $\pm$2K) after allowing the temperature to stabilize each time. The resistance

was measured using a digital ohmmeter (accurate to $\pm 0.01\Omega$) and dummy leads were employed for temperature compensation. As a check, readings were later obtained for a nominally identical strain gauge over the same range of temperatures. Very similar results were obtained for this gauge. Using the gradient of the graph (figure 4.2.3) the temperature coefficient r was found to be 17.6% per 100K, which corresponds closely to that cited by the manufacturer.

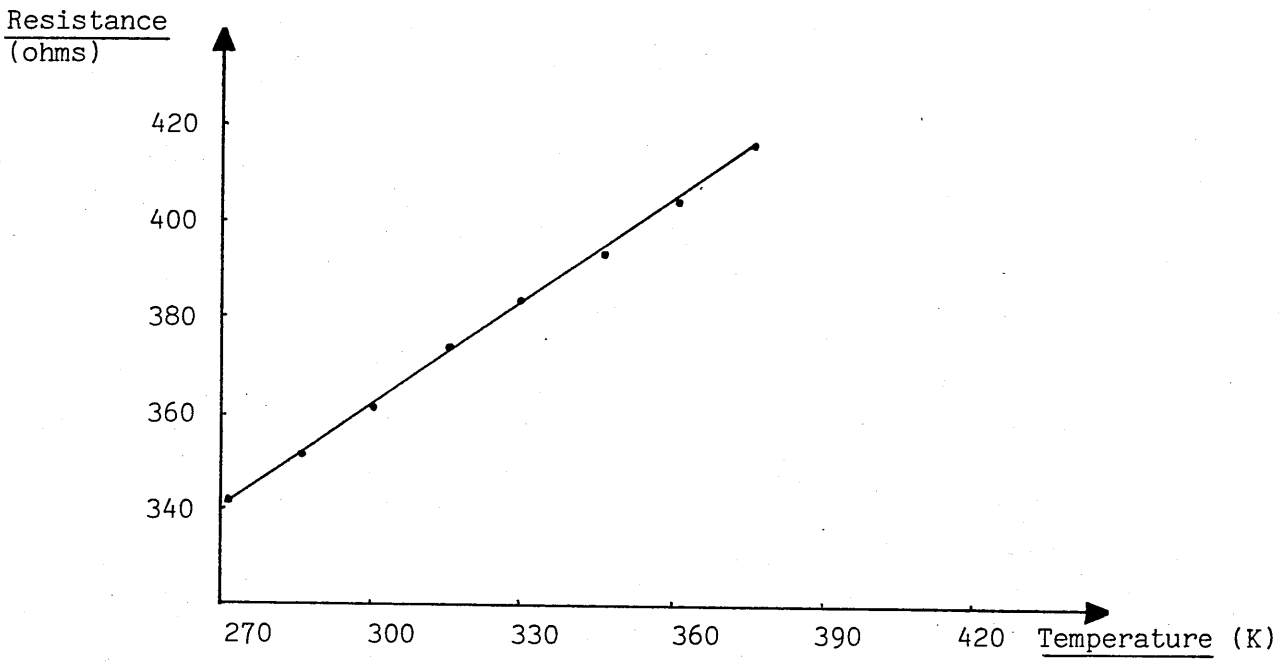

Variation of Gauge Resistance With Temperature

Figure 4.2.3

Values quoted by manufacturers for r are generally for unbonded gauges. The bonded temperature coefficient of resistance r_B consists of two parts, namely an intrinsic temperature coefficient of resistance r and an apparent strain contribution due to the difference in thermal expansivity between the gauge and the substrate. Hence, if the gauge is bonded to a substrate of coefficient of thermal expansivity α_S then:

$$r_B = r_S + (\alpha_S - \alpha_G) k \qquad 4.2.4$$

Where α_G is the coefficient of thermal expansivity of the semiconductor strain gauge and k is the gauge factor. For silicon α_G is about 2.5×10^{-6} mm/mm/K. Table 3 gives typical values of r, expressed as a percentage per 100K, and gauge factor, for p and n-type gauges of various doping levels.

p-type silicon			n-type silicon	
r: % per 100K	k		r: % per 100 K	k
7.2	100		3.6	-100
5.4	115		10.8	-110
10.8	130		23.4	-120
18.0	140		28.8	-130
32.4	155		43.2	-135

Temperature Coefficient of Resistance r, for Different Gauge Factors
(Based on values given by Kulite[56])

Table 3

When wire or metal foil gauges are used their thermal expansivity coefficients may be modified to provide compensation for the apparent strain arising from the differential coefficient of thermal expansivity of the substrate. This is not possible in the case of semiconductor strain gauges and other means of compensation must thus be devised.

4.3 COMPENSATION FOR THERMAL ZERO SHIFT

This shift in bridge zero due to gauge resistance change with temperature can be compensated for in four main ways:

(i) Use of dummy gauge

(ii) Self-compensation

(iii) Dual element resistors

(iv) Parallel resistors.

(i) It was found that when a single p-type silicon gauge was used it was possible to provide temperature compensation for zero shift by introducing a dummy gauge in the bridge circuit. This was put in a gauge pair arrangement, as in figure 4.3.1. It was necessary to locate the

dummy gauge isothermally with the active gauge for precise compensation to be achieved, although such locations are not always convenient or practicable. With this arrangement a zero shift of 250 mV with a 50K temperature rise was reduced to 0.1 mV.

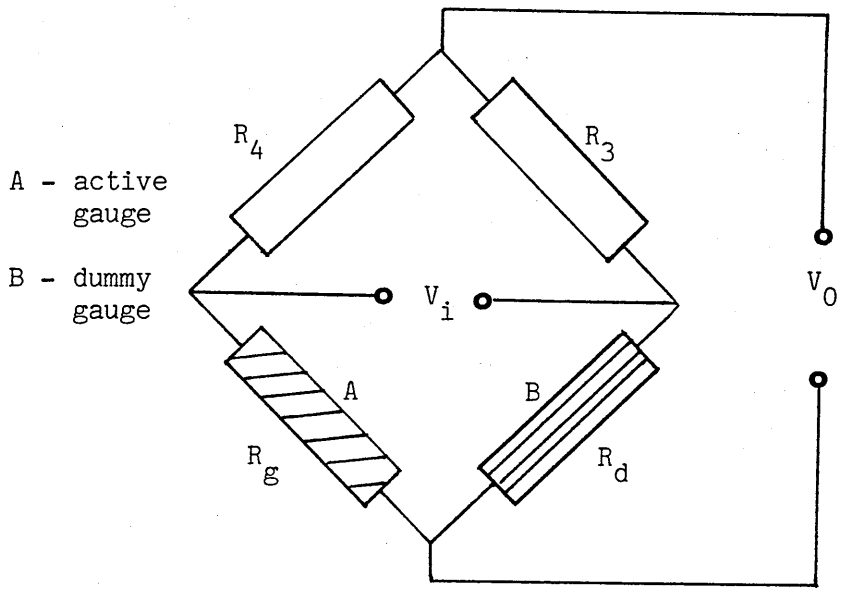

Zero Shift Compensation with Dummy Gauge

Figure 4.3.1

(ii) Zero drift can be reduced with self-compensation in an n-type silicon strain gauge. As shown in Table 3, semiconductor strain gauges made from n-type material have negative gauge factors. From equation 4.2.4 it can thus be seen that the value of r_B, the TCR of a bonded gauge, will be zero or have a negative value if the differential thermal expansivity $(a_S - a_G)$ is greater than r, the unbonded TCR.

(iii) It is possible to obtain dual element (ie p-type and n-type pairs) silicon semiconductor strain gauges. If these are put in adjacent arms of a Wheatstone bridge, then, depending on the value of α_S for the substrate, self-compensation can be accomplished.

In this case the thermal zero output voltage will equal zero when (for n-type gauges having k_n and r_n and p-type gauges having: k_p and r_p)

$$\alpha_S = \alpha_G + \frac{r_n - r_p}{|k_n| + k_p} \qquad 4.3.2$$

(NB Additional trimming using small pieces of wire with a high TCR inserted into appropriate arms of the bridge can further reduce apparent strain levels.)

(iv) When four p-type silicon strain gauges are used in a Wheatstone bridge circuit there will be zero output voltage for no applied strain if the bridge is exactly balanced (ie $R_1 R_3 = R_2 R_4$). However, there will be a thermal zero shift if the TCR of each arm is not identical. The latter condition is not easily achieved because the resistance of each gauge, bonding to substrate and bonded TCR must all be identical. Nevertheless, if a fixed resistor R_F, which has a low TCR is

connected across the arm of the bridge which has the largest TCR (eg R_2) this will reduce the effective TCR of that arm and so compensation for thermal zero shift is achieved. Simultaneously, the bridge can be re-balanced for zero strain by connecting a series resistor R_s, across the open node of the bridge as shown in figure 4.3.2.

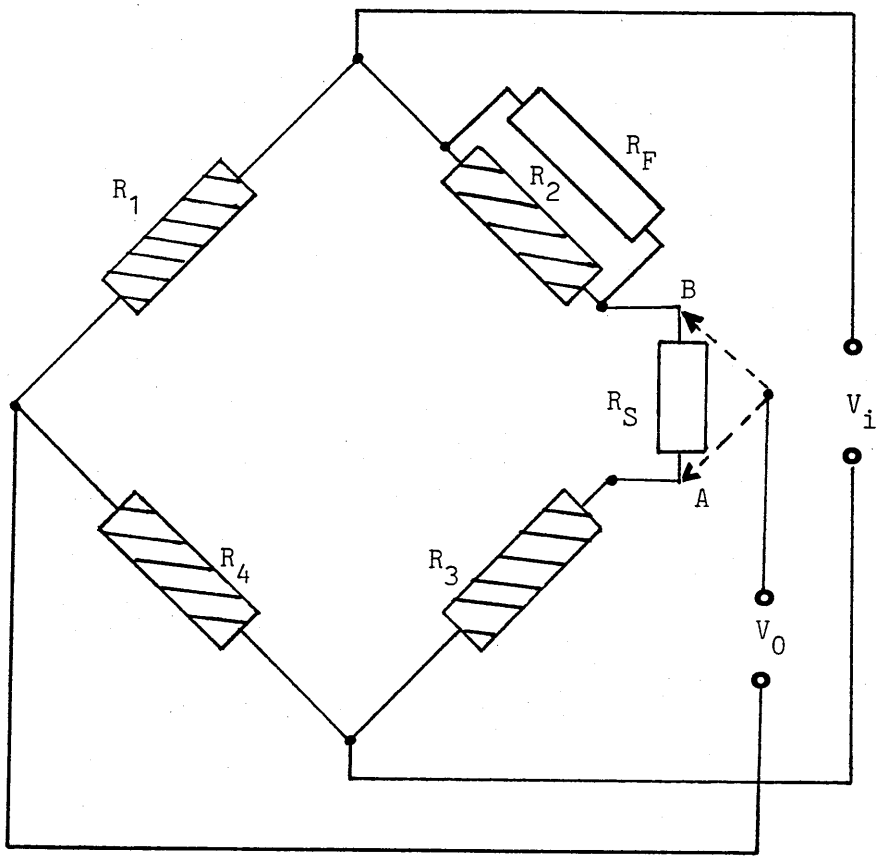

Modified Wheatstone Bridge for Thermal Zero Shift Compensation and Non-Zero Null

Figure 4.3.2

An experiment was carried out to explore this. The task of selecting the required series resistance R_S was achieved by initially using a decade resistance box for R_S and adjusting this until there was zero output voltage for no applied strain. Then the required value of resistance and the arm of the bridge (ie A or B in figure 4.3.2) to which it was connected was noted, as was ambient temperature, which was 293K.

The gauge assembly was then placed into a low temperature oven and the temperature raised (by 50K). After measuring the output voltage for no applied strain and noting its polarity a second decade resistance box (for R_F) was put in parallel with the bridge arm which had the largest TCR (as indicated by the polarity of the zero shift). A series of values for resistor R_F were substituted and, at each substitution, the value of R_S was adjusted to give zero output voltage for zero strain. The values of R_F and R_S were noted each time and then the gauge assembly was removed from the oven and allowed to return to the initial temperature of 293K.

The same pairs of values of R_F and R_S used at the elevated temperature were then substituted, in turn, at the lower temperature until no output was observed. Only one pair of resistances gave zero output voltage for both the low and elevated temperatures. Once this had been done the decade boxes were replaced by fixed resistors of the appropriate values.

In practice it was found that metal oxide resistors, which have a low TCR ($< 1 \times 10^{-4}\ \Omega\ K^{-1}$) were suitable for this application. A typical value for R_S which was used was 7Ω and the corresponding value for R_F was $20\ k\Omega$. For a different elevated temperature than that explored a different value pair of resistors would have been required.

If computer matched gauges are used then, according to some semiconductor strain gauge manufacturers,[57] thermal zero shift compensation may not be necessary for a number of applications.

4.4 TEMPERATURE COEFFICIENT OF GAUGE FACTOR

The gauge factor k not only depends upon the level of doping but also varies as a function of temperature. This is illustrated by figure 4.4.1 which shows the gauge factor of p-type silicon gauges at various degrees of doping and different temperatures. For silicon, r the temperature coefficient of resistance is positive but G, the temperature coefficient of gauge factor, is always negative. However, like resistivity, the magnitude of G decreases with increasing level of doping.

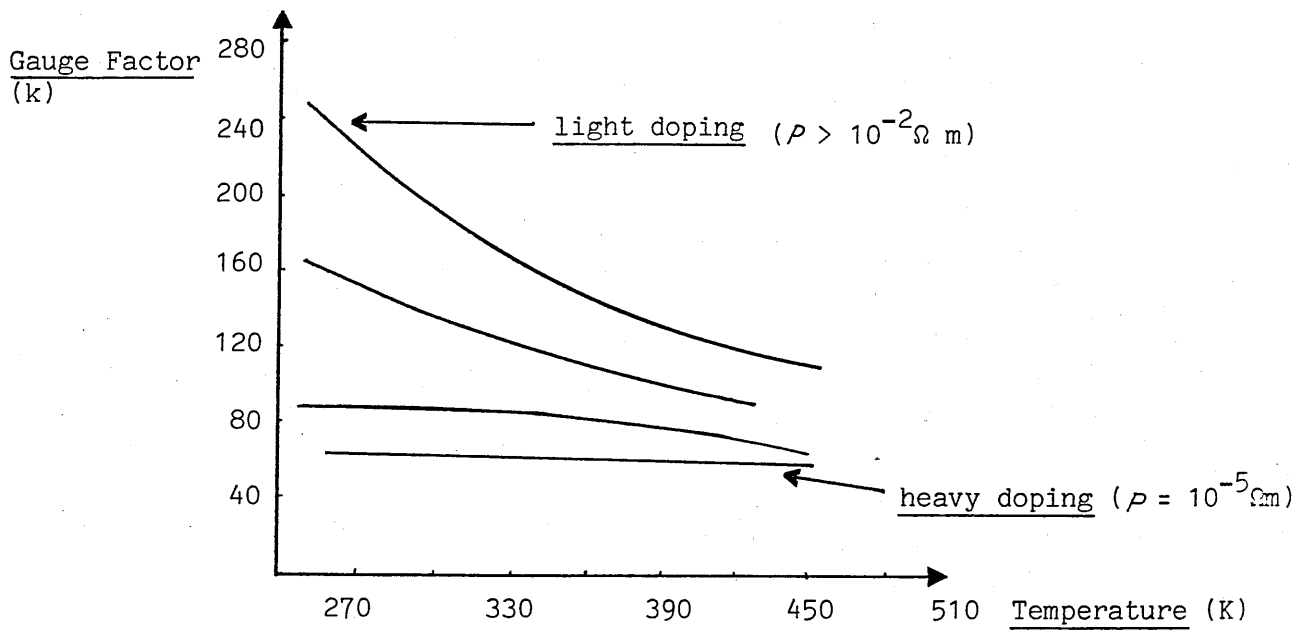

Variation of Gauge Factor with Temperature for Different Levels of Doping (p-type silicon)

Figure 4.4.1

If levels of doping are high (> 10^{25} atoms m^{-3}) then the gauge factor is virtually independent of temperature. However, partly because of the difficulty in producing highly doped material of uniform impurity concentration on a production basis, manufactured gauges have somewhat lower levels of doping (< 10^{24} atoms m^{-3}) and gauge factors such as those shown in Table 4. If higher levels of doping are used the gauge factor is reduced accordingly.

p-type silicon			n-type silicon	
Gauge Factor. k	Temp coeff of gauge factor: G (% per 100K)		Gauge Factor. k	Temp coeff of gauge factor: G (% per 100 K)
100	- 10.8		-100	-21.6
115	- 14.4		-110	-23.4
130	- 18.0		-120	-27.0
140	- 19.8		-130	-32.4
155	- 23.4		-135	-36.0

(Values are for unbonded gauges based on values given by Kulite[56]

Temperature coefficient of gauge factor

Table 4

The linear temperature dependence of k may be expressed as:

$$K_T = K_0 (1 + GdT) \qquad 4.4.1$$

k_T is the value of the gauge factor at an elevated temperature T, where T = T_0 + dT, and k_0 is the gauge factor at temperature T_0. The unbonded temperature coefficient of gauge factor is represented by G, for which typical values are given in Table 4.

Account must be taken of the interaction between a semiconductor strain gauge and the substrate to which it is bonded because E, the Young's modulus of the substrate, can change with temperature. The magnitude of E for many common materials decreases with temperature according to the linear relationship:

$$E_T = E_0 (1 + m\, dT) \qquad 4.4.2$$

Where T is an elevated temperature, equal to T_0 + dT, and m is the temperature coefficient of Young's modulus (thermoelastic coefficient). Hence, the effective temperature coefficient of gauge factor G_B, for a bonded semiconductor strain gauge, is:

$$G_B = G - m \qquad 4.4.3$$

For most metals m is approximately minus 4% per 100K rise in temperature.

4.5 COMPENSATION FOR TEMPERATURE COEFFICIENT OF GAUGE FACTOR

Investigations were carried out of five possible means of compensating for errors arising from G, the temperature coefficient of gauge factor. A fundamental difference between the first two means investigated was the type of circuit energization employed. Two other means involved different ways of providing constant current through the strain gauge in a bridge circuit. The five methods may be put into four main groups A, B, C and D; as follows:

A (i) Circuit compensation for constant voltage bridge supply

(ii) Circuit compensation for constant current bridge supply

B Constant current through gauge using series resistor

C Compensation using thermistor(s)

D Compensation by matching temperature coefficients of resistance and gauge factor.

Method A (i)

For constant voltage circuit energization compensation can be achieved with a series resistor R_S, introduced into the bridge circuit as shown in figure 4.5.1.

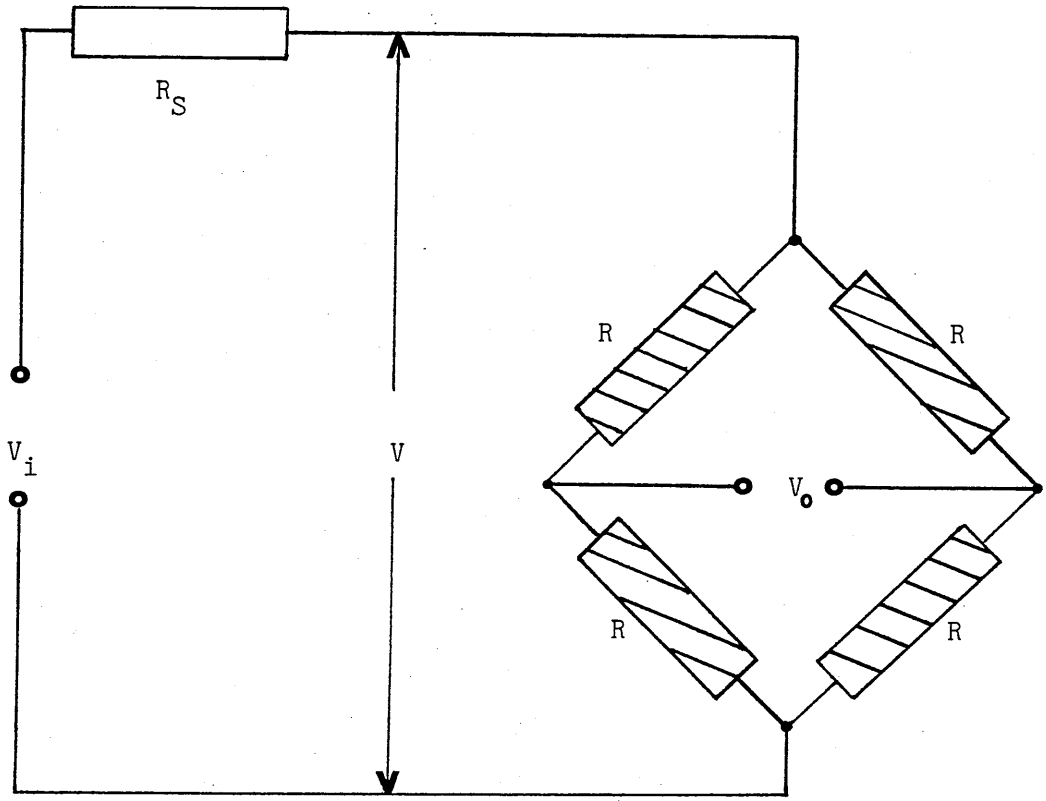

Circuit for Constant Voltage Supply to Compensate for Loss of Strain Sensitivity with Temperature Increase

Figure 4.5.1

Compensation is achieved, in this case, by virtue of the fact that the temperature coefficient of gauge resistance is positive while the temperature coefficient of gauge factor is negative (see Tables 3 and 4 respectively) for p-type silicon gauges.

This was investigated experimentally and it was found that, provided the magnitude of the temperature coefficient of gauge resistance was greater than that of the temperature coefficient of gauge factor for the bonded strain gauge, it was possible to select a value for R_S (which acts as a voltage divider) such that, when the temperature is increased, the voltage at the strain gauge was increased at a rate equal to the decrease in gauge factor.

The circuit can be considered as a voltage divider with the bridge treated as a single resistor with a positive temperature coefficient of resistance and the bridge voltage is caused to vary in proportion to the ratio of the two resistances. Thus when the temperature increases V_0 falls R rises, reducing current, increasing V and thence restoring V_0.

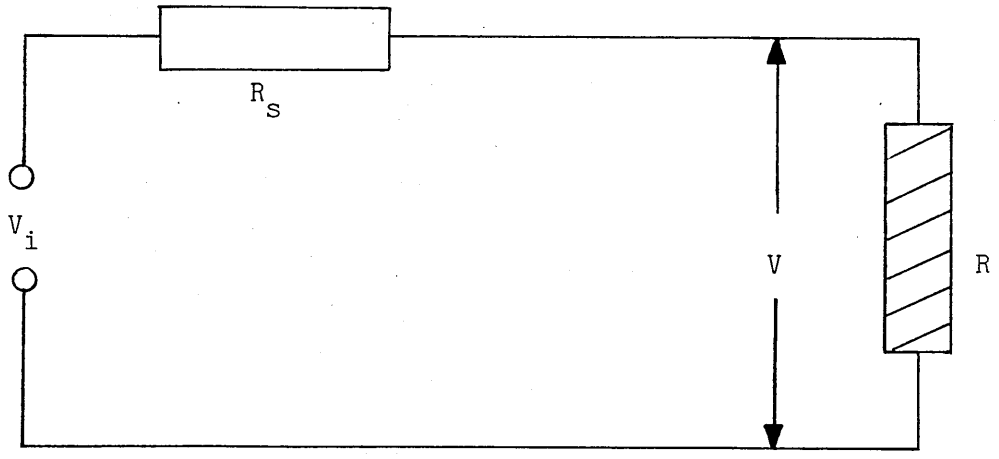

Basic Thermal Compensation Circuit for Constant Voltage Energization

Figure 4.5.2

From figure 4.5.2 it can be seen that the gauge (or bridge) energization voltage V is:

$$V = V_i [R/(R_S + R)] \qquad 4.5.1$$

Where V_i is the (constant) voltage input and R is the gauge resistance. If four strain gauges are used in a symmetrical bridge the bridge input resistance is also R and changes with temperature according to the relationship:

$$R_T = R_0 (1 + r_B dT) \qquad 4.5.2$$

R_0 is the resistance at room temperature and R_T is the resistance at an elevated temperature T (ie $T = T_0 + dT$). As in equation 4.2.2, r_B is the bonded gauge temperature coefficient of resistance.

Now at room temperature T_0 the application of a strain ε produces a signal output dV_0, which, from equation 4.5.1, will be given for a full bridge by:

$$dV_0 = V_i \, [R_0/R_s + R_0)] \, k_0 \varepsilon \qquad 4.5.3$$

At an elevated temperature T, the signal output was dV_T, where:

$$dV_T = V_i \, [R_T/(R_s + R_T)] \, k_T \varepsilon \qquad 4.5.4$$

From equation 4.4.1, $k_T = k_0 \, (1 + GdT)$

$$\text{Thus, } dV_T = V_i \left[\frac{R_0 \, (1 + r_B \, dT)}{R_s + R_0 (1 + r_B dT)} \right] k_0 \, (1+GdT) \, \varepsilon \qquad 4.5.5$$

(In the case of constant current energization V_i is replaced by IR.)

Compensation is achieved if $dV_T = dV_0$, and so R_s is found by equating equations 4.5.3 and 4.5.5.

According to Kulite[56] this gives:

$$R_s/R_0 = |G_B| \left[[r_B/(1 + r_B\, dT)] - |G_B| \right]^{-1} \qquad 4.5.6$$

To a first approximation the term $r_B dT$ is much less than 1. Thus:

$$R_s/R_0 \simeq |G_B| \,/\, (r_B - |G_B|) \qquad 4.5.7$$

but, from equation 4.2.4, $r_B = r + (a_s - a_G)\, k$

$$\therefore\ R_s/R_0 \simeq \frac{|G_B|}{r + (a_s - a_G)\, k - |G_B|} \qquad 4.5.8$$

It can be seen from equation 4.5.7 that compensation may be achieved provided that $r_B > |G_B|$.

The value of r_B is the same for a full bridge as for a single bonded gauge, but for a half active bridge the value is half that of a single bonded gauge.

This method of thermal compensation was tested with a p-type silicon gauge bonded to stainless steel, with an unstrained resistance of 351Ω at room temperature. The gauge factor at room temperature was 140, the bonded temperature coefficient of gauge factor G_B was - 13% per 50K and the bonded temperature coefficient of resistance r_B, calculated from equation 4.2.4 was 20.1% per 50K. Thus the gauge satisfies the criteria that $r_B > |G_B|$. Then, using equation 4.5.7:

$$R_S = \underline{643}\ \Omega$$

To examine the effect of employing a series resistor of this value the gauge was subjected to 300 μ strain at room temperature (293K), then again at a temperature of 343K using the circuit shown in figure 4.5.1, but with a single gauge. The output voltage was recorded in each case and again with the compensating resistor removed. Table 5 gives these output voltages.

Temperature (K)	dV (mV)
293 (with compensation) 343 " 343 (without compensating resistor)	52.0 50.8 47.4

Output Voltage for Compensated and Uncompensated Gauge

Table 5

The difference in output for the compensated and uncompensated gauge at 343K is roughly equivalent to a reduction of 20 μ strain. The strain measured at 343K using this circuit is approximately 2% less than that measured at room temperature. This is within the experimental error incurred in transferring the loading system into the oven. Even this level of improvement may prove acceptable over a limited temperature range.

Method A (ii)

For constant current energization a shunt resistor R_p, in parallel with the bridge supply, was used. In this case the resistor was

selected such that it acted as a current divider so that the voltage at the strain gauge(s) increased at a rate which was equal to the decrease in gauge factor with rise in temperature. Figure 4.5.3 shows the circuit used for this. Constant current energization was provided using the system described in section 3.5.

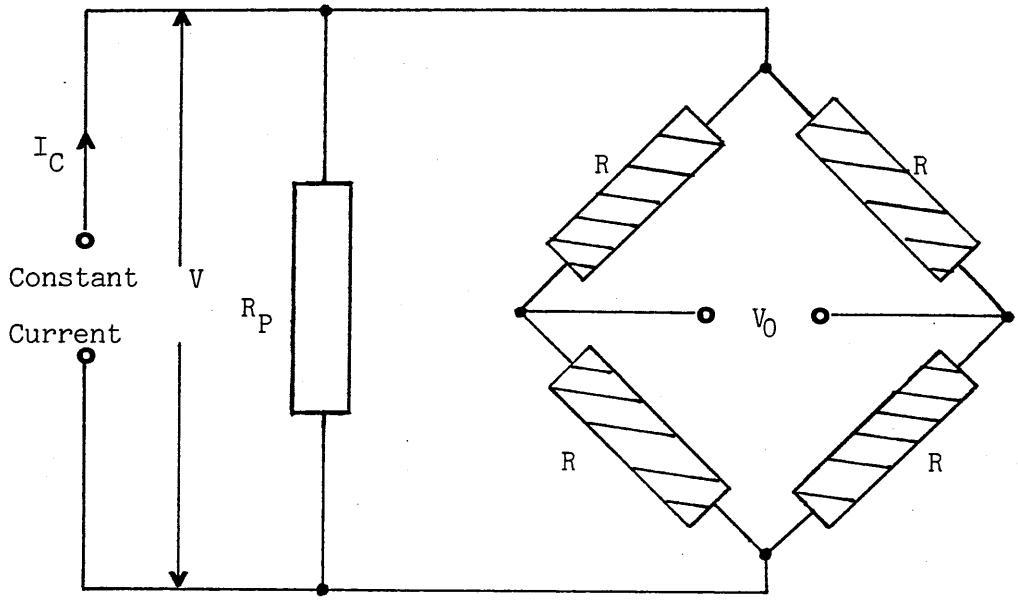

Constant Current Circuit Compensation for Loss of Strain Sensitivity with Temperature rise

Figure 4.5.3

This means of compensation was investigated experimentally using the same gauges, temperature increase and applied strain as used in the constant voltage energization investigation. In this case equation 4.5.1 becomes:

$$V = I_c R_p [R/(R_p + R)] \qquad 4.5.9$$

As before, the gauge resistance at room temperature is R and, for a symmetrical bridge of four gauges of resistance R, the bridge input resistance is R, and changes with temperature accordinging to equation 4.5.2. By Thevenin's theorem, R_p works out to be the same value resistance as the series resistance with constant voltage energization.

When tested experimentally, using the same applied strain and elevated temperature as in the constant voltage case, it was found that the uncompensated strain magnitude was 19 μ strain lower than that measured when the compensating shunt was introduced. As before, the compensated strain magnitude was lower (almost 2%) than that measured using this circuit at room temperature.

If high precision is required then measurements would need to be taken so that the actual temperature coefficients of gauge factor and resistivity could be detemined for the particular bonded gauge(s) rather than using manufacturer's values. Then the calculated values of R_s or R_p

would provide compensation for loss in gauge factor with temperature rise which would be specific for the gauge(s) and conditions.

Method B

When the temperature of a semiconductor strain gauge increases, R increases and since k is proportional to dR/R, it is decreased. This contribution to gauge factor reduction can be eliminated (Neubert[16]) by keeping the gauge current constant, since output voltage is then proportional to dR not to dR/R.

If constant voltage bridge energization is employed it is still possible to provide approximately constant current through a gauge by simply putting a high resistance in series with it. (This method was not tested experimentally.)

Method C

Compensation similar in principle to method A, but which can be used with any relative values of r_B and G_B, can be achieved by using a thermistor with a negative temperature coefficient of resistance (NTC). This can be either in series or parallel with a fixed resistor in order to adjust the resistance and TCR of the combination. The values must be

chosen for this so that the voltage across the bridge increases (due to the decrease in thermistor resistance with temperature increase) to compensate for the reduction in circuit sensitivity.

Although this was not investigated experimentally, the arrangement shown in figure 4.5.4 could be used with either a single gauge or with several gauges in a bridge.

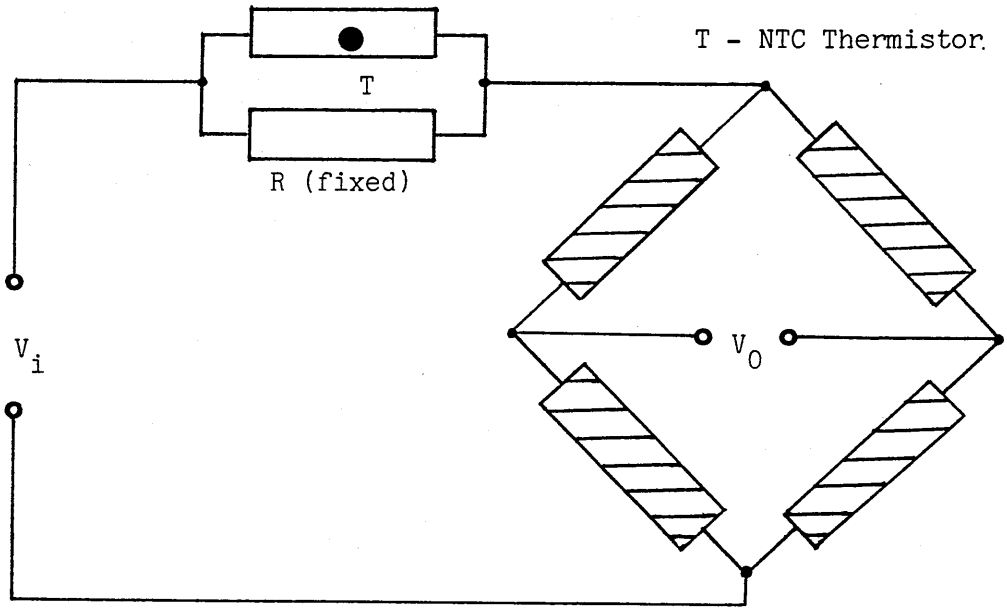

Temperature Coefficient of Gauge Factor Compensation using a Thermistor

Figure 4.5.4

It is necessary that the thermistor circuit is at the same temperature as the strain gauge(s).

Method D

Baker[32] points out that if the gauges have a bonded temperature coefficient r_B equal to, but of opposite sign to their temperature coefficient fo gauge factor, then if constant current bridge energization is used the bridge will be self compensated. Any adjustments required to the compensation can be made using a shunt resistor, as shown in figure 4.5.3.

4.6 COMPENSATION FOR TEMPERATURE EFFECTS ON CIRCUITS

In addition to changes in semiconductor strain gauge resistance and gauge factor with temperature change, when long leads are used there may be changes of lead resistance and also contact resistance with temperature. Although the effects are small they may be significant when gauges are compensated for temperature effects.

Mansfield[58] has shown that these additional changes will bring about a reduction in the gauge factor as follows:

$$k_N = k\,[R/(R + R_{L1} + R_{L2} + R_{C1} + R_{C2})] \qquad 4.6.1$$

k_N is the new, reduced gauge factor, R is the gauge resistance, R_{L1} and R_{L2} are lead resistances and R_{C1} and R_{C2} are contact resistances, as shown in figure 4.6.1.

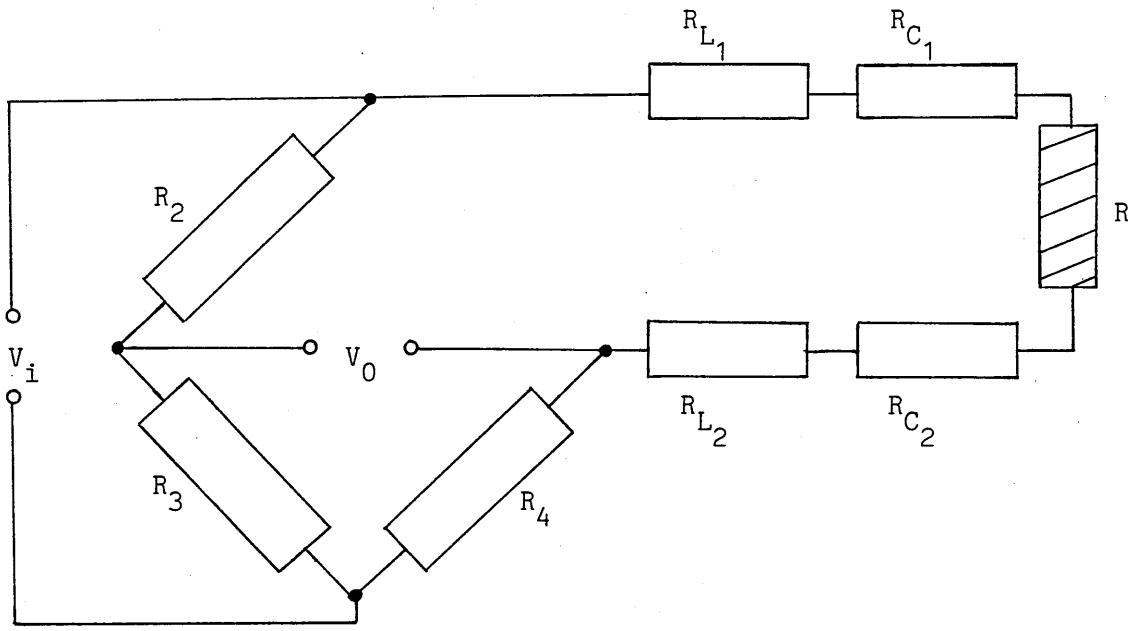

Two Lead Wire System for Quarter Active Bridge

Figure 4.6.1

If it is not possible to determine the reduced gauge factor then the effects may be reduced with a three lead wire configuration (figure 4.6.2).

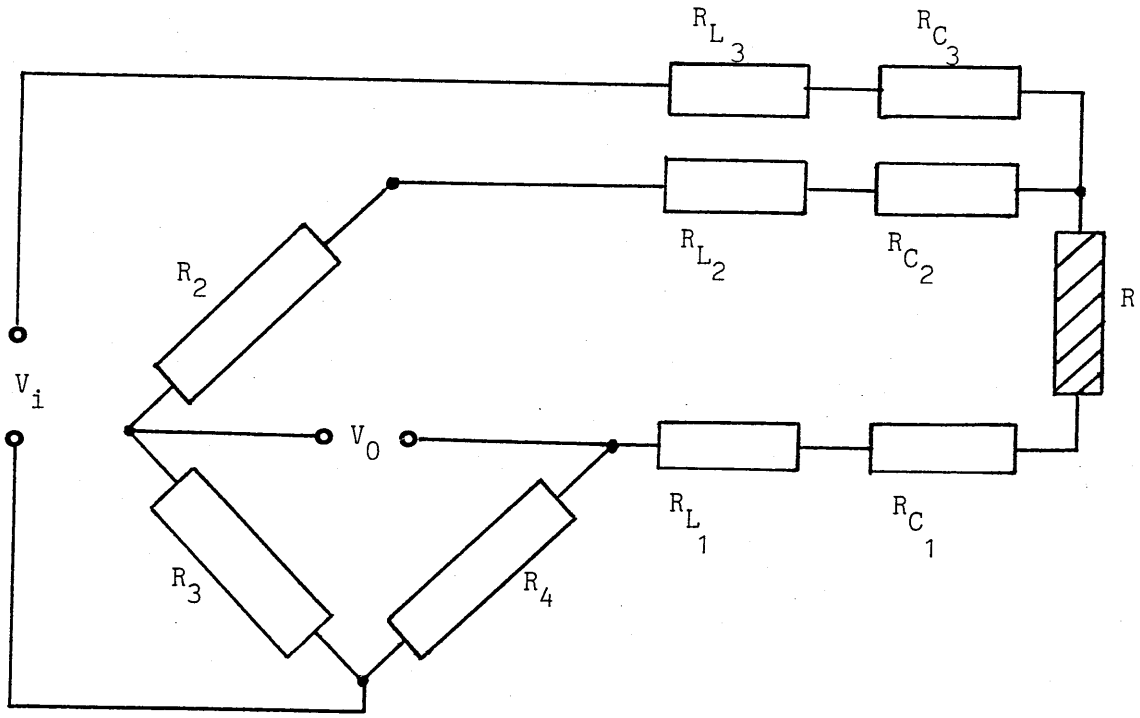

Three Lead Wire Configuration for Quarter Active Bridge

Figure 4.6.2

In effect, the extra lead transfers one of the original lead wires into an adjacent bridge arm (in this case the arm containing R_2). This is achieved by using the extra lead for the bridge supply and connecting it to the junction of the active gauge and one of the bridge completion leads. If R and R_2 are of the same value and if the two bridge completion wires have equal resistance, experience the same ambient conditions, have the same specific heat capacity and mass then the reduction in gauge factor can be halved (equation 4.6.3).

The balance equation must be modified to account for the change in lead resistance (dR_{L1} and dR_{L2}) and contact resistance (dR_{C1} and $dR_{C}2$) with temperature change. Thus it becomes:

$$[R+R_{L1}+dR_{L1}+R_{C1}+dR_{C1}]R_3=[R_2+R_{L2}+dR_{L2}+R_{C2}+dR_{C2}]R_4 \qquad 4.6.2$$

As can be seen from equation 4.6.2, R_{L1}, R_{C1} and R_{L2}, R_{C2} are on opposite sides of the equation. Thus effects are now attributable to differences between them (ie not their sum, as when a two lead wire system, such as shown in figure 4.6.1, is used). Moreover, the reduction in gauge factor (equation 4.6.1) is now covered by one lead only and so is reduced by a half to:

$$k_N = k\,[R/(R + R_{L1} + R_{C1})] \qquad 4.6.3$$

An experiment was carried out to explore this, employing a 1000Ω p-type silicon gauge. First, a two lead wire system (figure 4.6.1) using lead wires 5 m long was set up, and the entire circuit placed in an oven and the temperature raised by 50K. A load producing a known strain was

employed and the bridge output was measured using a digital voltmeter. A three lead wire system (figure 4.6.2) was then set up by adding another 5 m long lead wire to the two lead wire system. When the oven temperature was raised by 50K and the same strain applied as before, the measured bridge output was about 2% higher. This difference means that there are thermal effects which bring about a reduction in gauge factor.

It is suggested by Mansfield[58] that a balancing resistor should be placed across the bridge resistors (R_2 and R_3). Then any change in either the lead resistance (R_{L3}) or the contact resistance (R_{C3}) of the third lead and the bridge completion wire will not produce zero shift.

For a symmetrical bridge or for a half active bridge the third lead could be put in the output circuit. However, if it is put in the supply circuit it will induce less noise in the high impedance detector.

If an asymmetrical bridge is used, with the asymmetry across the supply ($R_2 \neq R_3$), then the third lead should only be in the supply circuit, since the lead must be in series with the same resistance value in order

for the compensation to be effective.

4.7 GENERAL OBSERVATIONS AND COMMENTS

As Welsh[59] has pointed out, the employment of inorganic bonding agents, rather than organic epoxy bonding, can result in improved thermal stability and, hence, improved accuracy of strain measurement. This is because inorganic bonding media generally have thermal expansivity coefficients similar to those of metal substrates.

When using semiconductor strain gauges care must be taken to avoid exceeding the safe gauge current, as indicated in section 3.5. Any reduction in gauge size must be accompanied by a reduction in gauge current, and if substrates have low thermal conductivity, then lower gauge currents are also recommended than for use with metal substrates.

Some manufacturers[60] have devised integrated semiconductor pressure transducers with passive temperature compensation using on-chip balancing resistors. The required resistor values are conventionally determined such that they affect the bridge balance. It is claimed[61] that, if the appropriate dopant level is selected and constant current energization is employed then almost complete compensation can

be achieved over a temperature range from somewhat below room temperature to more than 50K above room temperature. Integrated semiconductor transducers with on-chip passive temperature compensation have also been devised[61] for use at cryogenic temperatures.

An active temperature compensation system for use with semiconductor pressure transducers has been devised by Welsh et al[62]. This uses a temperature stable resistor in series with a regulated voltage supply and a bridge. If the bridge temperature changes the excitation current and hence the voltage across the resistor changes. This voltage is used to control continuously both the offset and gain characteristics of a signal conditioning amplifier. The amplifier and resistor are housed in a common unit which is remote from the pressure transducer. Under specified conditions, Welsh et al. claim to be able to reduce zero offset errors to $\pm$0.05% of full-scale reading per 50K and gain characteristics have been reduced from a 2% variation to 0.2% variation of reading for this same temperature range.

4.8 SUMMARY

Semiconductor strain gauges display four undesirable thermal characteristics to a greater degree than wire or metal foil gauges. Namely:

(i) Temperature coefficient of resistivity

(ii) Temperature coefficient of gauge factor

(iii) Variation of gauge non-linearity with temperature rise

(iv) Apparent strain induced by differential thermal expansion between the gauge and substrate.

The temperature coefficient of resistivity of semiconductor strain gauges is positive for temperatures from somewhat below room temperature to several hundred kelvin above room temperature. Increased dopant level reduces the magnitude of the temperature coefficient of resistivity.

The shift in Wheatstone bridge zero due to gauge resistance change with temperature can be compensated by:

(i) Use of dummy gauge(s)

(ii) Self-compensation

(iii) Dual element gauges

(iv) Parallel resistors.

The temperature coefficient of gauge factor is negative and can be reduced by increased dopant level. Compensation may be achieved by:

(i) Circuit compensation by series resistor (constant voltage)

(ii) Circuit compensation by parallel resistor (constant current)

(iii) Constant current through gauge using series resistor

(iv) Compensation using thermistor(s)

(v) Compensation by matching temperature coefficients of resistance and gauge factor.

Changes in lead and contact resistance with temperature can result in reduced output, but if a third lead wire is introduced into the bridge supply circuit this reduction can be halved.

On-chip passive temperature compensation systems for semiconductor pressure transducers have been devised, and active temperature compensation systems are currently being developed.

CHAPTER 5

Photoelectric Sensitivity of Semiconductor Strain Gauges

5.1 INTRODUCTION

Relatively high ambient light levels have been found to influence the resistivity of semiconductor strain gauges[18, 32]. Xavier and Vogt[63] observed both a photovoltaic and a photoconductive effect when silicon semiconductor strain gauges were illuminated with fluorescent light of quite high intensity (> 4000 lux). Both effects were reported as showing a maximum for illumination by sources with wavelengths between 800 nm and 900 nm, but were not found to influence significantly either gauge accuracy or response.

An attempt was made in the present study to explore the static photoelectric response of typical silicon semiconductor strain gauges illuminated by various light sources including monochromatic and high intensity sources. After undertaking various preliminary experimental investigations a detailed study was carried out to examine the dynamic photosensitivity of semiconductor gauges. This was done with gauges

illuminated by a xenon flash (of the type typically employed for photography) and quite a pronounced response, compared to the static response, was detected with the aid of a transient recorder.

5.2 OPTICAL RESPONSE OF P-N JUNCTIONS

The photovoltaic effect is normally observed when a p-n junction is illuminated by light of a suitable frequency and it is found that a voltage is developed across the junction. In this case the voltage is limited in magnitude to the barrier height of the particular junction. The polarity will be the same as the forward bias voltage when the junction is employed as a rectifier. The open-circuit photovoltage V_{oc} is given by:

$$V_{oc} = \frac{KT}{e} \ln \left[\frac{e A G (l_p + l_n)}{I_s} + 1 \right] \qquad 5.2.1$$

K is Boltzmann's constant T is the absolute temperature, e is the electronic charge, A is the area of the junction, G is the optical generation rate, l_p and l_n are the hole and electron diffusion lengths, respectively, and I_s is the reverse saturation current.

In the case of the semiconductor strain gauge there is no p-n junction but a photovoltaic effect may occur at the metal contact junction if they are not properly ohmic, but retain some rectifying characteristic. Similar behaviour to the p-n photojunction is expected.

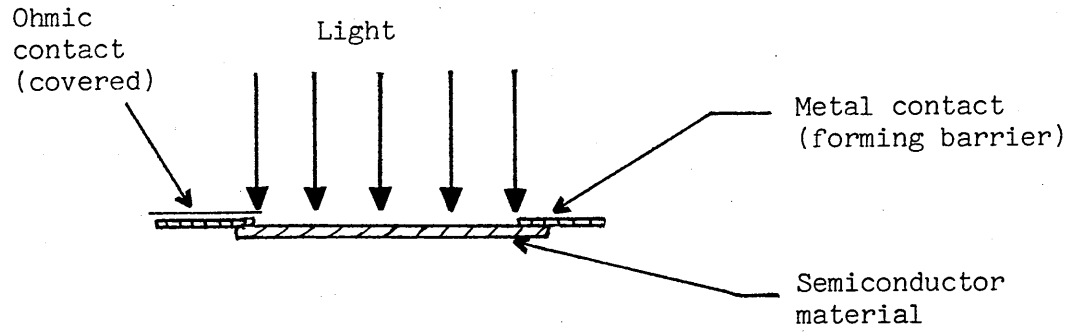

Semiconductor Gauge Under Light Radiation

Figure 5.2.1

The magnitude of the voltage measured, as in figure 5.2.1 between one of the metal contacts and the second contact, is equal to the photovoltage and is dependent on the dopant level.

The influence of illumination level is illustrated by figure 5.2.2, which shows photodiode characteristics for three different levels of illumination. This is photoconductive operation, and as can be seen, an increase in light intensity does not alter the shape of the characteristic but shifts it lower down the current axis.

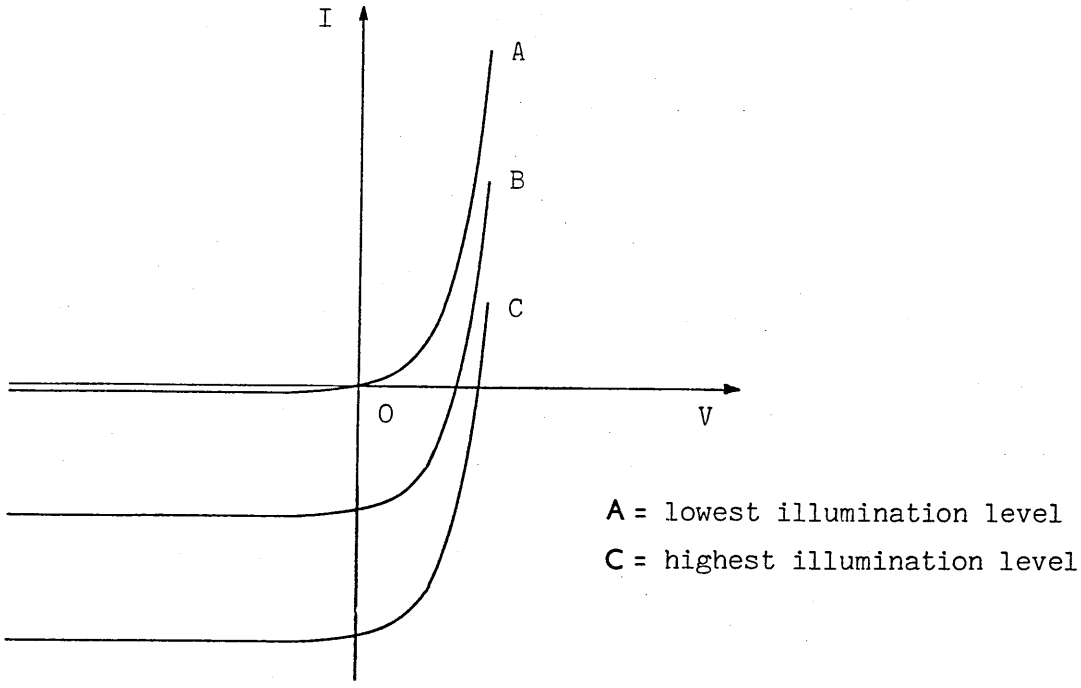

Diode Characteristics for Three Different Illumination Levels. To show the influence of light intensity. (Photo conductive operation)

Figure 5.2.2

The diode equation in this context is:

$$I = I_s \left[\exp \frac{eV}{KT} - 1 \right] - I_p \qquad 5.2.2$$

where the total diode current is I, I_s is the saturation current, I_p is the

optically generated current (photocurrent) and V is the voltage across the diode. The open circuit photovoltage is then given by the intersection of these characteristics with the voltage axis, and its variation with light intensity is illustrated in figure 5.2.3. The limit of the photovoltage is the contact potential of the junction. Thus, maximum photovoltage depends on the doping level.

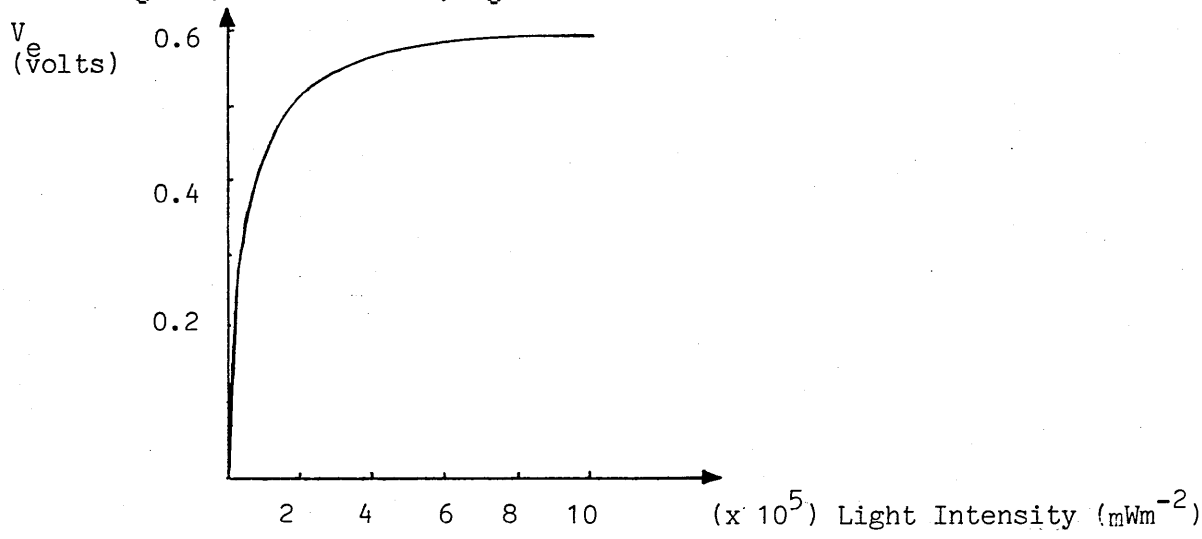

Photovoltage for a Silicon p-n Junction for Different Light Intensities (Pankove[64])

Figure 5.2.3

Although, for a semiconductor strain gauge, the dopant density is fixed, there will be a change in band structure, and hence barrier properties, when the gauge is strained. Thus the photovoltage V_e may change.

5.3 PHOTOCONDUCTIVITY IN BULK SEMICONDUCTORS

Photoconductivity is the increase in conductivity due to absorbed photons creating free carriers. If no light is incident on the semiconductor material shown in figure 5.3.1 then the only carriers present will be thermally generated ones.

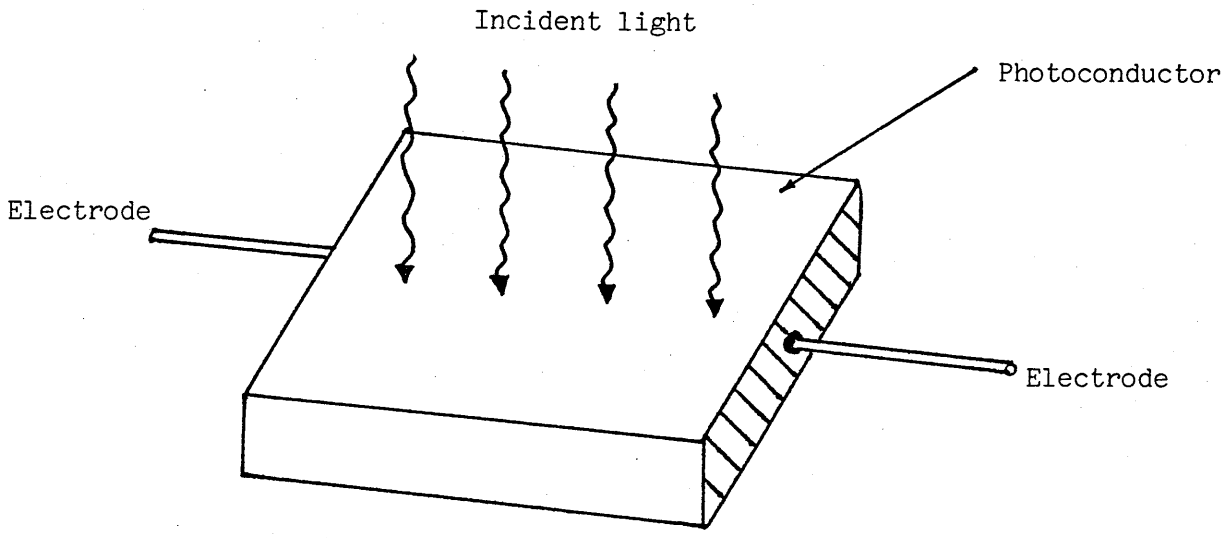

Photoconductor Under Illumination

Figure 5.3.1

When a bias is applied to the photoconductor with no light incident upon it the current flowing is known as the 'dark current'. If light is incident on the photoconductor there will be photogenerated electron-hole pairs produced in addition to the existing thermally generated population. This

additional current is known as the 'photocurrent'. This current is only detectable if it is a significant fraction of the dark current. The two basic cases to consider are intrinsic photoconduction and impurity photoconduction. The former is when a photon raises an electron from the valence band to the conduction band, hence producing a free electron and a free hole.

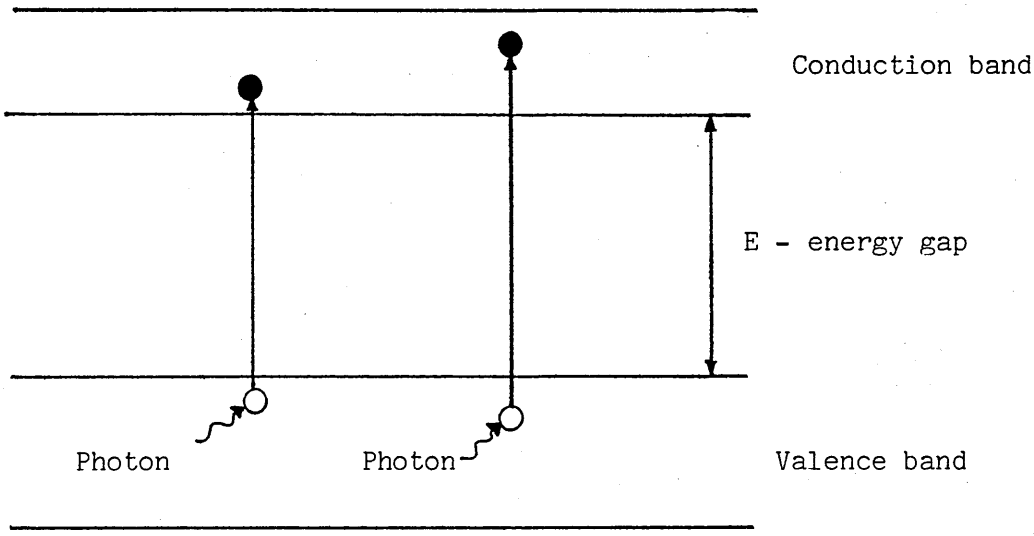

Photoconductivity

Figure 5.3.2

Impurity photoconduction occurs when a photon ionises an acceptor or donor atom. Only one free carrier is produced in this case. The energy required is far less than the band gap energy E (figure 5.3.2) of the semiconductor.

For a photoconductor to have high sensitivity to light it is necessary that mobility μ is high and carrier lifetimes are long. The number of electron-hole pairs generated per second N, depends on wavelength;

$$N = \eta P \lambda / (hc) \qquad 5.3.1$$

(η is the quantum efficiency, P is the optical power at wavelength λ, h and c are constants). The geometry of the device influences the sensitivity. To maximise the quantum efficiency at a given wavelength, the dimensions of the device must be in keeping with the absorbtion coefficient since, on passing through an absorbing medium, a beam of light is attenuated and the reduction in intensity I is proportional to the distance travelled.

If the intensity is reduced, over a distance δx, to $I - \delta I$ then:

$$\delta I / I = - \alpha \delta x \qquad 5.3.2$$

α is the absorbtion coefficient, and, in the limit:

$$dI/dx = -\alpha I \qquad 5.3.3$$

If I_0 is the intensity at the surface of the material, then after travelling a distance **x**, the intensity will be:

$$I = I_0 \exp(-\alpha x) \qquad 5.3.4$$

α varies with wavelength and, for silicon, the main feature is the absorbtion edge corresponding to photons with the band gap energy, at 1.13μm in wavelength. For shorter wavelength (higher photon energies) the absorbtion increases steeply. Thus, light from a blue source will be absorbed far more than light from a red source of illumination.

The responsivity of a photodiode is defined as the ratio of the photocurrent to the incident optical power. Figure 5.3.3 shows the characteristic for a silicon photodiode. As can be seen the peak response is at about 0.9μm. The spectral output of the xenon flash tube is mostly within the range of this device.

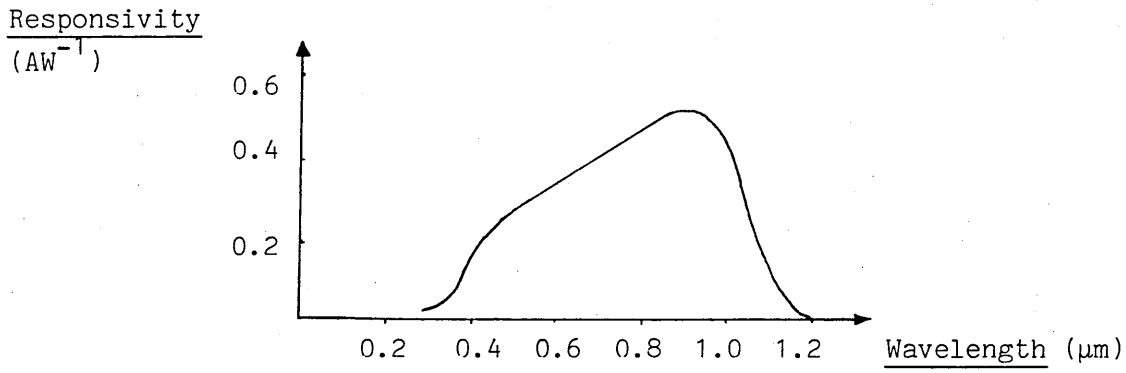

Responsivity Characteristic of a Silicon Photodiode

Figure 5.3.3

A p-i-n diode (p-type - intrinsic - n-type) consists of a layer of p-type material and a layer of n-type material, of typical doping densities 10^{24} atoms m^{-3} and 10^{22} atoms m^{-3} respectively, with a layer of very lightly doped material (eg 10^{20} atoms m^{-3}) between them. Hence the central region is almost intrinsic and the transition region is wide and virtually independent of both the exact doping level and voltage. Since the transition region is wide (where the photogenerated carriers drift) compared to the neutral regions (where relatively slow diffusion occurs) the p-i-n diode is a high speed device. Section 5.6 describes experiments to compare the dynamic photosensitivity of a p-i-n diode with that of p-type silicon strain gauges illuminated by the same source, a variable xenon flash unit.

5.4 INVESTIGATION OF STATIC PHOTOELECTRIC RESPONSE

This investigation was intended to provide qualitative information concerning the influence of static sources of illumination on the resistance of silcon semiconductor strain gauges. Since p-type silcon gauges are most commonly used the studies concentrated on these, of 500 Ω unstrained resistance at room temperature.

(i) Photovoltaic effect

Semiconductor strain gauges mounted on thin steel strip, as described in chapter 3, were chiefly employed for these studies. A special room was used which had a heater fitted with a thermostat to provide a constant temperature (292±1k). The gauges were located in a light-proof box which had an arrangement (see figure 5.4.1) to enable a known strain to be applied to the gauges. Light from the sources was passed through a tube so that it was incident normally on the gauges. As shown in figure 5.4.1, an infra-red absorber was fitted to the tube.

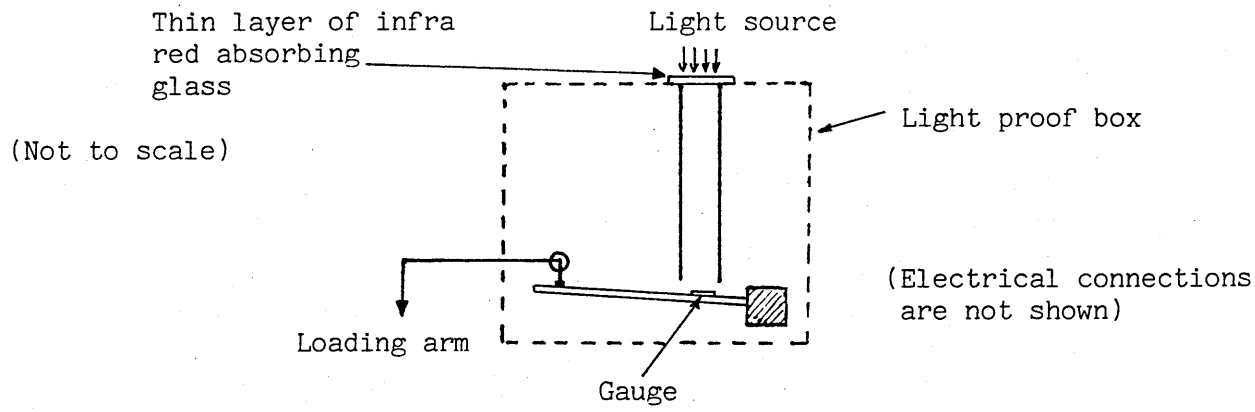

Basic Arrangement for Photoelectric Response Investigation

Figure 5.4.1

To explore a possible photovoltaic effect a small mask was made to cover the junctions of the lead terminals with the semiconductor material. The p-type silicon gauges were then illuminated for 100 seconds each time with a variety of light sources. Loads producing up to 300 μ strain on the gauges were employed.

When each of the following light sources was used, no open circuit voltage was detected when either junction was masked, when no junction was masked or both junctions masked. Neither was any voltage detected when each of these tests was repeated and the gauge subjected to various strains. The digital voltmeter used was set on a 50 μV range and could be read to 0.1 μ V.

Sources

(a) 60W tungsten filament lamp

(b) 80W flourescent tube

(c) 60W quartz halogen lamp: maximum illumination level 5000 lux at 0.01 m (operated at various power levels)

(d) 1mW (output) helium-neon laser: emission wavelength 600nm

(e) 60W ultra-violet lamp: emission wavelengths 300 to 400nm.

The fluorescent tube used was of somewhat higher intensity (about 5000 lux measured with a sensitive photometer) than that used by Xavier and Vogt[63], who did detect a small response.

The entire series of experiments was repeated, first, using p-type silicon strain gauges of unstrained resistance 350 Ω and 1200 Ω respectively, and second, using n-type silicon gauges of unstrained resistance 350Ω and 1000 Ω. In no case was an open circuit voltage detected. Neither was any voltage detected when the infra-red absorber was removed and the gauges illuminated with the various light sources.

As a check, the digital voltmeter used in these investigations was replaced by an oscilloscope. This could detect a voltage change of

0.01 μV, but it was not found that, for any of the strain gauges, a deflection corresponding to an open circuit voltage was produced on the oscilloscope screen.

No sign of rectifying properties were found from electrical measurements on the gauges. It is thus likely that photovoltaic effects seen by other workers are the result of poorly formed contacts which inadvertently possess Schottky junction characteristics.

(ii) Photoconductive effect

With both junctions of the silicon strain gauge covered by the mask investigations were undertaken to discover if the gauges exhibited a photoconductive effect. The gauges were connected to a sensitive digital ohmmeter (resolution $\pm$0.001 Ω) and the change in resistance dR when the gauges were illuminated by the different sources of illumination was recorded. This was all carried out at room temperature (292K). Typical results obtained for a p-type silicon strain gauge located 100mm below the light sources, are given in Table 6.

No illumination	Illumination source	dR (ohms)
Unstrained Resistance R (with no light) 515.002 ohms (steady reading over 5 minutes)	Daylight (not sun) Fluorescent tube Laser (helium-neon) Quartz-halogen lamp	0.022 0.040 0.062 0.085

Change in Resistance, dR, for Different Sources of Illumination Compared to no Illumination

Table 6

When the gauge was subjected to an applied strain of about 300 μ strain (tensile and compressive strains were used) changes in resistance, dR', were again observed when the gauge was illuminated by the various sources. The magnitude of dR' was very slightly higher in each case, than when the gauge was illuminated but unstrained. For example, in the case of the quartz halogen lamp illumination the value of dR' was 0.088 Ω , compared to 0.085 Ω as given in Table 6. Although the difference between these figures is negligible in practice, the actual

magnitude of dR is equivalent to about 2 μ strain, and so cannot be ignored. Even with normal daylight dR is equivalent to over 0.5μ strain.

Similar corresponding characteristics were observed when p-type silicon gauges of unstrained room temperature resistance 350 and 1200 Ω and n-type silicon gauges of resistance 350Ω and 1000 Ω, were studied under the same conditions. In each case the sources of longer wavelength produced the greatest change in resistance. (The maximum again was equivalent to nearly 2 μ strain.) A small change in resistance was observed when each gauge was illuminated by an ultra-violet lamp which was equivalent to almost 1 μ strain.

When the infra-red filter was removed from the arrangement shown in figure 5.4.1 and the gauges were illuminated by sources such as the tungsten filament lamp (for 10 minutes), then, as expected, there was a gradual change in gauge resistance associated with the resulting increase in temperature. The greatest change for this source was equivalent to over 50 μ strain.

Since no calibrated light source or means of accurately controlling the power output of the sources was available, these

investigations were basically qualitative. However, since an immediate change in gauge resistance was found with the infra-red filter in position, and also when sources such as a fluorescent light and an ultra-violet light were used, a photoconductive rather than a purely thermal mechanism is indicated.

5.5 INVESTIGATION OF GAUGE DYNAMIC PHOTOSENSITIVITY (pilot study)

The response of gauges to a short duration flash of light under relatively low ambient light conditions was measured. An opaque tube 25mm long was located over the strain gauges to prevent stray light falling on them and a xenon flash tube was placed above this. For the pilot experiments the p-type gauges were provided with a 6V power supply and an appropriate value resistor, such that they were dc coupled with a transient recorder* as shown in figure 5.5.1. The output from the recorder was fed to a Hewlet Packard 85 microcomputer and then to an x/y plotter. As before, the gauge junctions were masked. The xenon flash unit had a fixed flash duration of 0.5 ms.

* (see Appendix 2 for details of this)

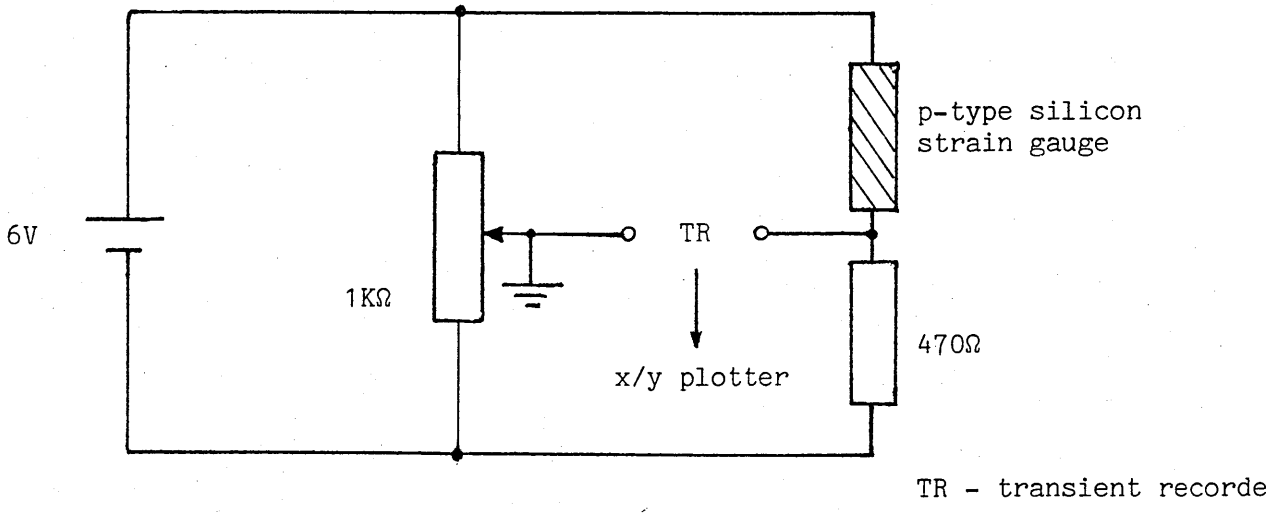

Basic Circuit Arrangement for Dynamic Photosensitivity Investigation

Figure 5.5.1

The bridge circuit was balanced by adjusting the 1K Ω potentiometer. Using the transient recorder sample rates of 2μs per sample (1024 samples) and 5μs per sample were employed. The strain gauge was illuminated normally with the xenon flash, which had a lens and reflector. These measurements were all undertaken at a temperature of 293 ±1K. To confirm that the response was attributable to optical radiation, the light from the flash tube was stopped by an opaque screen from reaching the surface of the strain gauge. No response was found in this case.

Representative data, obtained for p-type silicon gauges, of unstrained resistance 500Ω at room temperature, are shown in figures 5.5.2 and 5.5.3. These are for sample rates of 2μs and 5μs per sample, respectively. The output voltage change dV for these corresponds to almost 2μ strain.

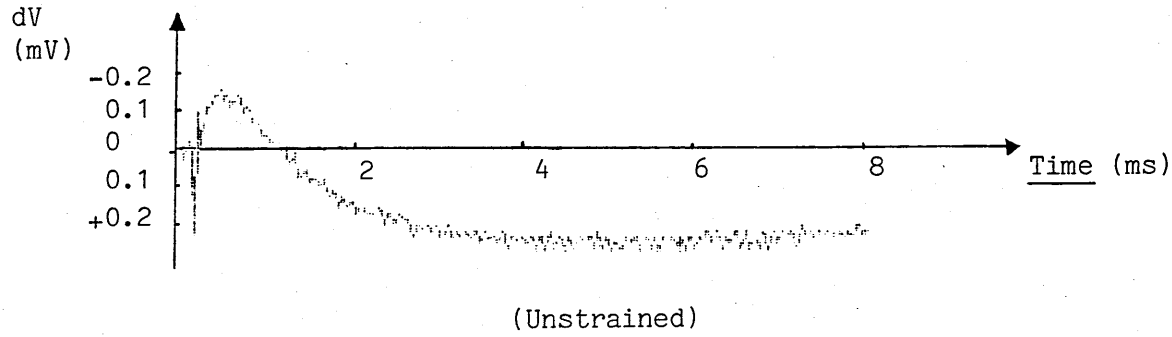

Response of p-type Silicon Gauge: 2μs per sample

Figure 5.5.2

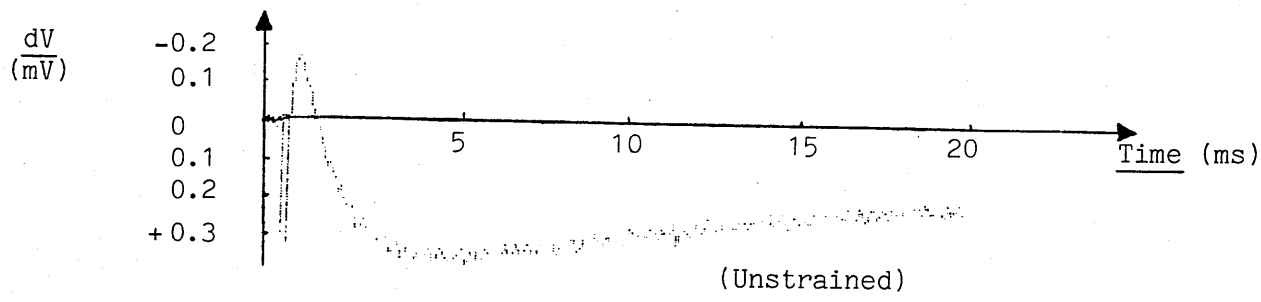

Response of p-type Silicon Gauge: 5μs per sample

Figure 5.5.3

Calculation of carrier drift and diffusion times

After undertaking various measurements with p-type silicon strain gauges, calculations were made in order to provide an estimate of the likely inherent response time of the gauges.

For example, the carrier drift transit time t, for a typical p-type silicon strain gauge of mobility 0.15 m^2/Vs, active length 0.5×10^{-3}m and field of 15×10^3 V m^{-1} is:

t = drift length /V

$= 0.5 \times 10^{-3}/(0.15 \times 15 \times 10^3)$

$= \underline{2 \times 10^{-7}\ s}$

If the carrier life time is very short (and evidence presented later will support this), then many carriers will not have time for transit and so photosensitivity will be low.

The diffusion time τ for such a gauge is:

$\tau = w^2/2D$. Where w is the diffusion distance (0.5×10^{-3}m) and D is the diffusion coefficient (0.0039 $m^2\ s^{-1}$ for electrons and 0.0012 $m^2 s^{-1}$ for holes in silicon).

Therefore, $\tau = \underline{2.56 \times 10^{-5} s}$ for electrons

and $\underline{8.33 \times 10^{-5} s}$ for holes.

Carriers take this amount of time to diffuse across typical p-type silicon strain gauges and a decay from a light signal is expected to last at least 100 μs. Much more is found, due to other mechanisms.

5.6 MAIN INVESTIGATION OF GAUGE DYNAMIC PHOTOSENSITIVITY

Having established that a photoconductive effect could be detected, a more comprehensive series of measurements were carried out on a variety of gauges.

In these investigations a variable duration xenon flash unit was employed. A p-i-n diode was also used to provide a basis for comparison of the dynamic photosensitivity of the silicon gauges. The basic system employed is shown in figure 5.6.1. To eliminate spurious electromagnetic effects the aperture and gauge mounting plate were earthed.

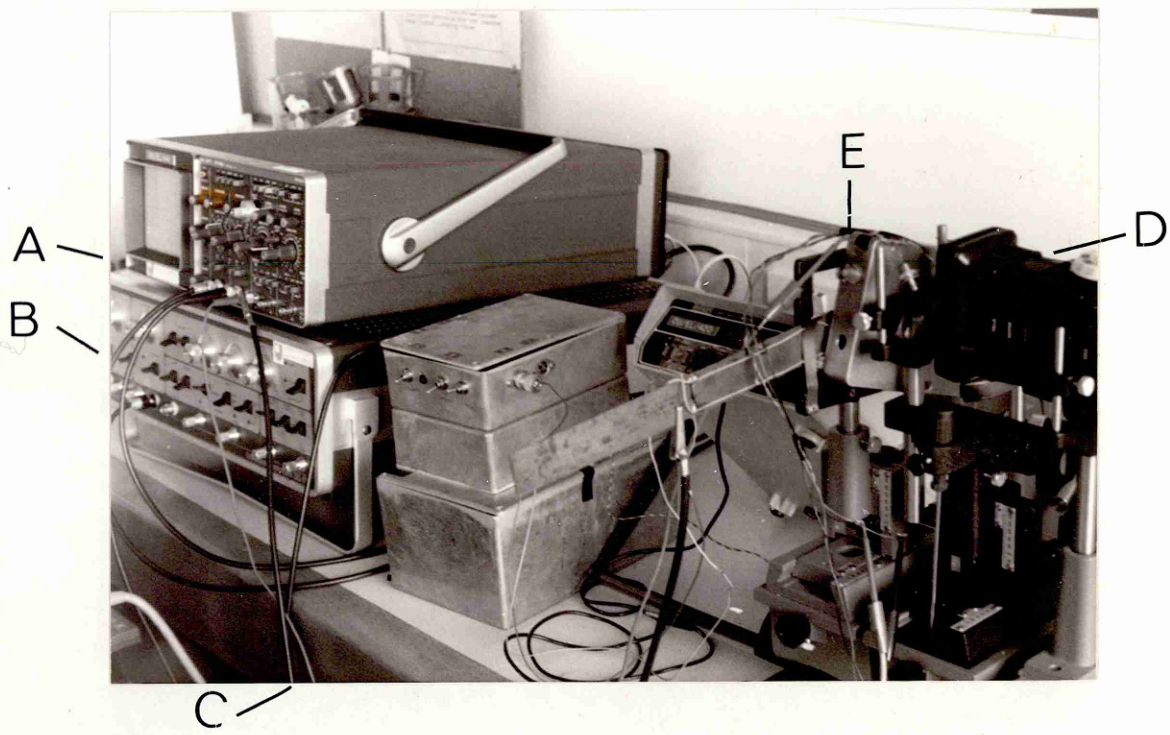

System Used in Main Experimental Investigation of Gauge Photoelectric Sensitivity with Xenon Flash Unit and Transient Recorder

Figure 5.6.1

The transient recorder (A) was connected to an oscilloscope for initial examination of the gauge response characteristic. After passing the information from the store of the transient recorder to the microcomputer (B) the characteristics could be processed and then printed using the x/y plotter (C). The top of the flash unit (D) can just be seen in front of the earthing plate which had the strain gauge (E) mounted behind it. Fuller details of the actual arrangement are shown schematically in 5.6.3.

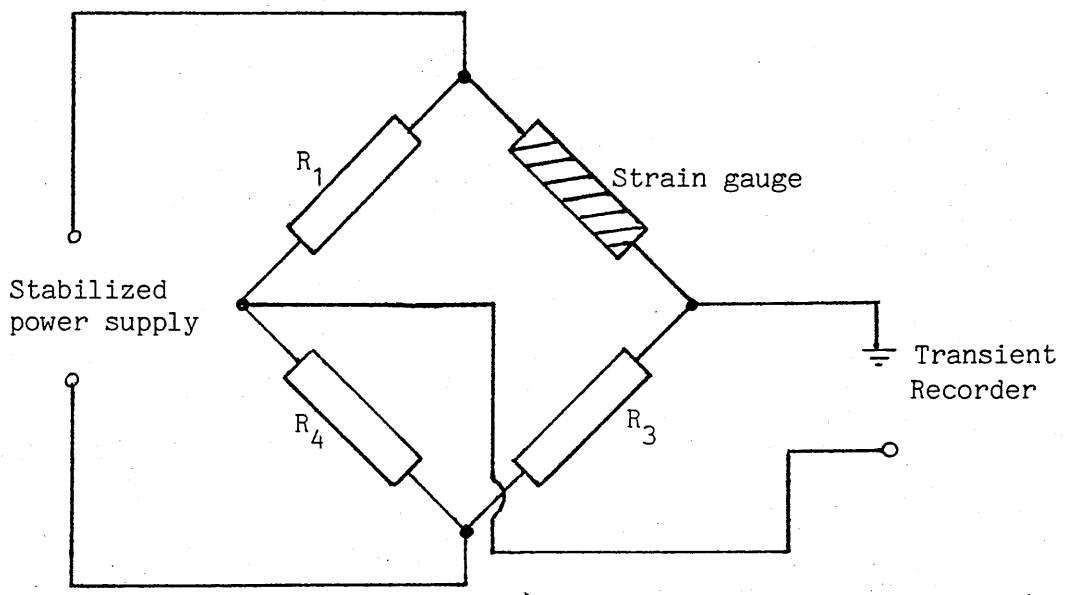

Basic Gauge Circuit

Figure 5.6.2

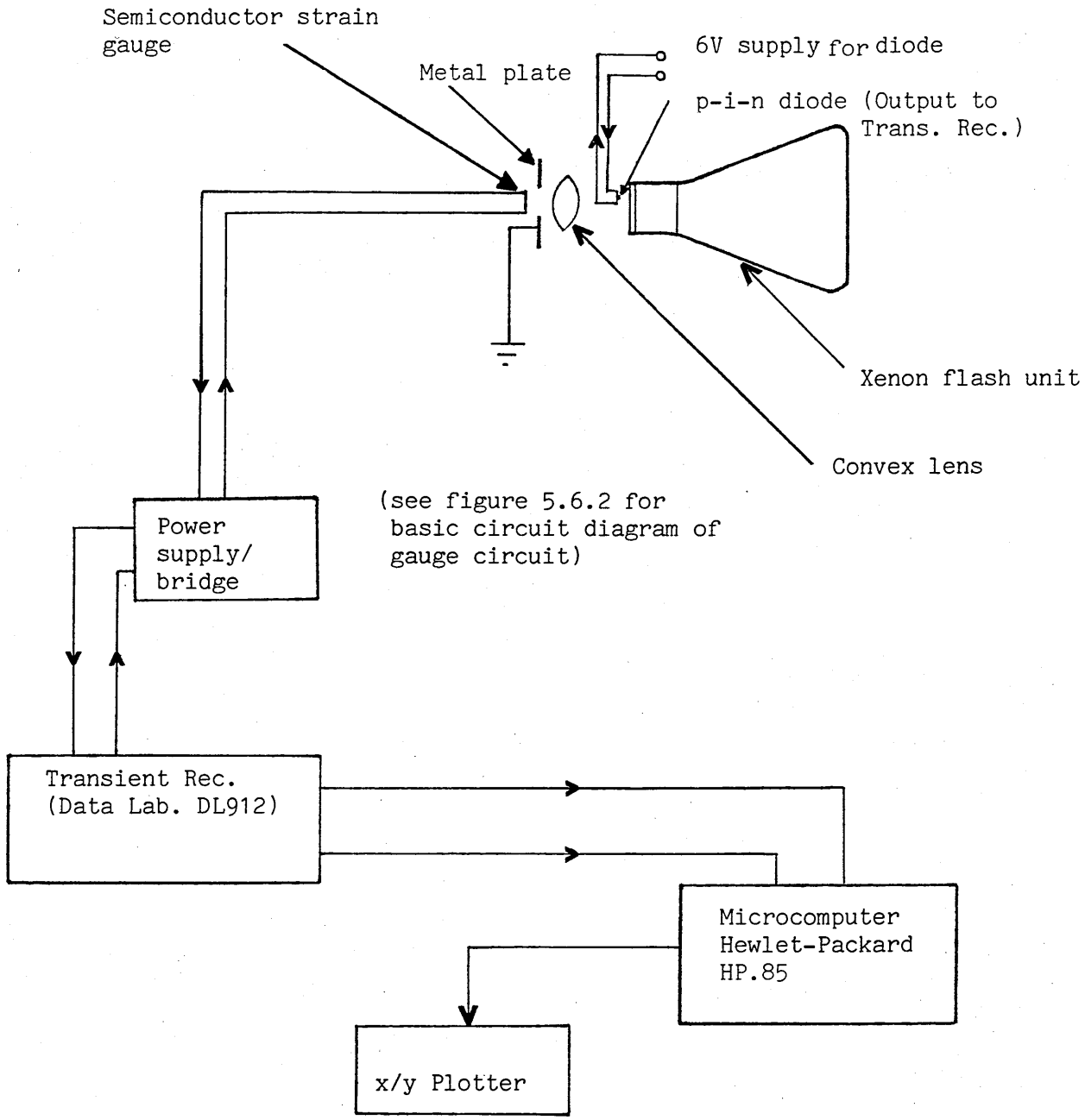

Schematic of System Used in Main Experimental Investigation with Xenon Flash Unit

Figure 5.6.3

For the main experiments a regulated power supply and bridge circuit was employed (see figure 5.6.2). In front of the strain gauge was an earthed metal plate which had a circular aperture. A photographic xenon flash unit (Vivitar 285) with variable flash duration was used. Light from this unit was focussed onto the aperture in the plate with a convex lens. A p-i-n diode having a specified responsivity of 0.55 AW^{-1} at 800 nm and a maximum rise time of 5 ns was located in front of the xenon flash unit to monitor the light. This was reverse biased with a separate 6V dc power supply. The response of the p-i-n diode was recorded simultaneously with that of the strain gauge for each flash.

The strain gauge was mounted on a separately earthed steel strip and the investigations were carried out at room temperature. Ambient lighting was normal daylight. A range of flash total power levels was used (see section 5.7), controlled by varying the flash duration. The flash unit was located normal to the aperature in the metal plate and on the axis, at a constant distance of 100 mm from it.

Outputs from both the strain gauge (unstrained) and the p-i-n diode were fed to the transient recorder, which was set at rates between 0.5μs and 2μs per sample. A range of response graphs was subsequently

recorded for both the strain gauge and the p-i-n diode for different xenon flash durations and at different sample rates. Each experiment was repeated with the gauges subjected to both tensile and compressive strains of about 300μ strain.

To check that there was no electromagnetic field coupling a cardboard screen was held between the xenon flash tube and the gauge and the flash tube was then operated, as before. This screen prevented the light from reaching the gauge and so any gauge response must be due to other effects. Again, no response was detected with the screen in position.

5.7 RESULTS OF MAIN INVESTIGATION OF GAUGE DYNAMIC PHOTOSENSITIVITY

Typical data, obtained with the experimental system shown in figure 5.6.3, are shown in the following figures. Figure 5.7.1(a) shows the response of a 500 Ω p-type silicon gauge with the xenon flash set at one quarter of full duration. Figure 5.7.1(b) shows the response of the p-i-n diode illuminated simultaneously with the gauge. The bridge output voltage change dV corresponds to about 2 μ strain.

The gauge response with the xenon flash output set at half power (ie same intensity as before but nominally twice the duration) is shown in figure 5.7.2(a). This was recorded at a rate of 2μs per sample compared to 0.5μs per sample in the previous case. Bridge output voltage change dV corresponds, in this instance, to over 2 μ strain. The response of the p-i-n diode illuminated simultaneously with the gauge is shown in figure 5.7.2(b). Similar characteristics were observed both for different output power levels of the xenon flash unit, and for other p-type silicon gauges of higher and lower unstrained resistance than that of the gauge described here. No difference in the characteristics was observed when the gauges were subjected to applied strains.

Owing to the speed and linearity of the p-i-n diode, figures 5.7.1(b) and 5.7.2(b) probably follow the light waveform quite closely. But, although obviously linked to the light history, the waveform recorded from the semiconductor strain gauges is distinctly different. At the beginning of the light pulse there is an anomalous decrease in conductivity, followed by a comparatively slow ramp up. When the xenon flash is cut off, the reverse is found: there is a small anomalous increase in conductivity followed by a slow decay to the original value.

With uncontrolled experiments like these on uncharacterized materials it is impossible to be specific on the exact mechanisms involved. However, it is possible to put forward some plausible ideas which are compatible with these observations.

The slow rise and fall of photoconductivity are totally in accord with previous measurements (eg Haynes and Hornbeck[65] and Hornbeck and Haynes[66]) on p-type and n-type silicon, where the principal mechanism was demonstrated to be traps. It is likely that the present strain gauges have a very high density of traps and recombination centres due to the unpassivated and unprotected cut surfaces. It is assumed that, at the start of the flash, there are many unfilled traps. As new free carriers are generated, they begin to fill these traps, in which they cannot contribute to conduction. Thus the steady state photoconductivity is delayed. Similarly, when the radiation ceases, the traps release carriers over a range of characteristic times which depend on the exact nature of the defects. Thus enhanced conductivity is prolonged. The timescales of the long rise and fall in the present case are compatible with measurements made by Haynes and Hornbeck[65] and Hornbeck and Haynes[66].

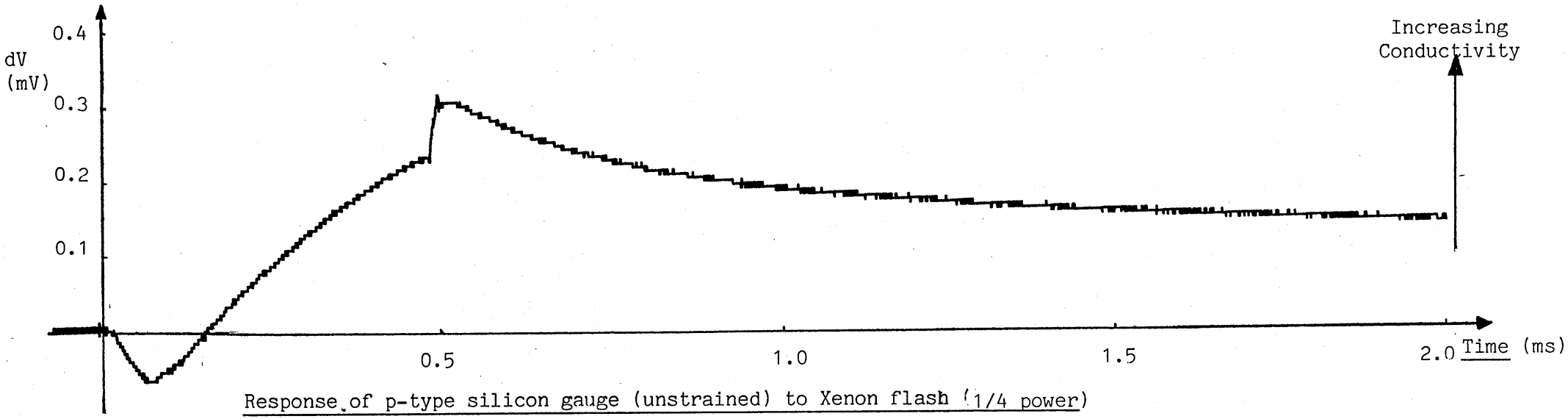

Response of p-type silicon gauge (unstrained) to Xenon flash (1/4 power)

Figure 3.7.1 (a)

Sample rate: 0.5 μs per sample

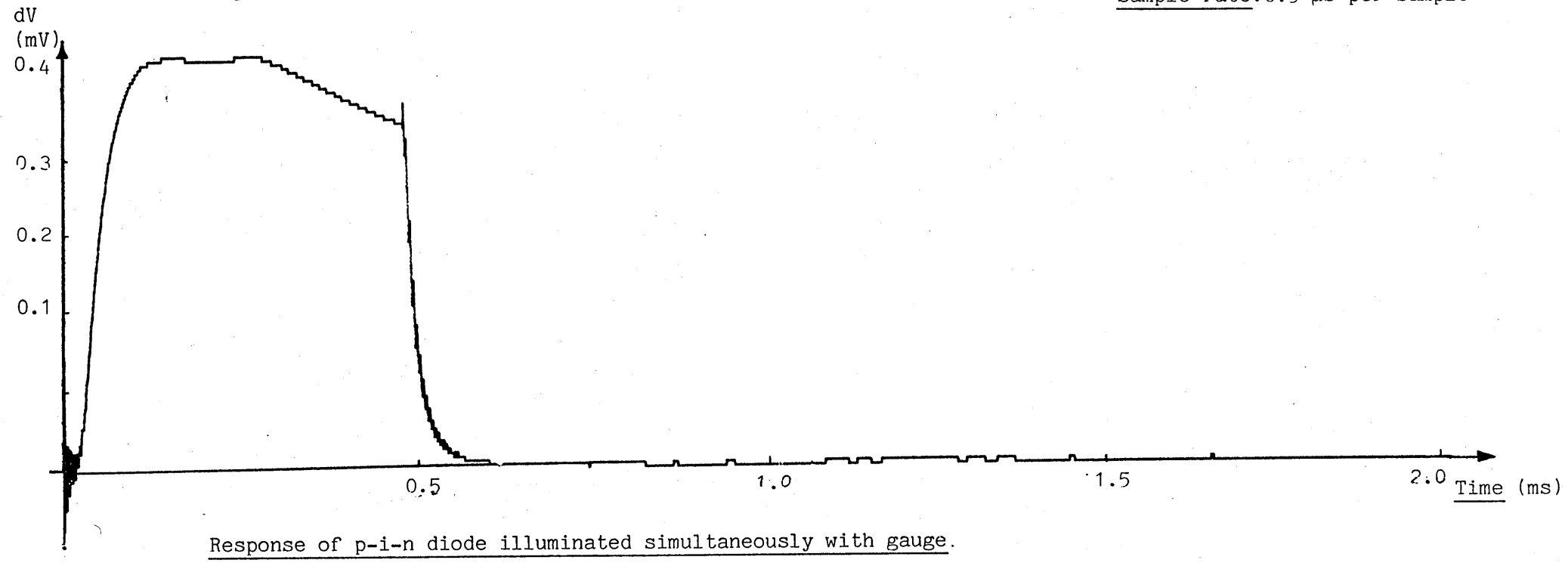

Response of p-i-n diode illuminated simultaneously with gauge.

Figure 3.7.1 (b)

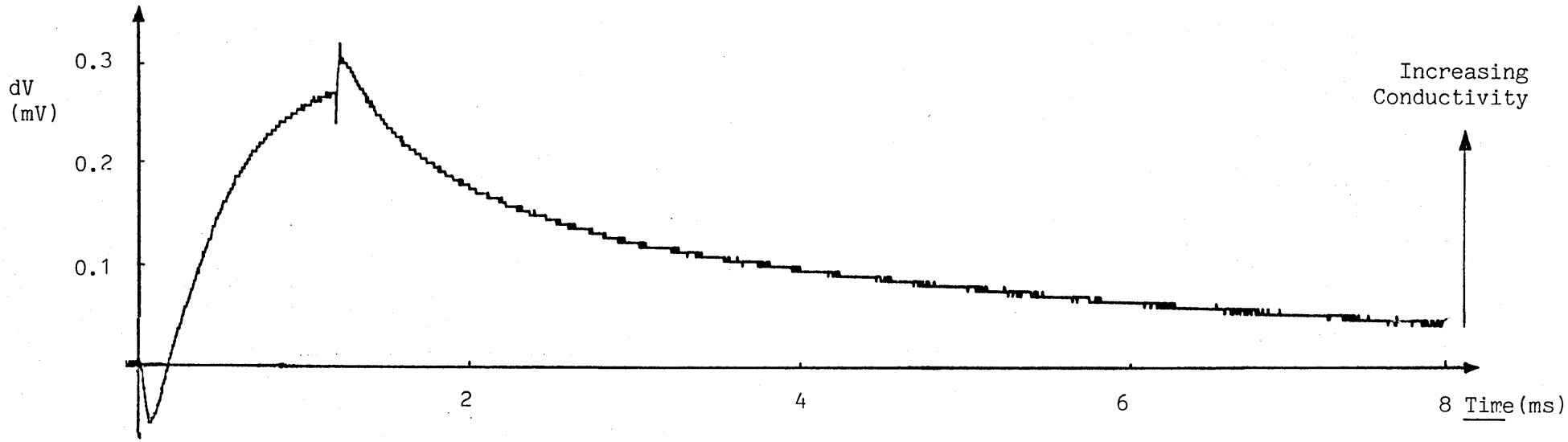

Response of p-type silicon gauge (unstrained) to Xenon flash ($\frac{1}{2}$ power)

Figure 3.7.2 (a)

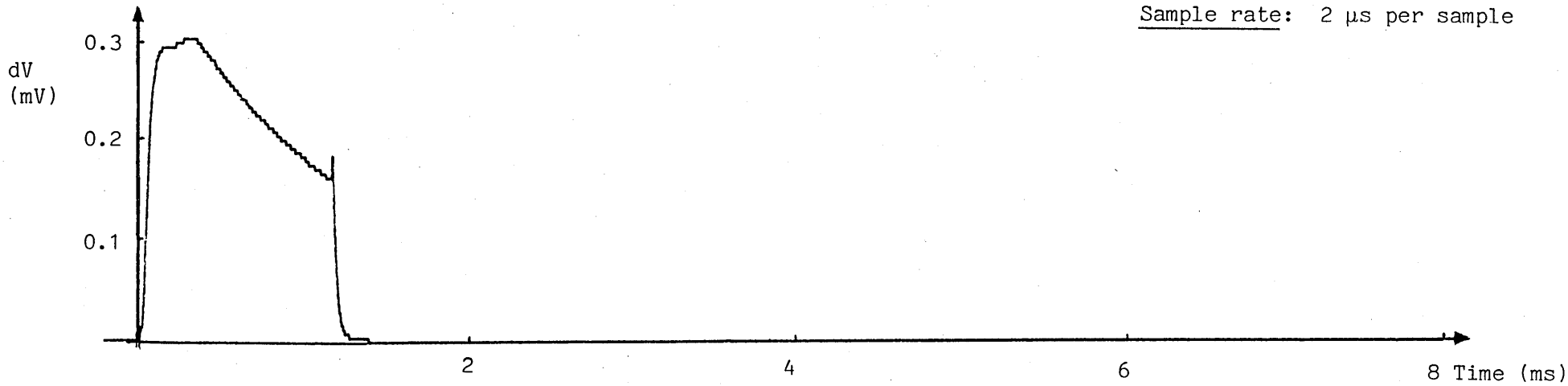

Response of p-i-n diode illuminated simultaneously with gauge

Figure 3.7.2 (b)

However, if trapping was the only mechanism then the measured waveform is expected to be like figure 5.7.3(a).

Waveform Due to Trapping as the Principle Mechanism

Figure 5.7.3(a)

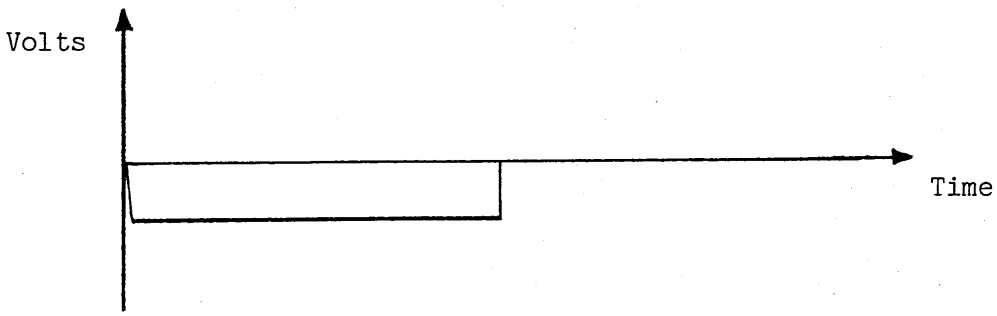

Additional Waveform Component

Figure 5.7.3(b)

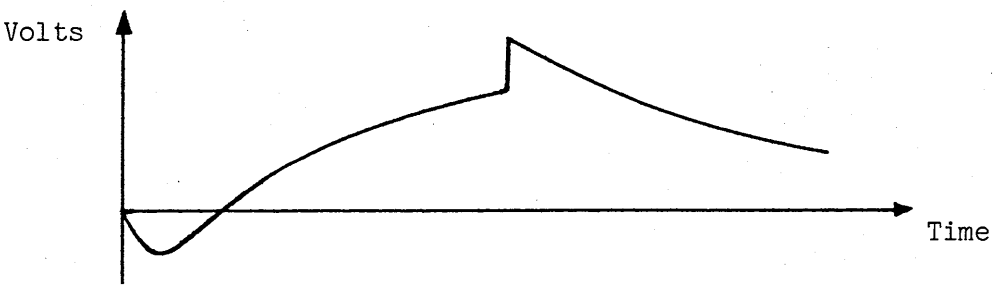

Superimposed Waveforms

Figure 5.7.3(c)

In fact, the measured waveforms are more like figure 5.7.3(c), containing an additional component, shown separately in figure 5.7.3(b).

There are two possible explanations for this additional response. First, it is possible that because of the wide and time-varying spectral range of the radiation, that at the beginning of the flash existing free carriers are being excited into localised states (not necessarily within the band gap) by a certain range of photon energies. Therefore, until the free carrier population is built up again by the normal excitation processes (delayed by trapping) then the conductivity is decreased. At the end of the flash the conductivity is quickly restored, demonstrating that if they exist, then these immobile states have a very short characteristic lifetime.

The second explanation for the anomalous features is that there is a small photovoltage being generated somewhere in the system that is in opposition to the imposed current flow. No separate evidence has been found for this, but further investigation is necessary to rule it out altogether.

5.6 COMMENTS ON THE FINDINGS OF THE INVESTIGATIONS

The qualitative investigations of the static photoelectric response of conventional p-type silicon strain gauges indicate that, despite previous reports[63], these gauges do not exhibit a photovoltaic effect when illuminated by daylight, various commonly used illumination sources, and a helium-neon laser of 1 mW output power, or an ultra-violet lamp.

Nevertheless, a small photoconductive effect was detected with these sources. No evidence of asymmetric behaviour at the gauge junctions was found but the photoconductive effect was found to be greater for longer wavelength illumination sources than, for example, an ultra-violet source. Since this effect may result in a change in resistance corresponding to several microstrain, account may need to be taken of this if precise strain measurements are required or if low levels of applied strain are being monitored. However, for most practical strain measurements undertaken with conventional p-type silicon gauges in normal environments the effect may be small enough to be ignored.

Only two different n-type silicon strain gauges were available for this investigation, but characteristics similar to those of the p-type silicon gauges were observed. These findings endorse those of Xavier and Vogt[63] concerning a photoconductive effect with silicon strain gauges. The fact that the corresponding strain magnitudes given in section 5.4(ii) are somewhat larger than those which Xavier and Vogt report may be due, in part, to the dopant levels employed in modern semiconductor strain gauges. Furthermore, there may also be differences in the intensity and sources of illumination employed. Finally, the reason why a photovoltaic effect was detected by Xavier and Vogt, but not in this investigation, could be due to improvements in the manufacture of semiconductor strain gauges, particularly the ohmic junctions with the contact wires.

Concerning the dynamic photosensitivity of silicon strain gauges it is suggested that, if the suggested trapping behaviour is the appropriate explanation of the observed effect, then the high trapping density probably indicates that there are many recombination centres as well - hence the carrier lifetime is very short. This is probably why the photoconductive effect, which depends on carrier lifetimes, is small.

5.9 SUMMARY

Silicon semiconductor strain gauges have been reported by Xavier and Vogt[63] as exhibiting both a photoconductive and a photovoltaic effect. The corresponding influence on gauge response and accuracy was not found by them to be significant.

Investigations in this project were undertaken of the static photoelectric response of silicon strain gauges using various common sources of illumination, including a fluorescent tube of somewhat higher intensity than that used by Xavier and Vogt. No photovoltaic effect was detected. This could be due to improvements in the manufacture of semiconductor strain gauges.

A photoconductive effect was observed and, in the case of quartz halogen lamp illumination, the change in gauge resistance with illumination corresponded to about 2 μ strain. This is somewhat larger than that reported by Xavier and Vogt. Apart from differences attributable to the sources of illumination this may be due to the fact that the dopant levels of modern semiconductor strain gauges are generally higher than those of gauges manufactured in the early 1960's.

When undertaking precise strain measurements it may thus be necessary to account for the influence of marked changes in illumination on measured strain magnitudes. A negligible increase in the effect was observed with increase in applied strain. There was no evidence found of asymmetric behaviour at the gauge junctions.

A study of the dynamic photoelectric response of p-type silicon strain gauges was carried out with a photographic xenon flash unit which had variable flash duration. A transient recorder was employed in the monitoring of this response and, to provide a comparison, a p-i-n diode was illuminated simultaneously with each gauge. Measurements and calculations were undertaken to obtain an estimate of the likely response time of the gauges. The values obtained for carrier drift time and diffusion times, although slow compared to a photodiode, suggested that a dynamic photoelectric response to such short duration light signals was possible.

The results obtained show that the gauges exhibited a significant response. No difference in the characteristics was observed when the gauges were subjected to applied strains. The slow rise and fall of photoconductivity observed for the gauges accords with

measurements of other investigations[65,66]. Trapping behaviour is suggested as being the probable explanation of the observed effect. Anomalous features of the characteristics are most likely to be attributable to the wide and time-varying spectral range of the radiation, or to small photovoltaic effects.

As the maximum change in bridge output voltage associated with this response is more than 2 μ strain, consideration may need to be given to this in certain strain measurement contexts. Further investigations could explore the effect with other semiconductor strain gauges, such as germanium gauges.

CHAPTER 6

Investigation of Potential Applications of Semiconductor Strain Gauges

6.1 INTRODUCTION

Following the investigations of the properties and performance of semiconductor strain gauges as well as means of compensating for certain gauge characteristics, studies were undertaken concerning potential applications to exploit these properties. These applied investigations took the form of two feasibility studies of potential uses.

The first investigation considered the possible use of semiconductor strain gauges for measurement and monitoring small dynamic strains in a nuclear radiation environment. Although there is some literature regarding the use of conventional strain gauges in nuclear radiation fields[67], a literature seach under taken by the United Kingdom Atomic Energy Authority did not identify any relevant literature concerning semiconductor strain gauges.

The other investigation concerned the employment of semiconductor strain gauges for 'condition monitoring' and performance diagnosis of internal combustion engine sub-units. This required time domain measurements to identify changes in induced static or dynamic strain over a considerable time period. It involved the simulation of wear or malfunction, such that possible associated changes in induced strain could be detected and monitored. An integrated and portable bridge/amplifier system was developed for use with semiconductor strain gauges in this context.

6.2 INVESTIGATION OF THE BEHAVIOUR AND USE OF SEMICONDUCTOR STRAIN GAUGES IN NUCLEAR RADIATION FIELDS

A number of investigators[68,69] have reported that some types of nuclear radiation have a significant effect on the electrical conductivity of semiconductors such as germanium and silicon. However, as previously indicated, no relevant literature concerning the effect of nuclear radiation fields, such as those emanating from a neutron source, on piezoresistance in semiconductors was identified. It was thus necessary to explore possible effects experimentally using typical silicon strain gauges and various neutron sources.

The first source which was employed was americium (Am) which decays by alpha emission to beryllium (Be). This was a 37GB$_q$ source and gave a neutron flux of about 3 x 10^6 neutrons s^{-1} with an average energy of approximately 3 MeV. The investigation was undertaken in a special room at the Radiation Centre, University of Birmingham, with radiation shields, remote handling equipment and radiation monitoring apparatus. The p-type silicon gauges were bonded to steel strip using P2 polyester adhesive and were clamped 5 mm directly below the neutron source as indicated in figure 6.2.1

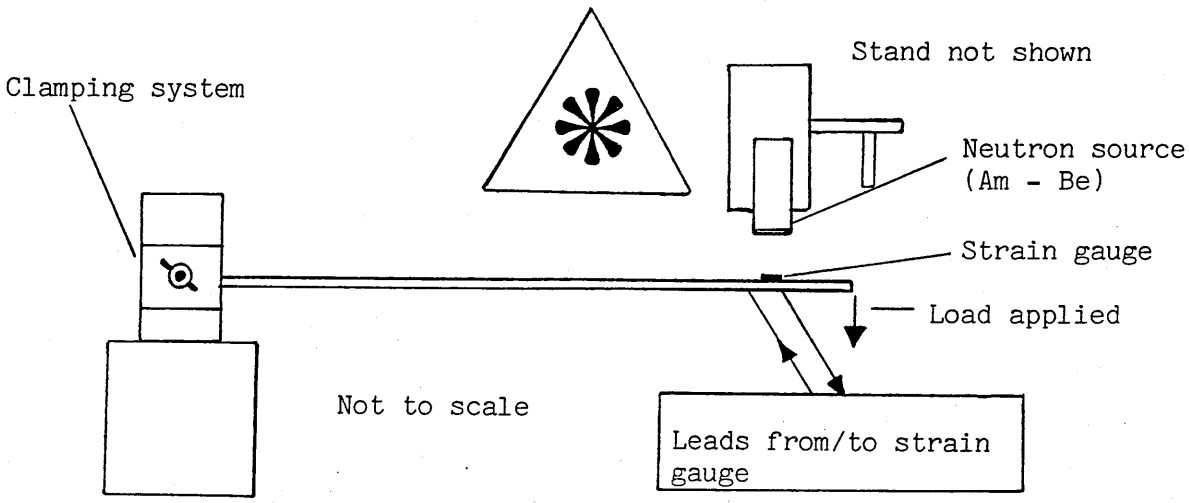

Basic Arrangement to Investigate the Effect of a Neutron Flux on Gauges

Figure 6.2.1

Initially, the resistance of the strain gauges was measured, both unstrained and strained, with no neutron flux. Ambient temperature

was 293(±1)K during the course of all the investigations in the special room. Known static tensile and compressive strains up to about 400 μ strain, were applied to the strain gauges and these strains were applied for a known, fixed time. Then the neutron flux was introduced and gauge resistance readings taken with no applied strain and then with the same applied strains and time durations previously employed with no neutron flux, namely 10 minutes.

With the aid of an electromagnet and lever system the gauge resistances were measured when subjected to dynamic tensile strains. Again this was undertaken with and without the gauge being subjected to a neutron flux. The resistance measurements were taken with the aid of a sensitive digital ohmmeter (±0.001Ω) located behind a thick lead wall and away from the neutron flux. After undertaking the static and dynamic experiments the strain gauges were subjected to longer exposures to the neutron flux between taking the resistance readings. These periods were 1 hour, then 4 hours, then 8 hours and so on, doubling each time up to 32 hours. The same investigation was repeated using two typical n-type silicon strain gauges of different resistivity at room temperature. A suitable germanium strain gauge was not available during these investigations.

Using an equivalent set of p-type silicon strain gauges, and equivalents to the two n-type gauges, a corresponding series of measurements were taken using a different neutron source. This source was a 37GB$_q$ californium (^{252} Cf) source which emitted, along with other radiation, a neutron flux which was somewhat greater than 3 x 10^6 neutrons S^{-1}. This is by spontaneous fission and the average energy of the neutrons is about 2 MeV. The basic arrangement employed is shown in figure 6.2.2 with the lead wall shield removed.

(see figure 6.2.2 overleaf)

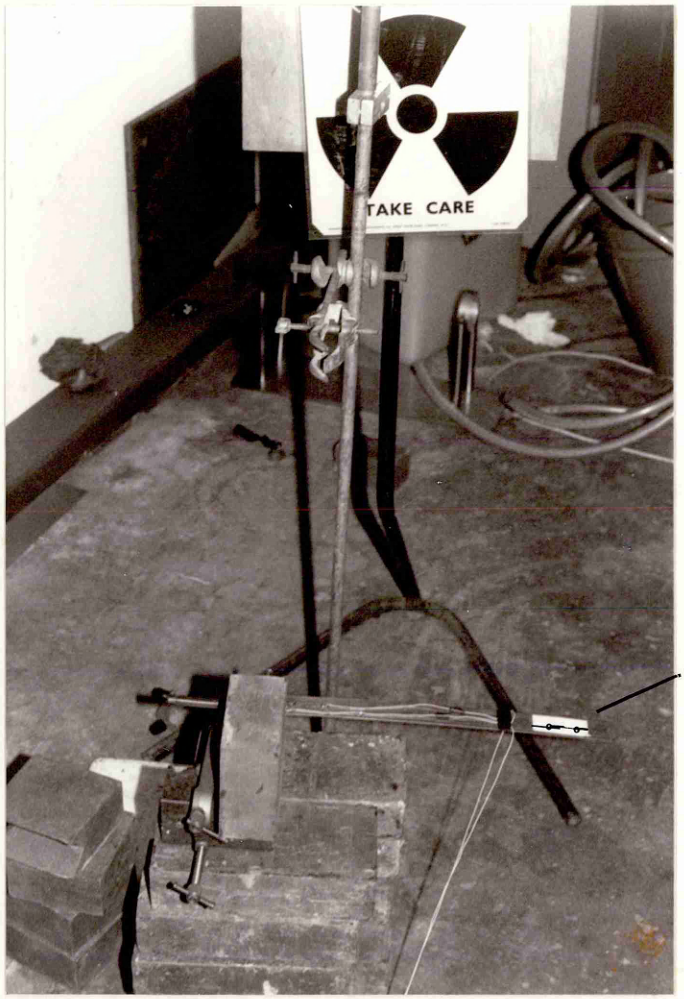

Basic Arrangement for Gauge Neutron Irradiation (source removed)

Figure 6.2.2

In order to explore the effect of a high flux of fast neutrons the employment of a particle accelerator was necessary. Arrangements were made to use the 'Dynamitron' at the University of Birmingham Radiation Centre for these experiments. Figure 6.2.3 shows the Dynamitron accelerator with the equipotential rings which couple the radio frequency supply to solid state rectifiers. It was not possible to employ different duration exposures of the semiconductor gauges to the neutron flux or to examine many strain gauges. However, four different, new p-type silicon gauges and one new n-type gauge were subjected to the neutron flux and, as before, their resistance measured before and again after irradiation, both unstrained and subjected to static strains up to 400 μstrain. As a check, a set of readings was obtained using the strain gauge bridge/amplifier system, described in section 6.3.4, in place of the digital ohmmeter.

The Dynamitron provides:

(a) polyenergetic neutrons with energies in the range 0 - 7 MeV

(b) monoenergetic neutrons with energies between 0 - 6.3 and 15 - 20 MeV

Equipotential rings (These couple an RF supply to the assembly of rectifiers)

The dc high voltage is the sum of the individual rectified voltages.

Solid state rectifiers (In operation the accelerator is enclosed within a pressure vessel filled with sulphur hexafluoride)

Dynamitron Accelerator

Figure 6.2.3

6.3 RESULTS AND COMMENTS ON NUCLEAR RADIATION OF SEMICONDUCTOR STRAIN GAUGES

The nuclear radiation inside a nuclear reactor consists of a thermal neutron flux (eg 10^{12} neutrons s^{-1}) and some fast neutrons. This is why the typical p-type and n-type silicon gauges were exposed to sources of neutron flux and irradiated in the Dynamitron (where they would be exposed to high energy and fast neutrons). The second source of neutrons used (^{252}Cf) operates by spontaneous fission, which is the same mechanism as the fuel elements in a nuclear reactor.

The neutrons produced by the first source are of higher energy and their average is about 3 MeV, compared to 2 MeV for ^{252}Cf. Assuming an isotropic distribution from a point source 5 mm away from the semiconductor strain gauge means that the strain gauges were subjected to a maximum flux of about 1×10^{13} neutrons $m^{-1}\ s^{-1}$, which is quite high, but lower than that in a typical nuclear reactor. Nevertheless, information received from the Atomic Energy Authority suggests that the sources and measures used provided a satisfactory replication of a reactor radiation environment, for the purposes of this exploratory study.

It was found that quite short term or prolonged exposure to the two sources of neutron flux did not produce a detectable effect on either the unstrained or strained resistance of the p-type and n-type silicon strain gauges which were examined. Table 7 gives representative values obtained for a p-type silicon gauge irradiated by the ^{252}Cf neutron source for 10 minute exposures, at an ambient temperature of 293K.

Neutron flux.	Applied static strain (400μstrain)	Gauge resistance (ohms)
No flux	Unstrained	180.61
10 mins expos.	"	180.60
10 mins expos	Strained	207.32
No flux	"	207.33
No flux	Unstrained	180.60

Source: californium 252

Resistance of p-type Silicon Strain Gauges for Different Strain and Irradiation Conditions

Table 7

A similar picture was found for other p-type silicon gauges, and n-type silicon gauges for this source, and for the americium - beryllium source. No difference was found either for gauges subjected to dynamic strains with and without radiation from the neutron sources. Furthermore, the resistance values obtained for the gauges strained and unstrained before and following irradiation in the Dynamitron were also not found to be significantly different, overall. It is interesting that reference to data [68] concerning radiation properties indicates that the absorbtion cross sections for silicon are about the same for thermal and fast neutrons.

The findings of this feasibility study suggest that silicon strain gauges could be employed to monitor and measure small static and dynamic strains in a nuclear reactor environment because, even after exposure to the neutron sources for a total of over 60 hours, no significant change in the resistance or response of the gauges was detected. When the gauges were employed with the bridge/amplifier system, such as could be used in the actual monitoring of a unit employed inside a reactor, again no significant difference was found in the response with and without exposure to the neutron flux. Future investigations could be undertaken, subject to conditions and

arrangements being satisfied, of semiconductor gauges inside a reactor, where temperatures may be higher and temperature effect compensation could be required. In addition, a study could be made of the behaviour and response of germanium p-type and n-type strain gauges subjected to various sources of nuclear radiation.

6.4 MACHINE 'CONDITION MONITORING' AND PERFORMANCE DIAGNOSIS

This brief feasibility study arose from an examination of the potential use of the high gauge factor, small size and low hysteresis of semiconductor strain gauges, with appropriate temperature effect compensation. A low drift, low noise, linear dc bridge/amplifier system was developed for use in the context of monitoring certain mechanical sub-units of internal combustion engines. The strain gauges used were p-type silicon and these were employed for monitoring small, induced static and dynamic strains so that information could be obtained regarding the condition and wear of the sub-units, over time.

The main circuit of the linear amplifier/bridge system is shown in figure 6.4.1. This was based upon an SGA 100 integrated circuit dc amplifier which is commercially manufactured. A compact, regulated

power supply unit was constructed to accompany the bridge/amplifier unit so that a rugged, self-contained and portable system was produced. To attain high performance, reliability and compactness a printed circuit board was designed and fabricated for the strain gauge bridge/amplifier unit (see figure 6.4.3). The amplifier could be used with a full, half or quarter active bridge, as required.

In figure 6.4.1, which is shown overleaf, transistor T_1 is 2 N3053, T_2 is BFX29 and T_3 is BC207. All other values and specifications are shown in the figure.

See also figure 6.4.2 overleaf

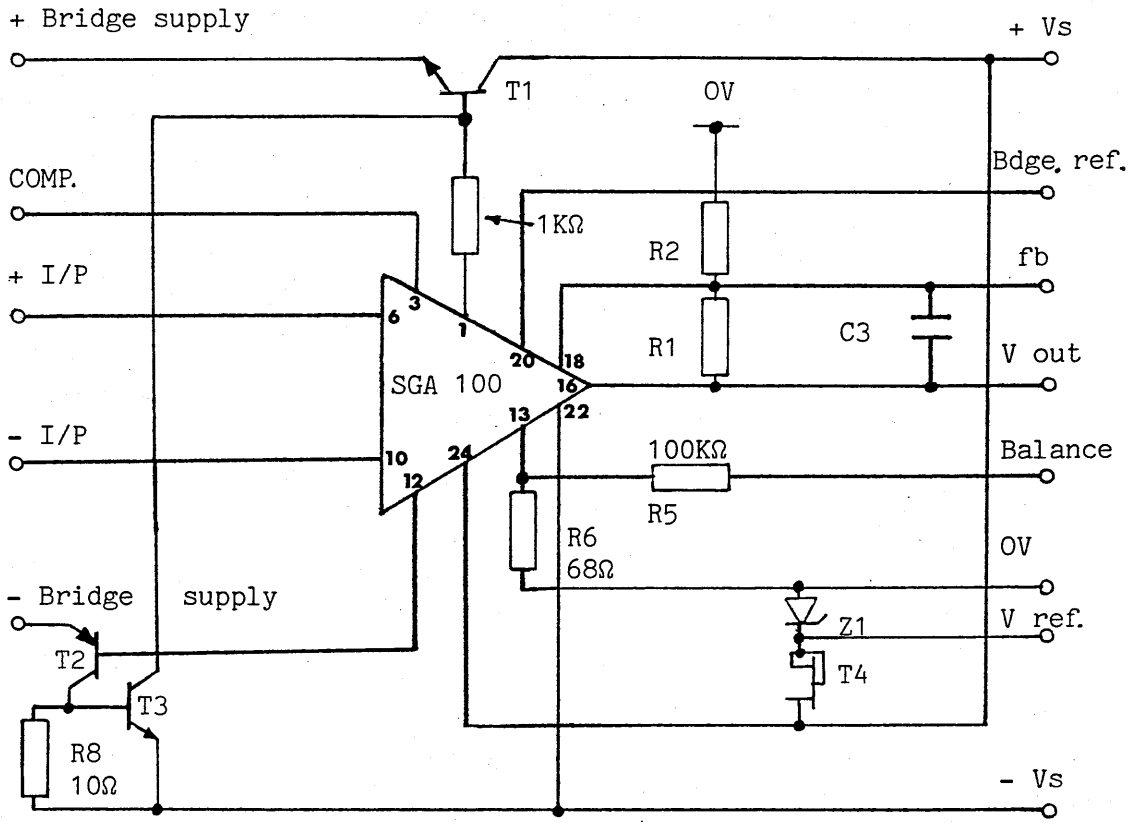

Z1 - IN823

T4 - BF224B

Main Circuit for Strain Gauge Bridge/Amplifier System

Figure 6.4.1

Figure 6.4.2 shows each of the main elements of the SGA 100 unit corresponding to the pin numbers shown in figure 6.4.1. (All positives pin 24, all negatives pin 22 - see Appendix 3.)

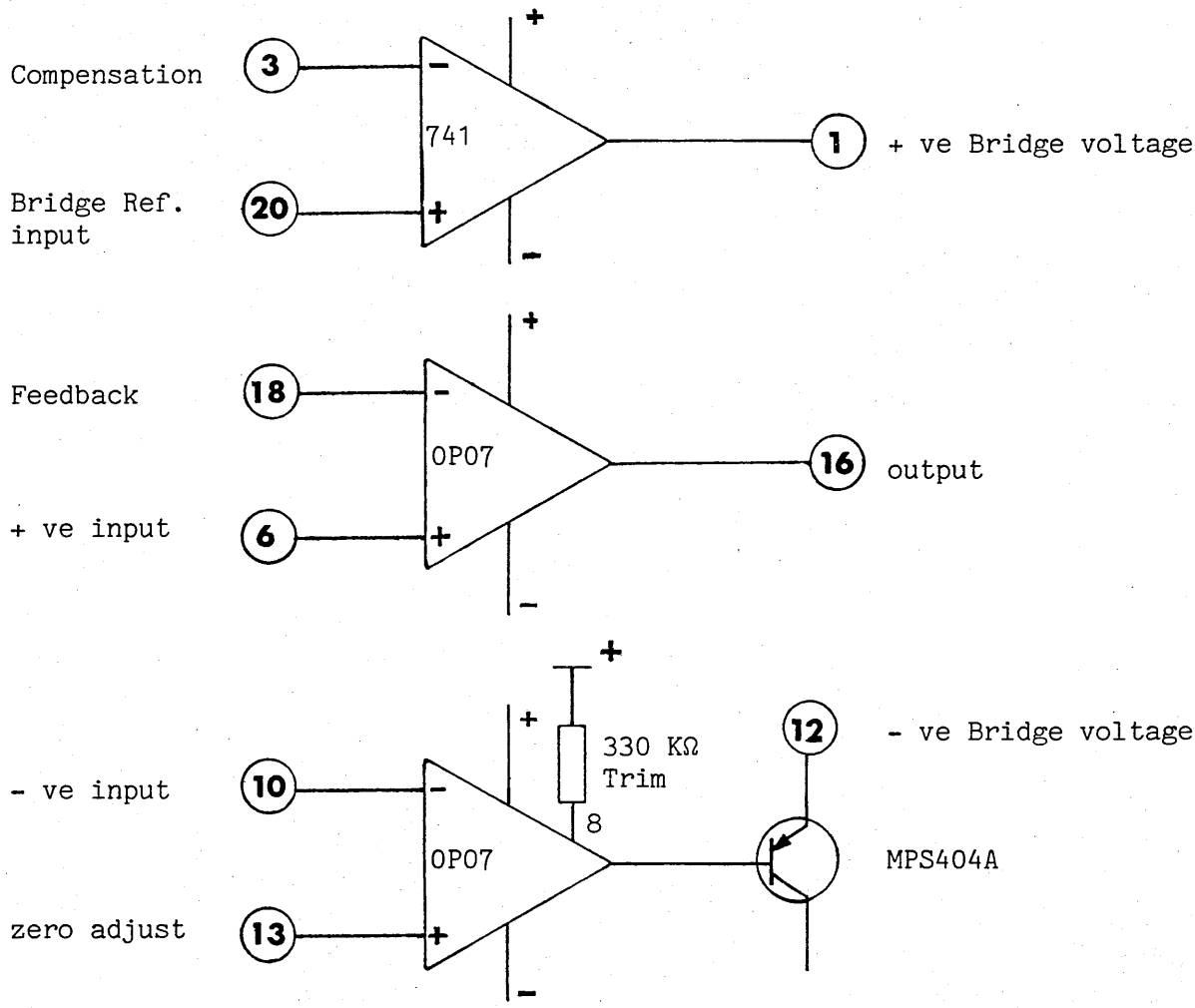

Main Elements of SGA 100 unit

Figure 6.4.2

The component values shown in figure 6.4.1 are the general values used, and it was found that the amplifier which was subsequently developed could be used for a wide range of gauge resistance values and resistance changes. By controlling the negative bridge supply voltage, such that the voltage at the negative terminal was maintained at zero volts, the problem of common mode rejection was overcome (ie by removing the common mode voltages). To minimise electromagnetic interference, which could be picked up by the leads to and from the unit, screening was employed, and, as this proved to be quite satisfactory, it was not found necessary to decouple the leads or to reduce the operating bandwidth of the system using capacitors. Amplifier white noise was minimised by the use of high quality resistors in the amplifier circuit (eg metal oxide resistors were used for the gain setting resistors (R_1 and R_2 in figure 6.4.1).

(see figure 6.4.3 overleaf)

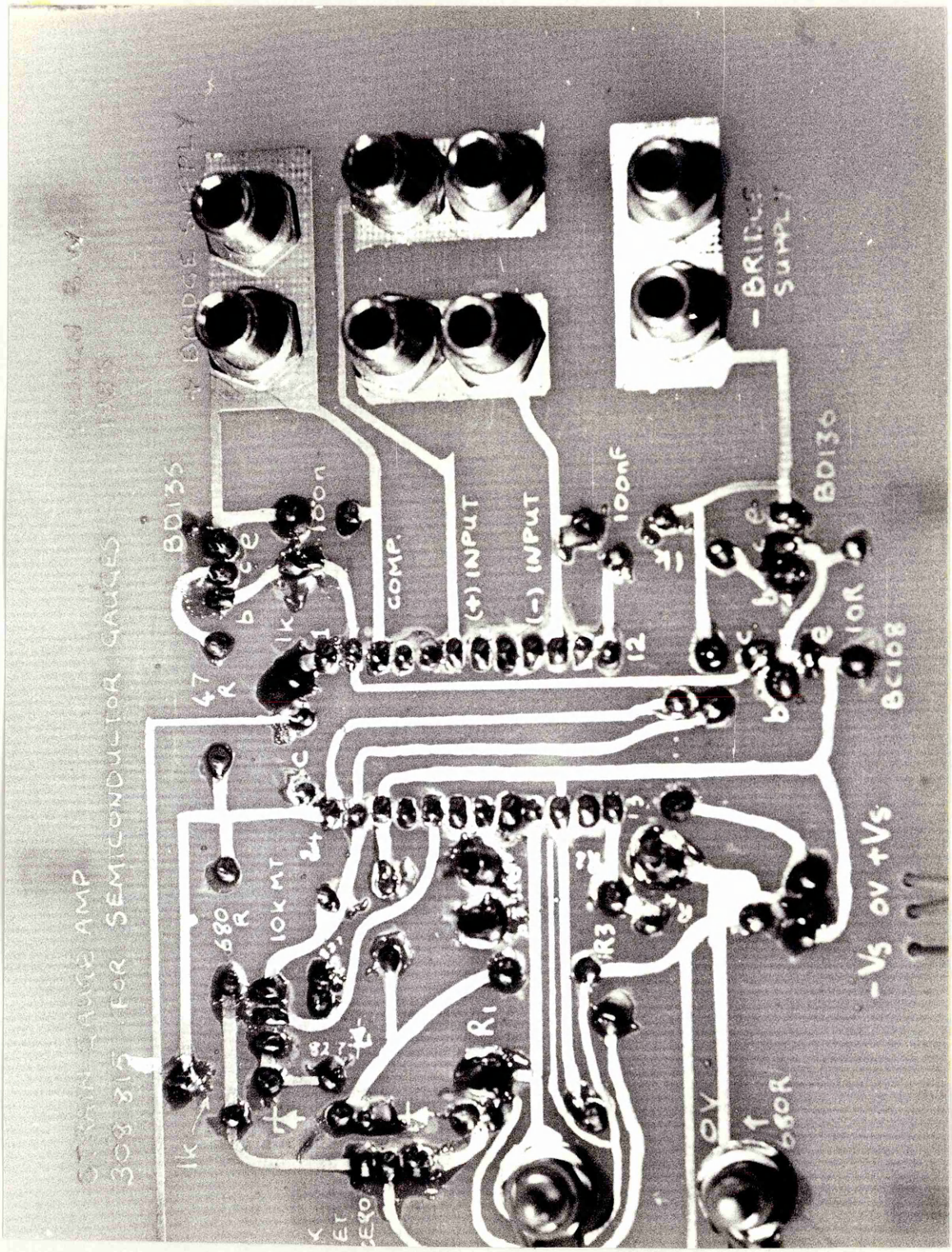

Printed Circuit Board Fabricated For Strain Gauge Amplifier/Bridge

(Fabricated using photo-resist board)

Figure 6.4.3

Figure 6.4.3 shows the basic printed circuit board for the semiconductor strain gauge bridge/amplifier unit. Some of the main circuit components on this board ar shown in figure 6.4.4, which is a photograph of part of the unit taken out of the containing box. This box was devised to enable the unit to be employed in environments where humidity and high dust levels could prove troublesome, if the circuit was not protected. It was anticipated that such environments would exist in the monitoring of some internal combustion engines.

(see figure 6.4.4 overleaf)

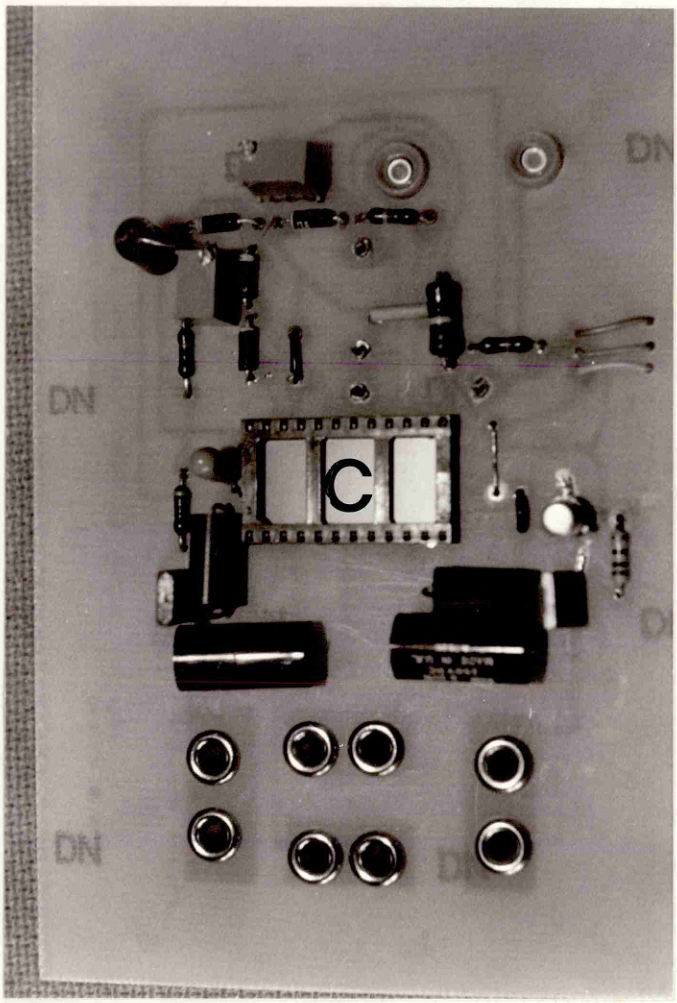

Part of the Main Components Section of the Strain Gauge Bridge/Amplifier Unit (C is the SGA 100 Socket)

Figure 6.4.4

The output voltage was monitored using a sensitive digital voltmeter such as that shown if figure 6.4.5. A more compact meter was subsequently employed for engine condition monitoring.

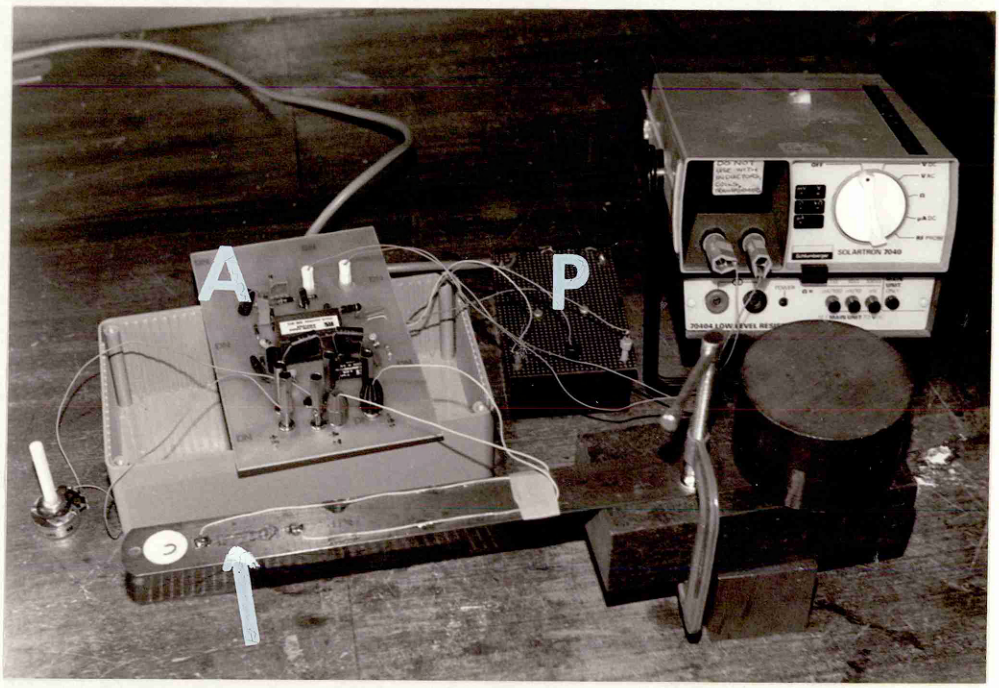

Basic Amplifier/Bridge Unit Set Up for Testing and Preliminary Investigation

Figure 6.4.5

The arrangement shown in figure 6.4.5 has the amplifier/bridge unit A removed from the box (the top of the box, which is not shown, has the calibration adjustment and zero adjustment controls mounted on it). In figure 6.4.5 the stabilsed 12V dc power supply unit P can be seen along with a mounted semiconductor strain gauge (arrowed) and a digital voltmeter. If required the whole system, including the digital meter, could be operated using sealed batteries rather than from ac mains power. (See Appendix 3 for brief details of the bridge/amplifier performance and characteristics.)

The applied investigation using this integrated bridge/amplifier system for semiconductor strain gauges required the taking of time-domain measurements of key parts of engine sub-units, such as fuel pumps, so that comparative data about changes in induced strains could be obtained. A profile could then be built up which could be used for assessing the future condition (ie reliability/performance) of key sub-units. This meant that reliable, relatively long-term monitoring of possible very small changes in induced dynamic or static strain must be provided and data appraisal undertaken at each data update. Evidence obtained from the initial periods of monitoring was used to determine the appropriate frequency of data updates. If the frequency was too

short then redundant data would be collected, but if it was too long then there would be insufficient warning of the onset of serious wear or malfunction.

Attempts were made to explore the condition monitoring of three different, typical, internal combustion engine sub-units. In each case, p-type silicon strain gauges of gauge factor 120 were employed. Compensation for temperature effects was undertaken using the appropriate methods outlined in chapter 4, such as the employment of dummy gauges and three lead wires. The investigations were of the folllowing:

1 Fuel pump unit

The strain gauge and dummy gauge were mounted in a typical fuel pump housing where it had been found, in initial trials, that small strains induced by worn bearings were transmitted and could be isolated. In figure 6.4.6 this unit is shown arrowed.

It was found not to exceed a temperature of 330K after protracted operation, but to prevent temperature changes due to external sources, fibre glass insulation was fitted around it. The strain gauges

were bonded using an inorganic bonding agent which had similar thermal expansivity to that of the metal, and a thermocouple was mounted next to them. All of these had the fibre glass lagging layer covering them.

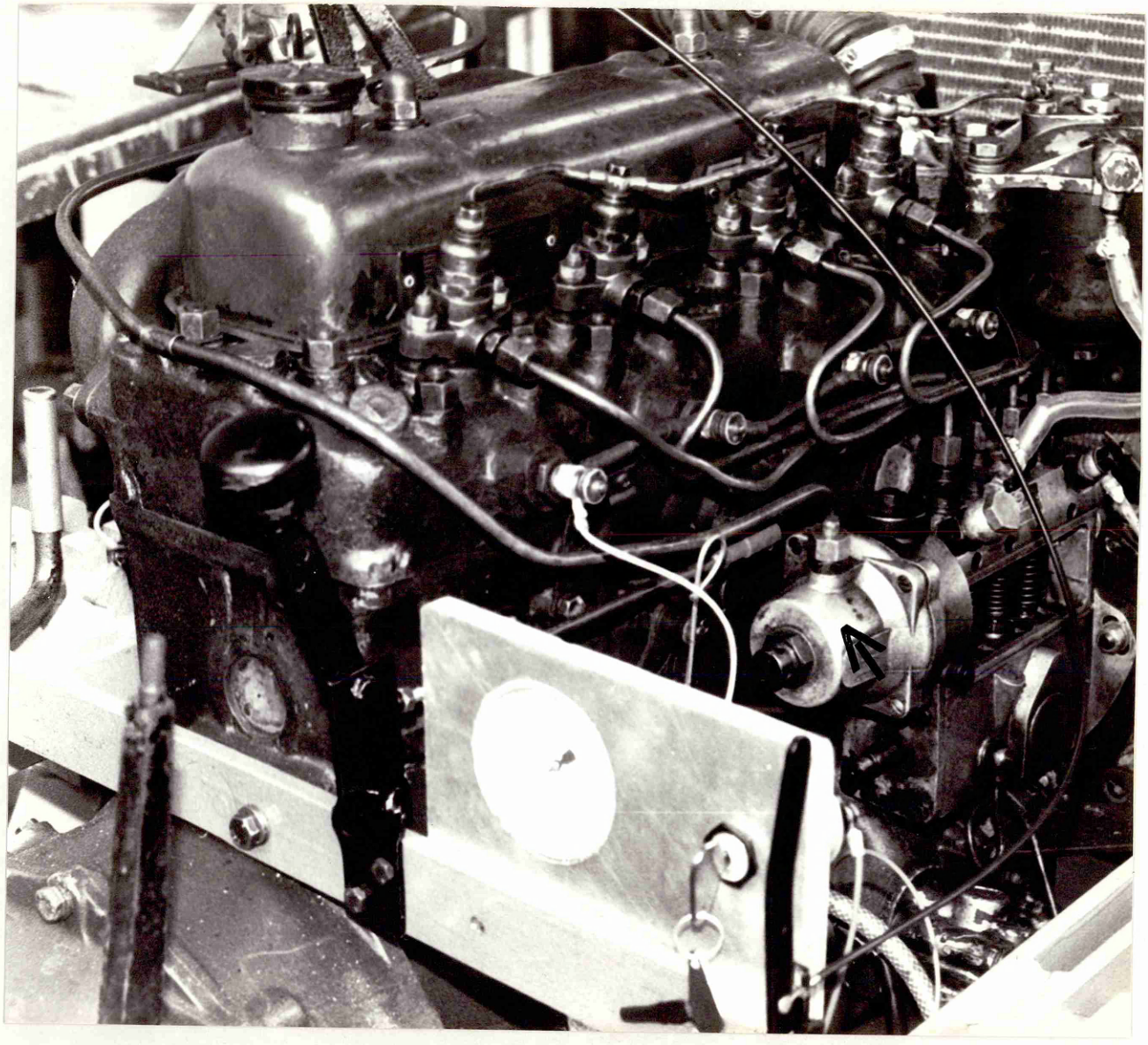

Diesel Engine: Fuel Pump Condition Monitoring

Figure 6.4.6

After preliminary calibration and setting up with a new pump bearing had been undertaken, the engine was set into operation and, after setting engine speed to a constant value and allowing conditions to come to equilibrium, the gauge output was monitored using the bridge/amplifier unit and a digital voltmeter set on a 50 mV ac range (which provided a rectified or rms output reading of $\pm$0.01 mV). The mean induced strain level was recorded and the mean temperature, measured by the thermocouple, was 328K. Then a bearing which was significantly worn but still functional was substituted in the unit and readings again taken, after allowing the system to come to equilibrium. It was found that the mean induced strain had risen, although the temperature was virtually unchanged. The worn bearing was known to have been used for about 5×10^3 hours. Thus, by monitoring a new bearing every 5×10^2 hours and putting the data into a microcomputer, then undertaking appropriate data analysis, it could be possible to predict the onset of serious wear and take remedial action before the unit failed. As a check, the original bearing was replaced and the engine operated as before. When the system had been given time to reach equilibrium the induced strain and temperature was monitored over several hours.

2 Lubricating oil pump unit

The system shown in figure 6.4.7 was employed in an attempt to monitor lubricating oil pump behaviour, for different brands of the same grade of oil and with simulated levels of wear, by measuring small changes in induced strain using gauges mounted on a small baffle inserted in the engine block. Engine speed was set a constant value of 2,000 rpm, a typical operating speed for such an engine.

(see figure 6.4.7 overleaf)

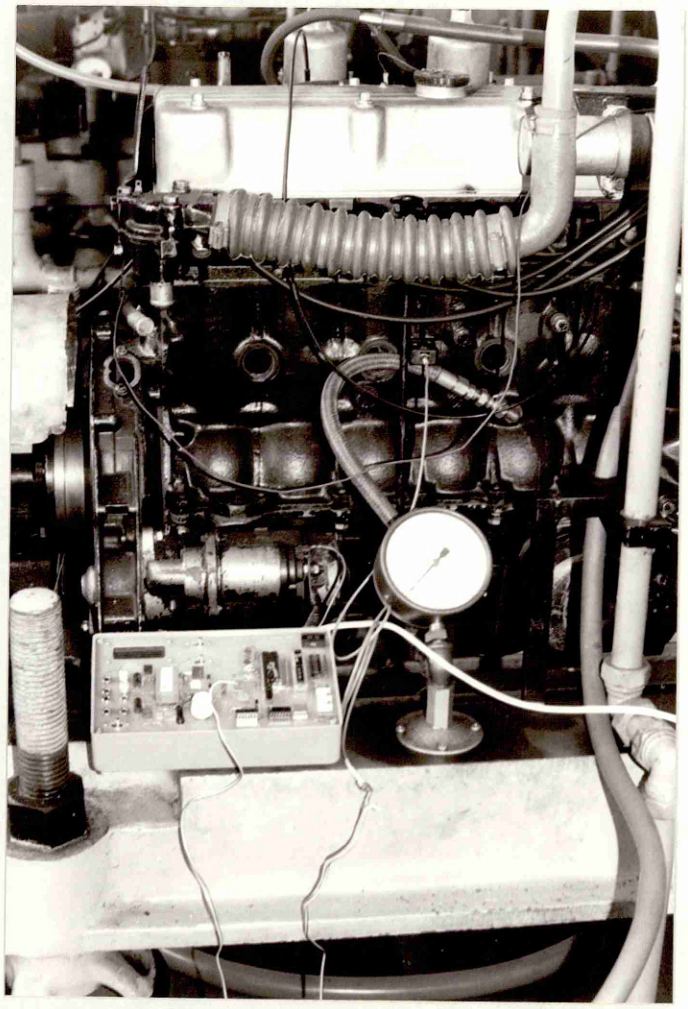

Petrol Engine: Oil Pump Condition/Performance Monitoring With Strain Gauge

Figure 6.4.7

Measurements of induced strain were taken using the same system and digital voltmeter as in the previous investigation. (See findings in section 6.5.) A single strain gauge and a dummy gauge were employed and these were bonded, using an inorganic adhesive as before, to the baffle. This adhesive was not affected by the oil.

3 Injector pump unit

This feasibility study concerned the monitoring of the condition, on an hourly time-domain basis, of a fuel injector pump unit of a diesel engine. The engine is shown in figure 6.4.8 with the bridge/amplifier unit in the foreground. In this case the possible influence of different brand fuels on induced strain levels had to be taken into account and so strain measurements were carried out, over the same total time period of 10 hours, for three different fuels being injected into the engine which was set at fixed speed. A fibre glass thermal shroud was used to maintain the temperature of the unit. (This is not shown in figure 6.4.8.)

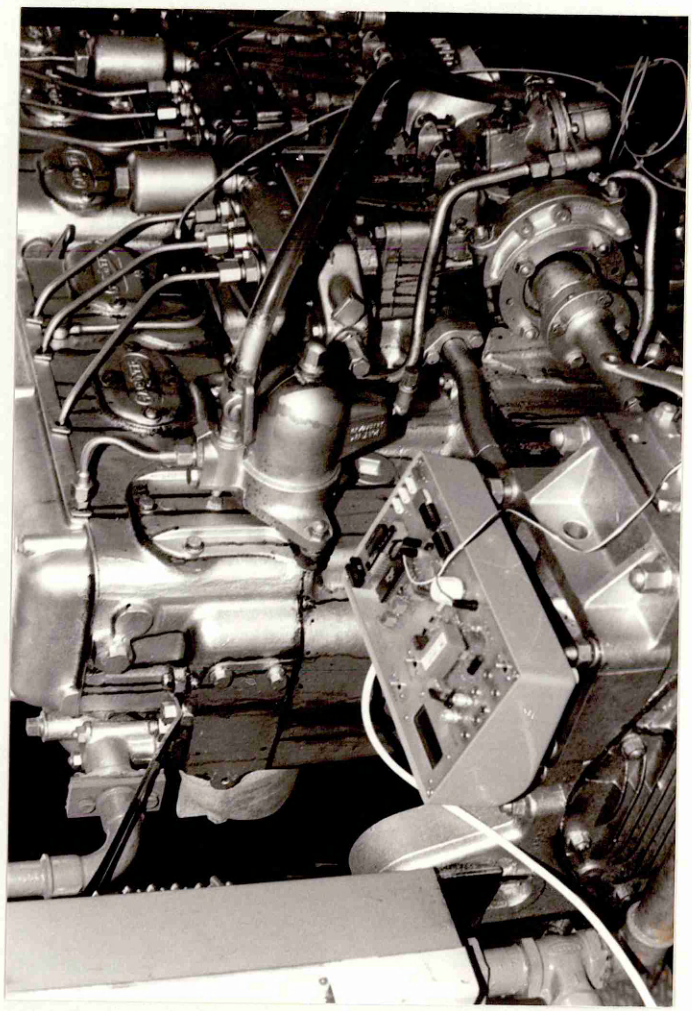

Diesel Engine: Monitoring of Injector Pump Unit with Strain Gauge

Figure 6.4.8

An injector pump element which was worn, but had not deteriorated to a serious state, was substituted and strain readings repeated, then the original unworn element was replaced and a series of readings taken again (see section 6.5). The same type of strain gauges employed in the previous investigations were used, and these were bonded inside the pump unit casing with an inorganic adhesive. As before, the integrated bridge/amplifier unit and digital voltmeter were employed with the strain gauge.

6.5 FINDINGS AND COMMENTS ON 'CONDITION MONITORING' USING SEMICONDUCTOR STRAIN GAUGES

1. Fuel pump unit Mean values of induced strain of 8 μ strain and 15 μ strain were observed for the new and worn fuel pump bearings, respectively. The mean temperature in each case was 328K. When the new bearing was later put back in place of the worn one the mean induced strain was found to be 9 μ strain at a mean temperature of 329K. It was still thus considerably lower than that found for the worn bearing and could, therefore, give a basis for condition prediction.

2. Lubricating oil pump unit When a new oil pump unit was monitored, induced strains on the specially devised baffle were not detected for any of the three different brands of oil. When a pump unit which was modified to simulate different amounts of wear was substituted, induced strains from 5 to 40 μ strain were detected for increasing amounts of simulated wear, at a given oil pressure and temperature. No detectable difference was observed in this respect for the different oils. This means that condition monitoring using a system such as that employed, may not require specific brand lubricating oils to be designated.

3 Injector pump unit For a new injector pump element there was no change detected in the induced strain during hourly monitoring over a 10 hour period, for each of the three different brand fuels employed. When the worn injector pump element was substituted the induced strain rose from 5 to 11 μ strain at the same constant engine speed, operating temperature and monitoring intervals. When the new element was replaced the induced strain was again found to be 5 μ strain under the same conditions as before. No difference in this strain magnitude, or that associated with the worn injector pump element, was detected when the different brand fuels were used. Thus, injector pump

condition monitoring, using such a system as that employed, may not require particular brands of fuel to be specified.

In each of the three investigations the bridge/amplifier unit performed satisfactorily and the temperature compensation measures adopted were found to be adequate. Moreover, as these investigations have indicated, it is possible to monitor small magnitude strain levels and identify small changes in these which could be related to the onset of mechanical failure or serious wear. However, it may not be possible to identify small induced strains for some units, or isolate these and use changes in induced strain levels to assess performance or to relate them to wear and malfunction.

Although the output voltage change from the integrated bridge/amplifier unit developed for this investigation was monitored with a digital voltmeter, a brief trial was made of the possibility of using a microcomputer in this context. This enabled actual strain magnitudes to be printed out directly and changes in strain over particular time intervals could be plotted on an x/y plotter or VDU screen. For this trial only simple dynamic strains and static strains on a long steel bar were examined.

Future investigations could explore the employment of such a system in applied machine 'condition monitoring' contexts. Appropriate software could be devised to include sub-routines to correct strain values for temperature or other effects, if required. Owing to the long fatigue life, small size, high gauge factor and low hysteresis of semiconductor strain gauges it could be possible to use such a system to provide long-term monitoring of very small changes in induced strain even for quite small mechanical sub-units.

6.6 SUMMARY

A potential use of semiconductor strain gauges which exploits their high gauge factor, small size and long fatigue life (compared to other types of gauge), is in monitoring dynamic and static strains in devices used in nuclear reactors and similar high radiation environments. Typical silicon semiconductor strain gauges were subjected to both short and prolonged exposure, of up to 60 hours, in a neutron flux provided by a high energy particle accelerator. They were also exposed for periods of up to 32 hours to neutron fluxes provided by both americium and beryllium sources. No effect on gauge response was found in any of these investigations and so semiconductor strain gauges could

be used in such high radiation environments, if appropriate temperature effect compensation was provided. Further investigations are suggested to explore the use of semiconductor gauges in nuclear reactors and to examine the effect of nuclear radiation on germanium gauges.

Another potential application of seminconductor strain gauges is the 'condition monitoring' of mechanical sub-units. An integrated bridge and low noise, linear amplifier system was developed for use with gauges in this context. Three different sub-units were monitored and, in each case, small changes in induced strain, which could be attributed to wear or malfunction, were detected, when worn components were substituted for new ones. A data logging system based on the system devised for this feasibility study could be developed for industrial use.

CHAPTER 7

General Conclusions, Comments and Suggestions for Further Investigation

7.1 INTRODUCTION

This study of semiconductor strain gauge theory and investigation of the performance and properties of semiconductor gauges has revealed various interesting facets which merit further exploration. It is regrettable that current literature in this sphere is somewhat scant because semiconductor strain gauges could be usefully exploited, as indicated, in a variety of contexts - particularly where their high gauge factor would be advantageous. Moreover, the investigations of gauge circuits and sytems to compensate for their relatively high temperature coefficient of gauge factor and temperature coefficient of resistance indicate that these undesirable features may be reduced to insignificant proportions. In addition, with improved control of dopant levels and the use of higher levels of doping, semiconductor strain gauges manufactured today are generally much superior to those made in the 1960's, when much of the research in this area was undertaken.

7.2 COMMENTS ON COMPARATIVE GAUGE PROPERTIES

A brief comparison of semiconductor strain gauges and metal wire and foil gauges was presented in section 1.6. Nevertheless, there are various other piezoresistive devices which can usefully be compared to typical semiconductor strain gauges. These include continuous metal film and discontinuous metal film resistors and cermet resistors. The properties of these devices are summarised in Table 8. As can be seen from this table, only continuous metal film resistors have good stability over time, but the gauge factor of these devices is low.

Investigations of thick film resistors by Canali et al[70,71] and Prudenziati et al[72] have shown that these devices have good stability over time and much higher gauge factors than either metal wire or continuous metal film resistors. Furthermore, these devices, which are obtained from an 'ink' containing submicron conducting particles and glass grains suspended in a viscous organic fluid, have low temperature coefficients of both resistance and gauge factor.

Type of material	Gauge Factor	Temp Coef of resistance (ppm/K)	Temp Coef of gauge factor (ppm/K)	Time Stability
Metal wire	2-5	20-4000	20-100	Very good
Continuous metal film	2-5	20-4000	20-100	Good
Discontinuous metal film	100	1000	-	Relatively poor
Cermet	100	1000	-	Quite poor
Thick film resistors	10-15	100	less than 500	Good
Semi-conductor	(±)40-175	400-9000	200-5000	Good

Comparative Data on Strain Gauge Properties[71]

Table 8

As the data presented in Table 8 shows, semiconductor strain gauges have higher gauge factors than other piezoresistive devices and this may be positive or negative (depending on the dopant). They also have good stability over time. Abramchuk et al.[25] report on the superiority of semiconductor strain gauges, compared to wire and foil

gauges, for investigating the rapid deformation processes in solids. In particular, they cite the high gauge factor of semiconductor gauges as being an important property in this context.

If measures and circuits devised to compensate for the relatively high coefficients of resistivity and gauge factor of semiconductor gauges (see Table 8) are adopted, then associated problems can be prevented. Furthermore, as Mallon et al[61] have proposed, improved control of the temperature properties of the piezoresistive coefficients for semiconductors may result from investigations of the use of modified dopants and additives. Moreover, as detailed in section 2.6, by introducing higher levels of doping, the non-linearity of semiconductor strain gauges may be significantly reduced.

It is suggested that, on the basis of the findings outlined in the preceding chapters, semiconductor strain gauges can be an invaluable means of measuring or monitoring a range of dynamic or static strains - especially low magnitude strains.

7.3 COMMENTS ON SEMICONDUCTOR STRAIN GAUGE PERFORMANCE AND USES

The importance of good bonding of strain gauges was discussed in section 2.3 and it was explained how various means of testing bonds were studied. Recent developments in adhesive technology[73] have provided new, inorganic bonding agents, which can match more closely the thermal expansivity of metal substrates and provide reliable bonding. This is a further improvement which enhances the potential of semiconductor strain gauges for wider areas of employment.

Extensive investigations of circuits for use with semiconductor strain gauges were described and recommendations made regarding these in chapters 3 and 4. An important outcome of these applied studies is that, with the improvements made in the compactness and robustness of electronic devices in recent years, reliable, yet low cost and high precision, strain measurements may be undertaken using semiconductor strain gauges. Moreover, as was demonstrated, a portable and adaptable low noise, low drift amplifier system, along with a bridge

and integrated power supply, can be devised for use with strain gauges. This means that semiconductor strain gauges may be used in various environments which may otherwise have proved unacceptable for their employment. For convenience, as described in section 6.5, the output from such a strain measuring system can be fed into a microcomputer so that a corrected readout of strain magnitudes may be provided, and stored if required. On the basis of the investigations undertaken, such a system could be used even when silicon strain gauges are subjected to a large and high energy neutron flux.

The feasibility of potential applications of semiconductor strain gauges and the integrated bridge/amplifier system in the contexts described in chapter 6 was found to be quite good. Other areas where the particular advantages of low cost, low hysteresis, high gauge factor and small size, combined with a small, reliable bridge/amplifier system may be exploited are in paramedical contexts and in situations where small strains arise due to small environmental differences.

With regard to paramedical uses one possible context which has been identified is the use of a group of gauges to monitor the low magnitude strains due to initial contractions of the uterus during the

onset of labour in childbirth. A group of semiconductor strain gauges could be mounted on a diaphragm and the resulting differential signal monitored and used to control devices such as automatic fluid drips. A low hysteresis and sensitive but robust system providing a large signal would be required in this context and a semiconductor strain gauge bridge/amplifier system could provide the necessary precise signal for this application.

A situation where the high gauge factor and small size, along with the low hysteresis of semiconductor strain gauges could be exploited is in monitoring rapidly changing strains due to small, sudden environmental changes. One such example is in the testing and development of underwater weapons. For example, data regarding the effects of different underwater environments on torpedoes is necessary so that resulting improvements can be made to their accuracy and ability to discriminate between targets. Owing to their low mass and small size it would be possible to employ sufficient semiconductor gauges to provide comprehensive data regarding the effect of small changes in underwater environments in inducing small strains or displacements in different regions of the torpedo. This data could be transmitted or stored on board the torpedo, or used to provide a basis for correction in

conjunction with microprocessors controlling the guidance and homing systems.

7.4 SUGGESSTIONS CONCERNING ASPECTS FOR FURTHER INVESTIGATION

A number of phenomena, findings and ideas, which are suggested as being worthwhile aspects for further investigation, have been identified or have evolved as a consequence of this investigation of semiconductor strain gauges. Four main areas, each involving various factors, have been identified.

(i) Research and development could be undertaken with the intention of further improving semiconductor strain gauge performance with the aid of special electronic circuits. One aspect could be the exploration of the use of pulsed bridge excitation as a means of increasing bridge output. This could be particularly valuable for applications involving transient measurements. Other investigations could be carried out with the aim of providing on-chip passive temperature compensation for both discrete and multiple semiconductor strain gauges. Similarly, investigations could be carried out with a view to devising simple, active temperature compensation systems which

could also extend the operating temperature range of semiconductor gauges.

(ii) The need for comprehensive investigations of the photoelectric sensitivity of semiconductor strain gauges was pointed out in section 5.7. However, investigations of the dynamic photosensitivity of semiconductor materials which were not examined in this study are also required.

(iii) Further investigations, which built upon the findings of the examination of the behaviour of silicon strain gauges subjected to a neutron flux would be useful. A study of the corresponding behaviour of germanium strain gauges may provide valuable comparative evidence.

(iv) In addition to exploring the potential future applications of semiconductor strain gauges and integrated bridge/amplifier systems proposed in the preceding section, new areas of possible use could be investigated. This could involve the refining and extending of the techniques and methods devised for the applications described in chapter 6, since it is suggested that both areas of potential employment could be fruitfully developed.

APPENDIX 1

BRIDGE OUTPUT AMPLIFICATION

The output of the Wheatstone bridge was amplified using an operational amplifier as shown in figure A.1.1.

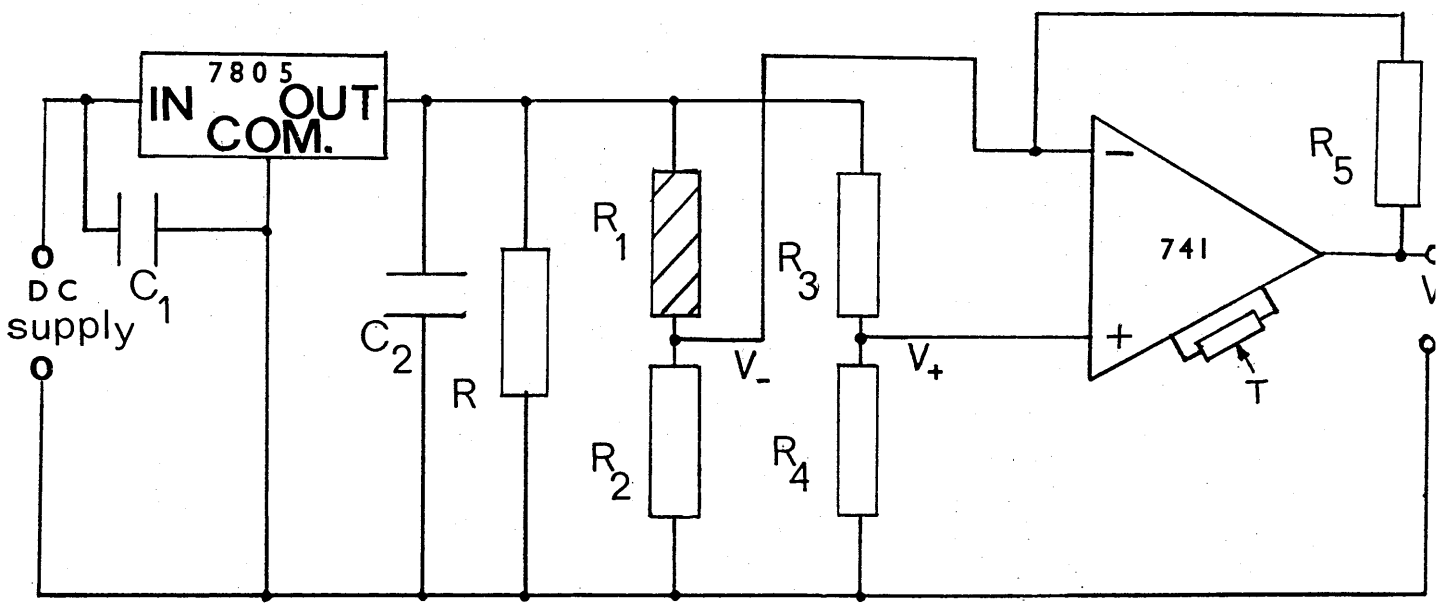

T - trim control

R_5 - 470KΩ

C_1 - 220nF

C_2 - 470nF

R - 4.7KΩ

Bridge with operational amplifier

Figure A.1.1.

The component values shown are typical of those used with a p- type silicon gauge of unstrained resistance 350Ω at room temperature and gauge factor 120. Resistors R_2, R_3 and R_4 were precision resistors (±0.1%). The offset trim control T, of the operational amplifier (eg 741), was adjusted so that the output of the amplifier was zero when the bridge was balanced.

Amplifications from 10 to 200 were used and, for an applied strain of only 10μ strain, this meant that an output V_o of about 450mV could be attained.

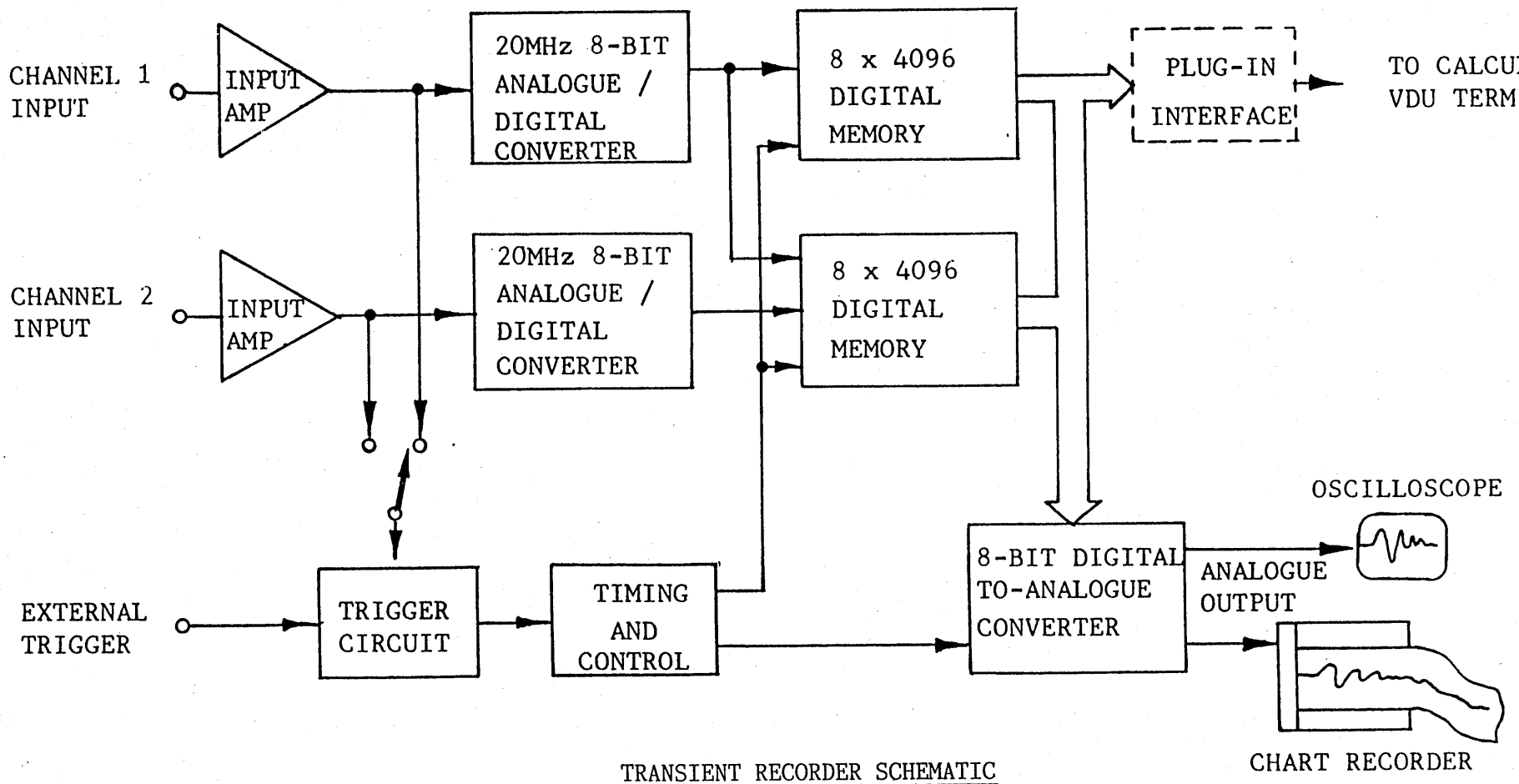

TRANSIENT RECORDER SCHEMATIC

Figure A.2.1.

APPENDIX 3

S.G.A. 100. Pin connections

+ Bridge Voltage	1	24	$+V_s$
N/C	2	23	N/C
Compensation	3	22	$-V_s$
N/C	4	21	N/C
N/C	5	20	Bridge Ref Input
+ Input	6	19	N/C
N/C	7	18	Feedback
N/C	8	17	N/C
N/C	9	16	Output
- Input	10	15	N/C
N/C	11	14	N/C
- Bridge Voltage	12	13	Zero Adjust

TOPVIEW

SEMICONDUCTOR LINEAR D.C. AMPLIFIER PERFORMANCE/CHARACTERISTICS

Supply Voltage	12V
Input offset voltage	1mV maximum
Input impedance	> 2.5MΩ minimum
Output current	5mA maximum
Closed loop gain (adjustable)	5 to 10,000
Common mode rejection ratio	> 100dB
Power dissipation	0.5W
Operating temperature	248 to 358K

REFERENCES

1. Thomson W, (Lord Kelvin) (1856) On the electrodynamic properties of metals. Proc. Royal Soc. pp 546-550

2. Hackemann P, (1938) Ein Beschleunigur.gsmesser nach dem piezoelektrischen Verfahren Jb.Dt.Luftf. Forsch.1 pp 628-9

3. Kluge G, Bochmann G, Brasack F (1940) Der Bremsvorgang an Kraftfahrzeugen und seine Messung. Dt. Kraftf. Forsch. 7.

4. Smith C. S, (1954) Piezoresistive effect in germanium and silicon. Phys. Rev, 94, pp 42-49.

5. Herring C, (1955) Transport Properties of a Many-Valley Semiconductor. Bell Syst. Tech J, 34 (2) pp 237-290.

6. Eisner R. L, (1955) Tensile test on silicon wiskers. Acta Met. 3, pp 1 - 2

7. Herring C and Vogt E, (1956) Transport and deformation potential theory for many-valley semiconductors with Anisotropic Scattering. Phys. Rev. 101, pp 944-961.

8. Morin, F, Geballe T. H, and Herring C, (1957) Temperature dependance of the piezoresistance of high purity silicon and germanium. Phys. Rev, 105, pp 525-539.

9. Mason W. P, and Thurston R.N, (1957) Use of piezoresistive material in the measurement of displacement, force and torque. J.Acc.Soc. Am.29, pp 1096-1101

10. Gohlke W (1941) Schwingungseigenschaften von Quarzdruckmessgeräten, V.D.I. Forschungsheft, Vol 407, pp 1 - 17.

11. Mason W. P, (1946) Elastic, piezoelectric and dielectric constants of sodium chlorate and sodium bromate. Phys. Rev. 70, pp 529 - 33.

12. Mason W. P. (1958) Physical accoustics and properties of solids. D. Van Nostrand. (New York)

13. Mason W. P. (1959) Semiconductors in strain gauges. Bell Lab. Record. 37, pp 7 - 9.

14. Geyling F. T, and Forst J. J, (1960) Semiconductor strain transducers. Bell Syst. Tec. J. 39, pp 705 - 731.

15. Vogt C. O, (1960) Semiconductor strain sensors. M.Sc. Thesis. Oklahoma State Univ.

16. Vogt C.O, (1960) The strainistor - a semiconductor strain sensor. 6th Nat. Flt. Test Symp, San Diego, Calif.

17. Wright W.V, and Sanchez J.C, (1961) Recent developments in Flexible silicon strain gauges. Inst. Soc. Am. Conf. Preprint 37-SL 61

18. Neubert H.K.P, (1967) Strain gauges kinds and uses. Macmillan (London)

19. Neubert H.K.P, (1975) Instrument Transducers: An introduction to their performance and design. Oxford Press (Oxford)

20. Gravel C. L, and Mallon J.R, (1971) Sensing with semiconductors. Industrial Research. (March)

21. Wallace R. H, (1972) Piezoresistive semiconductor gauges. Strain. 8, pp 162 - 164.

22. Castle P.F, (1974) A temperature compensated silicon strain transducer. Strain.10, pp 22 - 25.

23. Vaughan J, (1975) Application of B and K Equipment to strain measurements. Brül and Kjaer.

24. Welsh B. L, and Pyne C.R, (1977) A method to improve the temperature stability of semiconductor strain gauge pressure transducers. Royal Aircraft - Est. TR.77155

25. Abramchuk G.A, Alekhin V.A, Vashchenko A.P, Sandulova A.V, and Stepanov G.V, (1977) Characteristics of semiconductor strain gauge resistors in elastic waves. Problemy Prochnosti.6, pp 116 - 118.

26. Mallon J. R, and Kurtz A. D, (1979) Static Performance of integrated sensor transducers. 25th I.S.A. Symp. Anaheim. (U.S.A.)

27. Mallon J.R, Nunn T.A, and Kurtz A.D, (1981) Piezoresistive shear gauge. 1st Symp. Gauges and Piezoresistive materials. Arcachon.(France).

28. Mallon J.R, Kurtz A.D, and Nunn T.A, (1983) Microfabricated structures for silicon piezoresistive transducers. 2nd Int. Conf. Solid state transducers. Delft.(Holland)

29. Sze S. M, (1981) Physics of semiconductor devices. 2nd Ed. Wiley. (New York) pp 12 - 16

30. Kanda Y, (1982) A graphical representation of piezoresistive coefficients in silicon.I.E.E.E. Trans. Electron Devices. 29 pp 64 - 70.

31. Yamada K, Nishihara M, Shimada S, Tanaba M, Shimazoe M and Matsuoka Y, (1982) Nonlinearity of the piezoresistance effect of p-type silicon diffused layers. I.E.E.E. Trans. Electron Devices. 29, pp 71-77.

32. Baker M.A, (1982) Semiconductor strain gauges. In: Strain Gauge Technology. Eds. Window A. L and Holister G. S, App. Sc. Pubs. (London)

33. Welsh B, Pyne C.R, and Cripps B. E, (1983) Recent developments in the measurement of time-dependent pressures. A.G.A.R.D. (France) Conf. Proc. 348, pp 36.1 - 36.17.

34. (a) Hearn E. J, (1985) Private Comm.

(b) Mackinnon J.A, (1985) "

35. Seto J.Y.W, (1976) Piezoresistive properties of polycrysalline silicon. J.App.Phys. 47, pp 4780-83.

36. Nishidon S, Kongai M, and Takohashi K, (1983) Seebeck and piezoresistance effects in amorphous-microcrystalline mixed-phase silicon films and applications to power sensors and strain gauges. Thin Solid Films. 112.

37. Germer W, and Tödt W, (1983) Low cost pressure/force transducer with silicon thin film strain gauges. Sensors and actuators. 4. pp 183 - 89.

38. French P. J, and Evans A. G. R, (1984) Piezoresistance in polysilicon. Electronics Letters. 24, pp 999-1000.

39. Keyes R. W, (1986) High mobility F E T in strained silicon. I.E.E.E. Trans on Electron Devices. 33 pp 863.

40. Fraser D. A, (1984) The physics of semiconductor devices 3rd Ed. Clarendon Press. (Oxford)

41. Pearson G. L, Read W. T, and Feldmann W. L, (1957) Deformation and fracture of small silicon crystals. Acta. Met 5, pp 181

42. Kerr D. R, and Milnes A. G, (1963) Piezoresistance of diffused Layers. J.App Phys. 34, pp. 727-31.

43. Mallon J. R, and Hayer J.R, (1981) Integrated sensors for use at cryogenic temperatures. 27th I.S.A. Symp. Indiana. (USA)

44. Tufte O. N, and Stelzer E.L, (1963) Piezoresistive properties of silicon diffused layers. J. App. Phys. 34, pp 313.

45. Tufte O. N, and Stelzer E.L, (1964) Piezoresistive properties of heavily doped n-type silicon. Phys. Rev. 133, pp 1705.

46. Kurtz A. D, and Gravel C. L, (1967) Semiconductor transducers using transverse and shear piezoresistance. 22nd I.S.A. Conf. Chicago (USA)

47. Stein P. K, (1961) Adhesives: How they determine and limit strain gauge performance. In: semiconductor and conventional strain gauges. Eds. Dean M, and Douglas R. D, Academic Press (New York)

48. Mordan G. C, (1982) Adhesives and installation techniques. In: Strain Gauge Technology. Eds. Window G. L, and Holister G.S, App. Sc. Pubs. (London)

49. Shields J, (1970) Adhesives handbook. Butterworths (London)

50. Parkins J. R, (1968) Calibration and instrumentation of semiconductor strain gauges. Strain. 4, pp 10-18.

51. Wake W. C, (1976) General properties of polymers used in adhesives and sealants. In: Industrial adhesives and sealants. Ed. Jackson B. S, Hutchinson - Benham. (London)

52. Pople J, (1982) Errors and uncertainties in strain measurements. In: Strain Gauge Technology. Eds. Window G. L, and Holister G.S, App. Sc. Pubs. (London)

53. Sanchez J. C, and Wright W. V, (1961) Recent developments in flexible silicon strain gauges. In: Semiconductor and conventional strain gauges. Eds. Dean M, and Douglas R. D, Academic Press (New York)

54. Stein P, K, (1961) Strain gauge circuits for semiconductor strain gauges. In: semiconductor and conventional strain gauges. Eds. Dean M, and Douglas R. D, Academic Press (New York)

55. Open University (1985) Electronic materials and devices. Block 1. Resistors, resistivity and wafers. Open Univ. Walton Hall, Milton Keynes (UK)

56. Kulite (1985) Strain Gauge Data. Kulite Semiconductor Products Inc. New Jersey (USA)

57. Micro Gage (1986) Strain Gauge Data. Micro Gage Inc, California (USA)

58. Mansfield P, (1985) Electrical resistance strain gauge - theory, and practice 3. Trans. Tech. 8, pp 9 - 11.

59. Welsh B, (1984) European Conference on semiconductor transducer technology. Kulite. (Portugal)

60. Kulite (1980) Semiconductor strain gauge characteristics. Applic. Note AN-06A. Kulite.New Jersey (USA)

61. Mallon J. R, and Bernstein H, (1983) Temperature compensation and shunt calibration of semiconductor pressure transucers. 12th Trans. Workshop.Florida (USA)

62. Welsh B. L, Pyne C. R, and Cripps B.E, (L983) Recent developments in the measurement of time dependent pressures. 53rd AGARD Symp. Cesme (Turkey)

63. Xavier M.A, and Vogt C. O, (1961) Characteristics and applications of a semiconductor strain gauge. In: semiconductor and conventional strain gauges. Eds. Dean M, and Douglas R.D, Academic Press (New York)

64. Pankove J. I, (1971) Optical Processes in Semiconductors. Prentice-Hall (New Jersey)

65. Haynes J. R, and Hornbeck J.A, (1955) Trapping and minority carriers in silicon II.n-type silicon. Phys. Rev. 100, pp 606-14.

66. Horbeck J. A, and Haynes J.R, (1955) Trapping of minority carriers in silicon I. p-type silicon. Phys. Rev. 97, pp 311-321.

67. Perry C. C, and Lissner H. R, (1962) The strain gauge primer. McGraw Hill (New York)

68. Crawford J. H, and Cleland J. W, (1957) Radiation effects in semiconductors. In: Progress in semiconduction: 2. Wiley (New York)

69. James H. M, and Lark-Horovitz K, (1951) Localized electronic states in bombarded semiconductors. Z. Physik.Chem. 198, pp 107-26.

70. Caneli C, Malavasi D, Morten B, Prudenziati M, and Taroni A (1980) Piezoresistive effects in thick-film resistors. J. App. Phys. 51, pp 3282 - 88.

71. Caneli C, Malavasi D, Morten B, Prudenziati M, and Taroni A, (1980) Strain sensitivity in thick film resistors. I.E.E.E. Trans on comps. hybrids and Manuf. Tech. 3, pp 421-23.

72. Prudenziati M, Morten B, and Taroni A, (1981) Characterization of thick-film resitor strain gauges on enamel steel. Sensors and Actuators. 2, pp 17-27.

73. Shields J, (1974) Adhesive Bonding. B.S.I/C.E.I. Oxford Univ. Press (Oxford)